Tran-SET

Transportation Consortium of South-Central States

Solving Emerging Transportation Resiliency, Sustainability, and Economic Challenges through the Use of Innovative Materials and Construction Methods: From Research to Implementation

Development of a Self-Healing and Rejuvenating Mechanisms for Asphalt Mixtures Containing Recycled Asphalt Shingle

Project No. 17BLSU06

Lead University: Louisiana State University

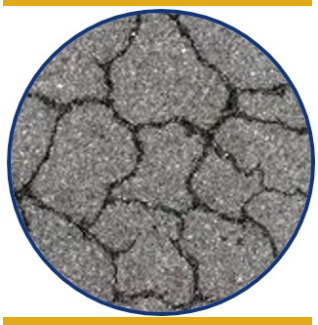

Enhancing Durability and Service Life of Infrastructure

Final Report

October 2018

Disclaimer

The contents of this report reflect the views of the authors, who are responsible for the facts and the accuracy of the information presented herein. This document is disseminated in the interest of information exchange. The report is funded, partially or entirely, by a grant from the U.S. Department of Transportation's University Transportation Centers Program. However, the U.S. Government assumes no liability for the contents or use thereof.

Acknowledgments

The authors acknowledge the financial support for this study by the Transportation Consortium of South Central States (Tran-SET), and the Louisiana Transportation Research Center (LTRC). Also, this study would have not been possible without the lab equipment support by LTRC to conduct different asphalt binder and mixtures tests. The authors would also like to express sincere thanks to Dr. Louay Mohammad and Dr. Samuel B. Cooper, III for their contribution to this study.

TECHNICAL DOCUMENTATION PAGE

1. **Project No.** 17BLSU06	**2. Government Accession No.**	**3. Recipient's Catalog No.**

4. Title and Subtitle Development of a Self-Healing and Rejuvenating Mechanism for Asphalt Mixtures Containing Recycled Asphalt Materials	**5. Report Date** Oct. 2018 **6. Performing Organization Code**
7. Author(s) PI: Marwa Hassan https://orcid.org/0000-0001-8087-8232 Post-doc: Max Aguirre https://orcid.org/0000-0001-9899-9235	**8. Performing Organization Report No.**
9. Performing Organization Name and Address Transportation Consortium of South-Central States (Tran-SET) University Transportation Center for Region 6 3319 Patrick F. Taylor Hall, Louisiana State University, Baton Rouge, LA 70803	**10. Work Unit No. (TRAIS)** **11. Contract or Grant No.** 69A3551747106
12. Sponsoring Agency Name and Address United States of America Department of Transportation Research and Innovative Technology Administration	**13. Type of Report and Period Covered** Final Research Report May 2017 – May 2018 **14. Sponsoring Agency Code**

15. Supplementary Notes
Report uploaded and accessible at: Tran-SET's website (http://transet.lsu.edu/).

16. Abstract
The objective of this study was to test the hypothesis that hollow-fibers encapsulating a rejuvenator product could improve both self-healing, rejuvenation, and mechanical properties of asphalt mixtures. Hollow-fibers containing a rejuvenating product were synthesized via a wet spinning procedure with sodium-alginate polymer as the encapsulating material. An optimization of the production parameters for the synthesis of fibers was performed to develop fibers suitable for high-temperature and shear stress environment typical of asphalt mixture production. A self-healing experiment was conducted to evaluate the healing/rejuvenation capabilities of sodium-alginate fibers in asphalt mixtures with varying types of binders and recycled materials. Based on the self-healing experiment, a 5% fiber content was determined to be the optimum fiber content to enhance the self-healing ability of asphalt mixtures. In addition, the effect of different fiber contents on binder blends and asphalt mixtures was evaluated by performing the Multiple Stress Creep Recovery (MSCR) and Semi-Circular Bending (SCB) tests. Results of the self-healing experiment showed that the enhancement in the healing recovery depends on the breakage of the fibers. When the fibers break, the rejuvenator is released resulting in softening of the binder. In contrast, when the fibers do not break, they act as a reinforcement for the mix. Loaded Wheel Tester (LWT) test results showed a performance improvement against permanent deformation for asphalt mixtures containing recycled materials with sodium-alginate fibers compared to conventional asphalt mixtures. Furthermore, SCB test results showed that the addition of sodium-alginate fibers enhanced the fracture properties of asphalt mixtures with Recycled Asphalt Shingle (RAS) at intermediate temperatures. Moreover, the addition of fibers in mixtures with recycled materials resulted in an improved performance against low-temperature cracking as the mixtures resisted higher stresses before failure.

17. Key Words Self-healing, polymer fibers, sustainable pavement, asphalt mixture, recycling, rejuvenator	**18. Distribution Statement** No restrictions.

19. Security Classif. (of this report) Unclassified	**20. Security Classif. (of this page)** Unclassified	**21. No. of Pages** 85	**22. Price**

Form DOT F 1700.7 (8-72) **Reproduction of completed page authorized.**

SI* (MODERN METRIC) CONVERSION FACTORS

APPROXIMATE CONVERSIONS TO SI UNITS

Symbol	When You Know	Multiply By	To Find	Symbol
		LENGTH		
in	inches	25.4	millimeters	mm
ft	feet	0.305	meters	m
yd	yards	0.914	meters	m
mi	miles	1.61	kilometers	km
		AREA		
in^2	square inches	645.2	square millimeters	mm^2
ft^2	square feet	0.093	square meters	m^2
yd^2	square yard	0.836	square meters	m^2
ac	acres	0.405	hectares	ha
mi^2	square miles	2.59	square kilometers	km^2
		VOLUME		
fl oz	fluid ounces	29.57	milliliters	mL
gal	gallons	3.785	liters	L
ft^3	cubic feet	0.028	cubic meters	m^3
yd^3	cubic yards	0.765	cubic meters	m^3
		NOTE: volumes greater than 1000 L shall be shown in m^3		
		MASS		
oz	ounces	28.35	grams	g
lb	pounds	0.454	kilograms	kg
T	short tons (2000 lb)	0.907	megagrams (or "metric ton")	Mg (or "t")
		TEMPERATURE (exact degrees)		
^oF	Fahrenheit	5 (F-32)/9 or (F-32)/1.8	Celsius	^oC
		ILLUMINATION		
fc	foot-candles	10.76	lux	lx
fl	foot-Lamberts	3.426	$candela/m^2$	cd/m^2
		FORCE and PRESSURE or STRESS		
lbf	poundforce	4.45	newtons	N
lbf/in^2	poundforce per square inch	6.89	kilopascals	kPa

APPROXIMATE CONVERSIONS FROM SI UNITS

Symbol	When You Know	Multiply By	To Find	Symbol
		LENGTH		
mm	millimeters	0.039	inches	in
m	meters	3.28	feet	ft
m	meters	1.09	yards	yd
km	kilometers	0.621	miles	mi
		AREA		
mm^2	square millimeters	0.0016	square inches	in^2
m^2	square meters	10.764	square feet	ft^2
m^2	square meters	1.195	square yards	yd^2
ha	hectares	2.47	acres	ac
km^2	square kilometers	0.386	square miles	mi^2
		VOLUME		
mL	milliliters	0.034	fluid ounces	fl oz
L	liters	0.264	gallons	gal
m^3	cubic meters	35.314	cubic feet	ft^3
m^3	cubic meters	1.307	cubic yards	yd^3
		MASS		
g	grams	0.035	ounces	oz
kg	kilograms	2.202	pounds	lb
Mg (or "t")	megagrams (or "metric ton")	1.103	short tons (2000 lb)	T
		TEMPERATURE (exact degrees)		
^oC	Celsius	1.8C+32	Fahrenheit	^oF
		ILLUMINATION		
lx	lux	0.0929	foot-candles	fc
cd/m^2	$candela/m^2$	0.2919	foot-Lamberts	fl
		FORCE and PRESSURE or STRESS		
N	newtons	0.225	poundforce	lbf
kPa	kilopascals	0.145	poundforce per square inch	lbf/in^2

TABLE OF CONTENTS

LIST OF FIGURES

LIST OF TABLES

ACRONYMS, ABBREVIATIONS, AND SYMBOLS

AASHTO	American Association of State Highway and Transportation Officials
ASTM	American Society for Testing Materials
BBR	Bending Beam Rheometer
$CaCl_2 \cdot 6H_2O$	Calcium Chloride Hexahydrate
Cw_0	Initial Crack width (mm)
Cw_t	Crack width at the time of analysis (mm)
DCB	O-Dichlorobenzene
DI	De-Ionized
DSR	Dynamic Shear Rheometer
G_{mm}	Maximum Theoretical Specific Gravity
H_e	Healing efficiency (%)
HMA	Hot-Mix Asphalt
HWTD	Hamburg Wheel-Tracking Device
IDT	Indirect Tensile Test
ITS	Indirect Tensile Strength
Jc-value	Critical Strain Energy Release Rate
LTRC	Louisiana Transportation Research Center
MSCR	Multiple Stress Creep Recovery
MWS	Manufactured Waste Shingles
NMAS	Nominal Maximum Aggregate Size
PCWS	Post-Consumer Waste Shingles
PEMA	Ethylene-Alt-Maleic-Anhydride
RAP	Recycled Asphalt Pavement
RAS	Recycled Asphalt Shingles
SEM	Scanning Electron Microscope
SBS	Styrene Butadiene Styrene
SCB	Semi-Circular Bending
TGA	Thermal Gravimetric Analysis

Tran-SET	Transportation Consortium of South-Central States
TSRST	Thermal Stress Restrained Specimen Test
UTS	Ultimate Tensile Strength
VDOT	Virginia Department of Transportation
3PB	3 point-bending

EXECUTIVE SUMMARY

The objective of the study was to evaluate self-healing of asphalt mixtures by mimicking the self-healing ability of human skin. Hollow-fibers containing a rejuvenator product were synthesized; self-healing and rejuvenating mechanisms were evaluated in asphalt mixtures containing recycled materials. The self-healing and rejuvenating processes consist of releasing the rejuvenator product by the breakage of the fibers when micro-cracks start to form in the asphalt mixture. Sodium-alginate was selected as the polymer shell material in the developed fibers based on its low-cost and biodegradability properties, which would provide a second release mechanism for the rejuvenator product in order to reverse the aging process after a number of years in service.

In this study, a commercial bio-oil, Rejuvn8, was selected as the core material in the developed fibers. Rejuvn8 was identified in past studies to be an effective rejuvenator product to reactivate the binder from recycled materials; thus, reducing the virgin binder needed to satisfy mix design criteria. The polymer fibers were synthesized via a wet-spinning process followed by a 48-hour drying period. The production parameters of the fibers were optimized to produce hollow-fibers with optimum thermal stability and tensile strength in order to resist asphalt mixing and production processes. Based on the optimization process, the optimum production parameters were a rejuvenator to shell material ratio of 1:1.5, 30% emulsifier content, and 40% plasticizer content. The tensile test results showed that the fibers synthesized with the optimum production parameters had an adequate tensile strength to resist shear stresses during the mixing process. Furthermore, the optimum production parameters enhanced the thermal stability of the fibers in order to avoid their degradation due to high-temperatures during the mixing process.

A self-healing experiment was conducted to evaluate the healing/rejuvenation effects of adding sodium-alginate fibers on asphalt mixtures with varying types of binders and recycled materials. The self-healing experiment test results showed that the addition of 5% fiber by weight of virgin binder resulted in the highest enhancement in healing of the evaluated mixtures. Therefore, a 5% fiber content was identified as the optimum fiber content in this study. The self-healing experiment also showed that the type of recycled materials influenced the healing/rejuvenation ability of the developed fibers. A validation of the optimum binder content was conducted by performing MSCR and SCB tests in a series of binder blends and asphalt mixtures. The validation process showed that the addition of 5% fibers enhanced the rutting susceptibility of the evaluated binder blend compared to the virgin binder. In addition, SCB test results showed that the addition of 5% fiber content enhanced the fracture resistance of asphalt mixtures containing Recycled Asphalt Shingles (RAS).

The study also evaluated the effects of adding sodium-alginate fibers on the rheological properties of binder blends with varying types of binders and extracted binders from RAS and/or Reclaimed Asphalt Pavement (RAP). Superpave PG Grading and the MSCR test were performed on the binder blends. Results showed that the addition of the synthesized fibers did not significantly affect the rheological properties of unmodified and SBS-polymer modified binders, as it did not change the final PG Grading of the evaluated binder blends. However, MSCR test results suggested an enhancement in performance against rutting of the binder blends with the addition of recycled materials and the developed fibers based on the non-recoverable creep compliance and percentage recovery.

The effects of adding the developed fibers on the mechanical properties of asphalt mixtures were evaluated by performing controlled laboratory tests in order to assess their performance against common distresses such as permanent deformation, fatigue cracking, and low-temperature cracking. The Loaded Wheel Tester (LWT) test results showed a performance improvement against permanent deformation in asphalt mixtures containing recycled materials with sodium-alginate fibers compared to conventional asphalt mixtures. Furthermore, SCB test results showed that the addition of sodium-alginate fibers enhanced the fracture properties of asphalt mixtures with RAS at intermediate temperatures. Moreover, the addition of fibers in mixtures with recycled material resulted in an improved performance against low-temperature cracking as the mixtures resisted higher stresses before failure.

IMPLEMENTATION STATEMENT

The results obtained from this study demonstrated the benefits of implementing rejuvenating fibers in asphalt mixtures in the South-Central region. In addition, the experimental data gathered throughout this research project have contributed to broaden the knowledge on the subject of innovative self-healing technologies in asphalt materials. Furthermore, the knowledge acquired in this investigation can be implemented in asphalt materials educational courses at LSU and other universities in the Transportation Consortium of South-Central States (Tran-SET) university consortium. Overall, this study has contributed to an emerging research field on the rejuvenation of asphalt mixtures that could potentially produce a new generation of asphalt mixtures with superior service life, lower initial cost, and less negative environmental effects.

1. INTRODUCTION

The use of recycled materials in Hot-Mix Asphalt (HMA) has increased due to the rising cost of petroleum-based products and the negative environmental impacts from carbon emissions associated with the production of asphalt binder. However, the main challenge of incorporating recycled materials in asphalt mixtures is the aged binder that increases the cracking susceptibility of the mix. Therefore, the aged binder in RAS and RAP tends to limit high content of recycled materials in the mix. The need to reverse the negative effects of recycled materials in HMA motivates researchers to identify and implement innovative and tenable approaches.

Asphalt rejuvenators have been introduced to rebalance the asphaltene-to-maltene ratio in an aged binder; this would reverse the aging process and thus restore the original properties of the binder. The application of rejuvenators has been used in maintenance activities on the top layer of the pavement in order to revive the oxidized top portion *(1)*. However, the depth of penetration of the rejuvenator as a surface treatment is a concern, which may negatively affect the effectiveness of this approach *(2)*. Self-healing mechanisms have emerged as an innovative approach to disperse the rejuvenator product into the asphalt mix.

Self-healing concept for asphalt pavement has its roots in biology, in which an injured skin and tissue can be self-healed, owing to the presence of nutrient supplies in the body that substitute the damaged parts. Developing self-healing mechanisms for asphalt pavements is promising as it would provide a more reliable and resilient design of asphalt mixtures to resist the initiation and propagation of cracking caused by vehicular and environmental loading; thus, improving the service life of the pavement.

1.1. Recycled Materials in Asphalt Pavements

Reclaimed asphalt pavement is a process in which asphalt pavement is removed during resurfacing, rehabilitation, or reconstruction operations. RAP materials are commonly used as a substitute for aggregate and virgin binder, but it also may be used as a granular base or subbase, a stabilized base aggregate, or as an embankment/fill material. A previous study compared the complex modulus of traditional HMA and HMA containing RAP *(3)*. Results showed that high percentages of RAP (25 and 40%) resulted in an increase in the complex modulus compared to the control mixture *(3)*. Another study evaluated the cracking susceptibility of HMA with RAP *(4)*. The results demonstrated that HMA with 20% RAP performed similarly to the control mixture; however, the cracking susceptibility increased with higher percentage of RAP in the mixture (e.g., 40%).

Another recycled material used in HMA is Recycled Asphalt Shingle (RAS). RAS is a material commonly used in the roofing industry, which consists of asphalt binder, mineral filler, organic paper felt, and glass fiber matting *(5)*. A study investigated the effect of incorporating 5% RAS on HMA performance against cracking and rutting *(6)*. The study concluded that there was no difference in cracking performance compared to the control mixture. Also, the rutting performance of the mixture containing RAS was within the guidelines of the Virginia Department of Transportation (VDOT). Furthermore, the PG of the recovered binder containing RAS showed an improvement at high-temperature. A similar study was performed

with HMA containing 5% Manufactured Waste Shingles (MWS). The study found that both fatigue cracking and rutting performance were similar to the control mixtures *(7)*.

1.2. Rejuvenation in Asphalt Pavements

A rejuvenator product is typically a cationic emulsion containing maltenes; it is added to an aged binder to recover the properties of the oxidized asphalt binder *(8)*. Studies have shown that asphalt rejuvenators are the most effective treatment to partially restore asphalt properties; i.e., restore the asphaltene to maltene ratio *(9)*. Another way that rejuvenator products decreased the oxidation process of the binder is by penetrating the asphalt and filling the voids as the rate of oxidation depends on the voids in the total mixture *(10)*. Furthermore, studies have shown that the use of rejuvenator products in mixtures with recycled materials increased the blending of the aged and virgin binders resulting in a reduction in the stiffness of the aged binder *(10)*.

A previous study evaluated three different rejuvenator products on recycled asphalt mixtures *(11)*. The study found that two rejuvenator products were successful in softening the aged binder. Furthermore, the study observed a reduction in both Marshall stability and resilient modulus of HMA with a rejuvenator product. Another study found that the use of rejuvenator products in asphalt mixture reduced hardening and temperature susceptibility of the pavement *(12)*. Shen et al. evaluated Superpave mixtures containing RAP with rejuvenator products to determine the mixture behavior in the Indirect Tensile Strength (ITS) and susceptibility against permanent deformation *(13)*. The study showed that the ITS of mixtures containing RAP with rejuvenator product had a similar performance to conventional mixtures. In addition, the results showed that all the evaluated mixtures satisfied the rut depth requirement of 8.0 mm.

Cooper et al. *(14)* studied the effect of four different rejuvenators on the performance of asphalt mixtures containing RAS. The use of a rejuvenator increased the recycled binder ratio but also showed an adverse effect on the intermediate and low-temperature performances of the mixture *(14)*. The effect of adding three different rejuvenator products on HMA containing RAS and RAP was evaluated by Mogawer et al. *(1)*. The study reported a reduction in the stiffness of the binder and an improvement in the cracking performance of the evaluated mixtures. However, the study showed a negative impact on the rutting and moisture susceptibility of the mixtures with the addition of the rejuvenator products.

It is worth noting that many studies reported that asphalt rejuvenators do not penetrate the asphalt pavement deeply enough to effectively restore the properties of the aged binder *(2)*. Therefore, asphalt rejuvenator products should be added to the asphalt binder during asphalt mixture production and not be used as a seal coat to avoid negative effects such as reduction in friction on the pavement surface and poor rejuvenation efficiency *(10)*.

1.3. Self-Healing Materials in HMA

An innovative method to address the poor penetration of a rejuvenator product is to incorporate microcapsules containing the rejuvenator. The concept of encapsulating a rejuvenator product is to release the product when the microcapsule breaks at a predefined stress. A previous study was successful in developing melamine-formaldehyde microcapsules via in-situ polymerization containing a recycling agent as core material *(15)*. The study observed that the selected rejuvenator product for the single-wall microcapsules had a positive influence at both

high- and low-grade temperatures of the evaluated binder. In addition, the authors developed double-walled microcapsules containing sunflower oil as a recycling agent using urea-formaldehyde/polyurethane as a shell material *(16)*. The study observed that the addition of a second wall in the microcapsules enhanced the thermal stability at high-temperature and the ability to encapsulate liquids in the long-term. A study evaluated the self-healing ability of microcapsules containing a rejuvenator product by inducing a crack using a three-point bending test under two environmental conditions: room-temperature and high-temperature *(17)*. The study reported a lower healing efficiency for the mixtures containing microcapsules compared to the control. Researchers concluded that a lower healing efficiency of the mixtures containing microcapsules was observed as not all microcapsules broke during the test since they were designed to break over time and not all at once.

Al-Mansouri et al. *(18)* developed calcium-alginate microcapsules containing sunflower oil as core material. The study found that the developed capsules had suitable thermal and mechanical properties to resist asphalt-mixing processes. The study conducted a self-healing experiment to evaluate the effect of the microcapsules and the healing temperature on the self-healing properties of asphalt mixtures with and without microcapsules. Results showed that the increased in microcapsule content had a significant influence on the healing levels, where a higher content resulted in higher healing efficiencies. In addition, the study concluded that the addition of calcium-alginate microcapsules enhanced the self-healing of the evaluated mixtures at healing-temperatures equal to or less than 30°C compared to mixtures without microcapsules. The study also reported that the mixtures without microcapsules had a better healing efficiency compared to the mixtures with microcapsules at healing-temperatures greater than 30°C.

Another study evaluated the effect of mixing and aging on the self-healing ability of calcium-alginates fibers containing sunflower oil *(19)*. The study observed that the addition of microcapsules did not improve the stiffness of mixtures compared to mixtures without microcapsules. The results also showed that mixing order and aging time did not have a significant influence on the flexural strength of the evaluated mixtures. Furthermore, the study observed that healing efficiencies varied depending on the order of addition of microcapsules, and mixtures with microcapsules showed higher efficiency levels than mixtures without microcapsules. Furthermore, the study observed that aging had a negative effect on the healing efficiency as mixtures without aging showed greater healing levels than mixtures with the aging process. Although a higher healing efficiency could be obtained with the addition of microcapsules with a rejuvenator product, studies have shown that the stiffness of HMA was reduced when microcapsules were added as the addition of sand like particles increased the rutting susceptibility of the mix *(20, 21)*.

The encapsulation of asphalt rejuvenators in sodium-alginate fibers emerged as a solution to address the negative effect of adding microcapsules in HMA. Sodium-alginate has been investigated in self-healing mechanisms such as the encapsulation of bacteria for concrete healing *(22)* and healing agents for thermoplastic composite material healing *(23)*. The low-cost, organic characteristics, low-environmental impact and self-degrading properties make this polymer a promising encapsulating material in asphalt pavement applications. A previous study successfully developed calcium-alginate fibers containing a commercial rejuvenator product, Modesel R20 *(24)*. The study performed an optimization process of the production parameters and it concluded that a ratio of 70:30 rejuvenator/alginate ratio produced suitable

fibers with thermal and mechanical properties suitable for asphalt mixing process. In addition, the study performed a self-healing experiment to evaluate the effect of fibers on the mechanical properties and healing efficiency of asphalt mixtures. Results for the self-healing experiment showed that the initial strength of asphalt mixtures was improved with the addition of the developed fibers, but the addition of the fibers reduced the healing capacity of the mixtures compared to mixtures without fibers. Lastly, the study concluded that the 5% fibers by weight of binder was the optimum fiber content for improving the initial strength of the evaluated mixtures.

Tabakovic et al. *(25)* evaluated the healing efficiency of a conventional mixture and a mixture with 5% calcium-alginate fibers by performing an Indirect Tensile Test (IDT) and comparing the initial strength and healed strengths at different healing periods. The IDT results showed that the initial strength of the mixture without fibers was higher than the mixture with fibers. However, the mixture with fibers had a higher ITS than the mixture without fibers after the first healing period. In addition, the study conducted a strain controlled 4-point bending tests to better simulate the damage that occurs in the field. Results of the 4-point bending tests showed that the mixtures containing fibers had a better stiffness recovering ability in comparison to the conventional mixture. The researchers concluded that compartment fibers containing a rejuvenator product are a promising self-healing mechanism to enhance the healing ability and mechanical properties of asphalt mixtures.

2. OBJECTIVE

The objectives of this study were the following:

- Develop a synthesis procedure for the production of sodium-alginate hollow-fibers containing an asphalt rejuvenator;
- Evaluation of the thermal stability and resistance to mixing processes of the fibers;
- Evaluation of self-healing efficiency of hollow-fibers, through crack healing and stiffness recovery of damaged mixture specimens under two different healing conditions;
- Assess the rheological properties of asphalt binder blends with the developed fibers through laboratory tests; and
- Evaluation of the performance against fatigue cracking, low-temperature cracking, and rutting susceptibility of HMA with fibers through laboratory tests.

3. SCOPE

A wet spinning process was used for the synthesis of rejuvenator-filled compartment fibers. A suite of laboratory experiments was carried out to evaluate the effects of varying the proportions of the production parameters in the thermal and mechanical properties of the hollow fibers. Thermal Gravimetric Analysis (TGA) test was conducted to evaluate the thermal degradation of the fibers from 25 to 600°C. A pullout test was conducted on the hollow-fibers for tensile strength evaluation. Two binder types (unmodified PG 64-22 and polymer-modified PG 70-22) were blended with the synthesized hollow fibers at different modification contents. Fourteen asphalt binder blends were prepared to evaluate the effects of adding the hollow-fibers in the rheological properties of the binder blends. Asphalt mixes were prepared using virgin and recycled materials from RAP and RAS and with different contents of hollow fibers. A suite of laboratory test was conducted on the prepared mixes to assess their performance against rutting, intermediate cracking, and low-temperature cracking.

4. METHODOLOGY

4.1. Synthesis of Sodium-Alginate Fibers

4.1.1. Chemicals

The encapsulated rejuvenator product, Rejuvn8, consisted of a green bio-oil product from Sripath Technologies (density 0.919 g/cm^3). The study used sodium-alginate as a shell material for the developed fibers. PEMA (ethylene-alt-maleic-anhydride) was utilized as a surfactant in an aqueous solution and a plasticizer material, Ethylene glycol, was added in the synthesis procedure. In addition, the coagulation bath consisted of a 0.6 Molarity (M) solution of calcium chloride hexahydrate ($CaCl_2 \cdot 6H_2O$).

4.1.2. Procedure for Fibers Preparation

The fibers synthesis procedure was performed by modifying the procedure presented by Mookhoek et al., who developed hollow-fibers containing o-dichlorobenzene (DCB) *(26)*. A wet-spinning process was performed to produce the hollow-fibers from an oil-in-water emulsion containing the shell material and the core material. Figure 1 shows a diagram of the wet spinning line used to develop the fibers. Sodium-alginate was selected as the shell material because it provides suitable properties such as water solubility, fast coagulation in the presence of divalent ions, and adequate mechanical properties *(27)*.

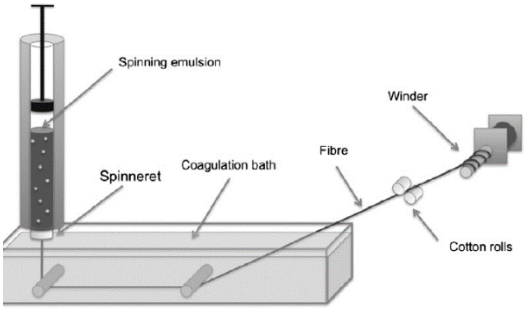

Figure 1. Wet-spinning line set-up *(26)*.

For the production of the fibers, 6 g of sodium-alginate was dissolved in 100 ml of de-ionized (DI) water using a high shear impeller at room temperature for 30 min. In addition, a 2.5 wt % polymeric surfactant solution, PEMA, was prepared by dissolving the copolymer in water at 70°C and mixing it for 60 min. The PEMA solution was allowed to cool down to room temperature. A healing solution of PEMA/rejuvenator was prepared by mixing different percentages of PEMA by weight of rejuvenator. PEMA was used to stabilize the healing solution. The healing solution was then mixed with the sodium-alginate solution at different rejuvenator-to sodium-alginate ratios at 40 rpm for 20 sec. The spinning of the fibers was conducted via a small-scale wet spinning pilot line. The pilot-size spinning line consisted of a motor-controlled plunger-extruder and a motor-controlled filament winder. A 100-ml syringe with an 18-gauge straight-cut needle was utilized to extrude the emulsion into the coagulation bath. The syringe was submerged into a coagulation bath containing a 0.6 M solution of calcium chloride hexahydrate ($CaCl_2 \cdot 6H_2O$) in water at room temperature. The coagulated fiber was removed out of the coagulation bath and it was coiled on a plastic bobbin under slight

tension at a constant rate matching that of the extrusion (i.e., draw ratio = 1). Afterwards, the bobbin with the fibers was placed inside a fume-cabinet at room temperature with air convection to dry slowly over at least a period of 48 hours before further testing.

4.2. Optimization Process for Sodium-Alginate Fibers Production

The optimization process consisted of two experiments. In the first experiment, the optimization process was conducted to evaluate the thermal stability and tensile properties of the evaluated fibers shown in Table 1 and to assess their resistance to asphalt mixing and production processes. In the second experiment, the optimization process evaluated the effects of fiber contents on the rheological properties of the binder blends. In the first experiment, the optimization process consisted of varying the following production parameters: percentage of emulsifier, percentage of plasticizer, and the amount of rejuvenator used. The impact on the stability of the solution containing the core and shell materials was evaluated with the variation in the percentage of the emulsifier. Furthermore, the addition of a plasticizer was evaluated to study its influence on the thermal stability of the developed fibers. Lastly, the different rejuvenator-to-shell material ratios were assessed in the experimental matrix to determine their effects on both thermal stability and tensile properties of the fibers. Table 1 summarizes the experimental test matrix for the optimization process.

Table 1. Test matrix for fiber's optimization.

Sample ID	Rejuvenator to Shell Material Ratio	Emulsifier Content (%)	Plasticizer Content (%)
Fiber1	1:1.5	30	-
Fiber2	1:1.5	40	-
Fiber3	1:1.5	50	-
Fiber4	1:1.5	30	10
Fiber5	1:1.5	30	20
Fiber6	1:1.5	30	30
Fiber7	1:1.5	30	40
Fiber8	2:1	30	10
Fiber9	2:1	30	40
Fiber10	3:1	30	10
Fiber11	3:1	30	40

4.2.1. Thermogravimetric Analysis (TGA)

Adequate thermal stability is needed for the fibers to resist high-temperature during asphalt mixture production. Thermal stability was evaluated by performing a TGA test at a rate of 10°C/min from room temperature (i.e., 25°C) to 600°C for the developed fibers in order to determine their high-temperature degradation rate.

4.2.2. Tensile Strength

Tensile strength was assessed to evaluate resistance of the fibers to breakage during the mixing processes. Based on the literature, the fibers should have an Ultimate Tensile Strength (UTS) greater than 12 MPa to resist typical stresses during asphalt mixing and production processes *(28, 29)*. The UTS of the developed fibers was tested in tension using a pullout testing system with a 50 N load cell at a crosshead speed of 5.0 mm/s.

4.3. Optimum Fiber Content in Asphalt Binder Blends and HMA

4.3.1. Asphalt Binder Blends Preparation

Table 2 details the second experiment conducted to predict the optimum fiber content based on the rheological properties of the binder blends. Asphalt binder from a recycled material (i.e., post-consumer waste shingles "PCWS") was added to the selected asphalt binder at 5% by total weight of virgin binder. Asphalt binder was extracted in accordance with AASHTO T 164 *(30)*. Afterward, the solution obtained from AASHTO T 164 —Method A *(30)* was distilled to a point where most of the Trichloroethylene (TCE) was removed and then carbon dioxide gas was introduced to remove all traces of trichloroethylene. This procedure was conducted in accordance with AASHTO R 59 *(31)*. The recovered asphalt binder was then blended with virgin binder at a 5% dosage rate. The asphalt binder blends shown in Table 2 were prepared by mixing virgin binder with the prepared fibers and extracted binder at a mixing temperature of 163°C. The different asphalt blends were prepared by using a high-shear blender at 3,600 rpm to achieve good mixing and dispersion of the fibers and extracted binder in the different asphalt binder blends. Virgin binder and extracted binder from recycled materials were blended for 10 minutes at 163°C. Then, the produced sodium-alginate fibers were added slowly to avoid conglomeration of fibers for an additional 20 minutes at 163°C.

Table 2. Test matrix for optimization of fiber content.

Binder Blend/Mixture Type	Type of Binder	RAS	Fiber Content
70CO	PG 70-22	-	-
70PG5P	PG 70-22	5% PCWS	-
70PG5P1F	PG 70-22	5% PCWS	1%
70PG5P3F	PG 70-22	5% PCWS	3%
70PG5P5F	PG 70-22	5% PCWS	5%

4.3.2. Hot-Mix Asphalt Mixtures Preparation

The test matrix shown in Table 2 was also adopted for mixture testing. Superpave asphalt mixtures were prepared in accordance with AASHTO R 35-09, AASHTO M 323-07, and Section 502 of the 2006 Louisiana Standard Specifications for Roads and Bridges. A Level 2 design ($N_{initial}$ = 8, N_{design} = 100, N_{final} = 160 gyrations) was adopted. The optimum asphalt content for each Superpave mixture was determined according to volumetric design criteria (air voids = 3% to 5%, voids in mineral aggregates ≥ 13%, and voids filled with asphalt = 68% to 78%), and densification requirements (%G_{mm} at $N_{initial}$ ≤ 89%, and %G_{mm} at N_{final} ≤ 98%). The RAS was incorporated into the evaluated mixtures at 5% by total weight of the mix. In addition, the developed sodium-alginate fibers were added in the asphalt mixture at different percentages by weight of the virgin binder as shown in Table 2.

4.3.3. Asphalt Binder Test

The MSCR test was performed on the asphalt binder blends shown in Table 2 in accordance to AASHTO TP 70, which consists of applying a low stress (0.1 kPa) for 10 creep/recovery cycles then the stress was increased to 3.2 kPa and repeated for an additional 10 cycles.

4.3.4. HMA Mixture Test

The SCB test was conducted at intermediate temperature to evaluate the effect of fiber content on the fracture resistance of the asphalt mixtures shown in Table 2. The SCB test was

performed in accordance to ASTM D 8044 *(32)*, which consists of applying a monotonically increasing load on long-term aged samples at a constant deformation rate of 0.5 mm/min until fracture failure.

4.4. Rheological Properties of Asphalt Binder Blends with Fibers

The objective of the binder experiment was to evaluate the effects of adding sodium-alginate fibers on asphalt binder blends containing recycled materials. The experimental test matrix is shown in Table 3. Two binder types were selected to evaluate the effect of adding the synthesized fibers: unmodified and SBS-polymer modified binders (i.e., PG 64-22 and PG 70-22, respectively). In addition, extracted binder from recycled materials (RAS and RAP) were incorporated in the selected binder blends at 5 and 20% by weight of virgin binder, respectively. As previously mentioned, the binder from the recycled materials was extracted in accordance with AASHTO T 164 and AASHTO R 59 *(30, 31)*. The recovered asphalt binder was then blended with the virgin binder at the dosage rate specified in Table 3. A high-shear blender rotating at 3,600 rpm at a mixing temperature of 163°C was used to prepare the selected asphalt binder blends and to achieve good mixing and dispersion of the fibers and extracted binder in the different asphalt binder blends.

4.4.1. Performance Grading (PG Grading)

Rheological tests such as Dynamic Shear Rheometer (DSR) and Bending Beam Rheometer (BBR) were used to assess the rheological properties of the asphalt binder blends shown in Table 3. PG grading was performed in accordance with AASHTO M 320 *(33)*.

4.4.2. Multiple Stress Creep Recovery (MSCR)

The MSCR test was conducted to characterize the rutting susceptibility of the different asphalt binder blends. As previously explained, the MSCR tests consists of applying creep and recovery periods and to measure the percentage recovery and non-recoverable creep compliance (J_{nr}). The MSCR was performed in accordance to AASHTO TP 70 at a testing temperature of 67°C.

4.4.3. Linear Amplitude Sweep (LAS)

The fatigue resistance of the prepared asphalt blends was characterized by conducting the LAS test. The LAS test consists of applying cyclic loading employing systematic, linearly increasing load amplitudes. The LAS was performed in accordance with AASHTO TP 101 *(34)* in samples aged using RTFO and PAV to simulate the aging of in-service asphalt pavements. LAS test was conducted to estimate two fatigue parameters ("A" and "B") based on the asphalt binder fatigue law ($N_f = A\ x\ {\gamma_{max}}^B$). The LAS test consists of two steps: (1) a frequency sweep test at a low strain amplitude of 0.1% is used to obtain undamaged material properties (parameter "B" of fatigue law); and (2) an amplitude sweep test with a series of cyclic loading at systematically linearly increasing strain amplitudes at a constant frequency of 10 Hz is used to determine the parameter "A" of the fatigue law through viscoelastic continuum damage (VECD) mechanics analysis.

4.5. Chemical Analysis of Asphalt Binder Blends with Fibers

4.5.1. High-Pressure Gel Permeation Chromatography

High Pressure Gel Permeation Chromatography (HP-GPC) was performed using an EcoSEC system (HLC-8320GPC) of Tosoh Corporation, equipped with a differential refractive index detector (RI) and UV detector. A set of four micro-styragel columns of pore sizes 200 Å, 75 Å (2 columns) and 30 Å from Tosoh Bioscience was used in the analysis. Tetrahydrofuran (THF) at a flow rate of 0.35 mL/ min. was used as the solvent. Columns were calibrated using polystyrene standard mixtures PStQuick B (MW= 5480000, 706000, 96400, 10200, and 1000 daltons), PStQuick E (MW= 355000, 37900, 5970, and 1000 daltons), and PStQuick F (MW= 190000, 18100, 2500, and 500 daltons) from Tosoh Bioscience. Filtered solutions prepared with the binder blends and THF solvent were processed through a 0.45-micron Teflon filters prior to running the HP-GPC test analysis. The concentration of asphalt solution was 0.5%.

4.5.2. Fourier Transform Infrared Spectroscopy (FTIR)

FTIR spectra were obtained using a diamond single reflection attenuated total reflectance (ATR) instrument (Bruker Optics alpha) with the following settings for data collection: 32 scans/sample, spectral resolution 4 cm-1, wave number range 4000-500 cm-1. A few drops of the GPC asphalt solution (0.5% in THF) was placed on the ATR crystal plate and the solvent allowed evaporating. The spectrum was collected after the complete evaporation of the solvent. FTIR spectra of the aged samples show a peak around 1700 cm-1, which is the characteristic of C=O species. The carbonyl index was calculated from the band areas measured from valley to valley [35] according to Equation (1). This was accomplished using the OPUS spectroscopy software provided with the Bruker FTIR instrument.

$$\text{Carbonyl Index (ICO)} = \frac{\text{Area around } 1700 \text{ cm}^{-1}}{\text{Area around } 1460 \text{ cm}^{-1} \text{ and Area around } 1375 \text{ cm}^{-1}} \quad [1]$$

Table 3. Test matrix for evaluation of rheological properties of asphalt binder blends with sodium-alginate fibers.

Blend ID	Asphalt Binder	RAS Content	RAP Content	Fiber Content
70CO	PG 70-22	-	-	-
70PG3F	PG 70-22	-	-	3%
70PG5F	PG 70-22	-	-	5%
70PG10F	PG 70-22	-	-	10%
70PG5P	PG 70-22	5% PCWS	-	-
70PG5P5F	PG 70-22	5% PCWS	-	5%
70PG20RAP	PG 70-22	-	20%	-
70PG20RAP5F	PG 70-22	-	20%	5%
70PG5P20RAP	PG 70-22	5% PCWS	20%	-
70PG5P20RAP5F	PG 70-22	5% PCWS	20%	5%
64CO	PG 64-22	-	-	-
64PG3F	PG 64-22	-	-	3%
64PG5F	PG 64-22	-	-	5%
64PG10F	PG 64-22	-	-	10%
64PG5P	PG 64-22	5% PCWS	-	-
64PG5P5F	PG 64-22	5% PCWS	-	5%
64PG20RAP	PG 64-22	-	20%	-
64PG20RAP5F	PG 64-22	-	20%	5%
64PG5P20RAP	PG 64-22	5% PCWS	20%	-
64PG5P20RAP5F	PG 64-22	5% PCWS	20%	5%

4.6. Effects of Sodium-Alginate Fibers on HMA Performance

4.6.1. Materials

An unmodified binder (i.e., PG 64-22), a SBS-polymer-modified asphalt binder (i.e., PG 70-22M), and aggregate (i.e., 16-mm gravel, 6.35-mm gravel, coarse sand, and fine sand) were selected to satisfy the mix design criteria for a 12.5 nominal maximum aggregate size (NMAS) asphalt mixture. Aggregate consensus properties were verified for all aggregate sources. The RAS used in this study was PCWS and were incorporated into the evaluated mixtures at 5% by the total weight of mix. In addition, RAP was incorporated in the selected mixtures at 20% by total weight of mix. Furthermore, the developed sodium-alginate fibers were included in selected asphalt mixtures at 5% by the total weight of the virgin binder; see Table 4.

4.6.2. HMA Mixture Design

The objective of this phase of the study was to evaluate the effect of adding sodium-alginate fibers on a Superpave asphalt mixture with a NMAS of 12.5 mm. Superpave asphalt mixtures were prepared in accordance with AASHTO R 35-09, AASHTO M 323-07, and Section 502 of the 2006 Louisiana Standard Specifications for Roads and Bridges. A Level 2 design ($N_{initial}$ = 8, N_{design} = 100, N_{final} = 160 gyrations) was used. The optimum asphalt content for each Superpave mixture was determined according to volumetric (air voids = 3% to 5%, voids in mineral aggregates ≥ 13%, and voids filled with asphalt = 68% to 78%), and densification requirements (%G_{mm} at $N_{initial} \leq 89\%$, and %G_{mm} at $N_{final} \leq 98\%$). Table 4 shows the description of the prepared asphalt mixtures.

Table 4. HMA mixture description.

Mixture	Asphalt Binder	RAS Content	RAP Content	Fiber Content	Total AC	Virgin AC	AC from RM	Recycled Binder Ratio
70CO	PG 70-22	-	-	-	6.3%	6.3%	0.0%	0 %
70PG5P	PG 70-22	5%	-	-	6.3%	5.5%	0.8%	12.7%
70PG5P5F	PG 70-22	5%	-	5%	6.3%	5.7%	0.6%	9.5%
70PG20RAP	PG 70-22	-	20%	-	6.3%	5.2%	1.1%	17.5%
70PG20RAP5F	PG 70-22	-	20%	5%	6.3%	5.4%	0.9%	14.3%
70PG5P20RAP	PG 70-22	5%	20%	-	6.3%	4.4%	1.9%	30.2%
70PG5P20RAP5F	PG 70-22	5%	20%	5%	6.3%	4.6%	1.7%	27.0%
64CO	PG 64-22	-	-	-	6.3%	6.3%	0.0%	0 %
64PG5P	PG 64-22	5%	-	-	6.3%	5.5%	0.8%	12.7%
64PG5P5F	PG 64-22	5%	-	5%	6.3%	5.7%	0.6%	9.5%
64PG20RAP	PG 64-22	-	20%	-	6.3%	5.2%	1.1%	17.5%
64PG20RAP5F	PG 64-22	-	20%	5%	6.3%	5.4%	0.9%	14.3%
64PG5P20RAP	PG 64-22	5%	20%	-	6.3%	4.4%	1.9%	30.2%
64PG5P20RAP5F	PG 64-22	5%	20%	5%	6.3%	4.6%	1.7%	27.0%

4.6.3. HMA Mixture Performance Tests

HMA mixtures presented in Table 4 were evaluated through laboratory tests to assess the performance of each mixture against intermediate-temperature cracking, permanent deformation, and low-temperature cracking. Asphalt mixture performance tests were conducted based on the test factorial shown in Table 5. Two mechanical tests and a simulative test (LWT) were conducted to characterize the performance of asphalt mixtures. According to the specimen details shown in Table 5, cylindrical specimens were fabricated using a Superpave gyratory compactor (SGC), except for the TSRST test. The laboratory TSRST

specimens were compacted into a rectangular slab, 260.8 mm wide by 320.3 mm long by 50 mm thick, using a kneading compactor. After compaction, the required beam specimens for the TSRST were obtained by sawing the rectangular slab to the required dimensions as shown in Table 5. The target air voids for all specimens prepared in this study were 7.0 ± 0.5%.

Table 5. HMA mixture performance tests.

Tests	Test Standard	Performance Characteristics	Specimen Details
SCB	ASTM D 8044	Intermediate Temperature: fatigue and fracture cracking resistance	ϕ150 mm × 57 mm
LWT at 50°C	AASHTO T 324	Rutting susceptibility and moisture resistance	ϕ150 mm × 60 mm
TSRST	AASHTO TP 10	Low temperature: thermal cracking resistance	50 ± 5 mm^2× 250 ± 5 mm length

4.7. Healing Efficiency of HMA Containing Sodium-Alginate Fibers

Table 6 presents the test matrix for the evaluation of the healing/rejuvenating efficiency of the prepared fibers. Six specimens were prepared for each evaluated mixture type, with three to be exposed to room-temperature healing conditions and three to be exposed to high-temperature healing conditions after inducing a crack in the specimens. Rectangular beam specimens with dimensions 40 x 40 x 160 mm (Figure 2a) were prepared by sawing a rectangular slab (i.e., 260.8 x 320.3 x 50 mm) to the required dimensions.

The self-healing test consisted of inducing micro-cracks in the rectangular beam specimens at room-temperature with a three-point bending setup with span length of 100 mm without any prior conditioning through a strain-controlled load applied at a rate of 0.5 mm/min, which allowed stopping the test before any sudden failure. Figure 2(b) shows the three-point bending setup adopted in the self-healing test. After inducing the crack in the beam specimen, an optical microscope was used to monitor the healing process of cracked specimens as a function of time, by adopting a magnification rate of 18x in order to measure the different cracks in the specimens. Immediately after crack measurements, specimens were subjected to a 6-day healing period under controlled environmental conditions (i.e., room temperature or high-temperature). Specimens were placed horizontally over a flat surface during the healing period. Cracks were monitored using the optical microscope at healing periods of 0, 1, 2, 5 and 6 days. The study performed a digital image analysis to measure the crack width over time. The healing efficiency of the specimens at the different healing periods was calculated as follows:

$$HE = (1 - \frac{Cw_t}{Cw_0}) * 100 \qquad [2]$$

where:
HE= Healing efficiency (%);
Cw_0 = Initial Crack width, mm; and
Cw_t = Crack width at the time of analysis, mm.

Table 6. Test matrix for self-healing experiment.

Mixture	Asphalt Binder	RAS Content	RAP Content	Fiber Content	Room-Temperature (25°C)	High-Temperature (50°C)
70CO	PG 70-22	-	-	-	3 Specimens	3 Specimens
70PG5F	PG 70-22	-	-	5%	3 Specimens	3 Specimens
70PG5P	PG 70-22	5%	-	-	3 Specimens	3 Specimens
70PG5P1F	PG 70-22	5%	-	1%	3 Specimens	3 Specimens
70PG5P3F	PG 70-22	5%	-	3%	3 Specimens	3 Specimens
70PG5P5F	PG 70-22	5%	-	5%	3 Specimens	3 Specimens
70PG20RAP	PG 70-22	-	20%	-	3 Specimens	3 Specimens
70PG20RAP5F	PG 70-22	-	20%	5%	3 Specimens	3 Specimens
64CO	PG 64-22	-	-	-	3 Specimens	3 Specimens
64PG5F	PG 64-22	-	-	5%	3 Specimens	3 Specimens
64PG5P	PG 64-22	5%	-	-	3 Specimens	3 Specimens
64PG5P5F	PG 64-22	5%	-	5%	3 Specimens	3 Specimens
64PG20RAP	PG 64-22	-	20%	-	3 Specimens	3 Specimens
64PG20RAP5F	PG 64-22	-	20%	5%	3 Specimens	3 Specimens

(a) **(b)**

Figure 2. (a) Rectangular specimen obtained by sawing rectangular slab and (b) three-point bending test setup.

5. RESULTS

5.1. Synthesis and Characterization of Sodium-Alginate Fibers with a Rejuvenator as a Core Material

Sodium-alginate fibers containing a commercial rejuvenator product (Rejuvn8) were prepared. An optimization study was conducted for the developed fibers by varying the production parameters and evaluating the effects of each parameter on the thermal stability and tensile strength of the fibers. The following production parameters were varied: percentage of emulsifier, percentage of plasticizer, and amount of rejuvenator used.

5.1.1. Thermogravimetric Analysis (TGA)

The thermal stability of the produced fibers was evaluated using TGA. The evaluated parameter in TGA was the percentage weight retained at 163°C. Table 7 summarizes the TGA test results for the different sodium-alginate fibers. Control fibers, sodium-alginate fibers with no additives, were prepared and tested in order to determine the effects of each production parameter on the thermal stability of the fibers. It is shown in Table 7 that the control fibers retained 68.6% of the initial weight at the evaluated temperature. In addition, it was observed that the increase in the emulsifier content from 30 to 50% resulted in a decrease in the weight retained of the fibers as Fiber 3 had a lower weight retained than Fiber 1 and Fiber 2. A plasticizer content at a dosage rate of 10 and 40% resulted in an increase in the weight retained of the fibers compared to the dosage rates of 20 and 30% of ethylene glycol. Furthermore, it was observed that the increase of rejuvenator to shell material ratio from 1.5:1 to 3:1 resulted in the fibers with the highest weight retained of the initial weight.

5.1.2. Tensile Strength

The resistance of the developed fibers to breakage during mixing and production processes was evaluated by measuring the tensile strength of the fibers. Prior to testing, the developed fibers were aligned within a custom paper window with a window gauge length of 66 mm. Super glue was used to fix the fibers in the paper window to avoid any undesirable deformation outside of the window gauge. Furthermore, the paper window was clamped in the tensile machine using two fixed grips and the paper window was cut without any preload in the fibers. The tensile test was performed at a constant rate as shown in Figure 3(a). Figure 3(b) shows a broken sodium alginate fiber after a tensile test was performed.

Table 7 shows the results of the tensile strength test of the fibers. For each prepared fiber type, ten fibers from three different batches were tested. As shown in Table 7, Fiber 6, Fiber 7, Fiber 8, and Fiber 11 satisfied the threshold level of a tensile strength greater than 12 MPa. The UTS test results showed that an increase in the tensile strength of the fibers resulted in lower failure strain percentages as shown in Fiber 4 and Fiber 7. In addition, a relationship between stiffness and tensile strength was observed as the stiffness increased with the increase in the tensile strength of the fibers.

Table 7. Optimization test results of sodium-alginate fibers; (a) TGA results, (b) UTS test analysis.

(a)

Sample ID	Temperature (°C)	Weight Retained (%)
Fiber 1	163	76.2
Fiber 2	163	77.3
Fiber 3	163	67.3
Fiber 4	163	82.1
Fiber 5	163	77.1
Fiber 6	163	76.9
Fiber 7	163	81.5
Fiber 8	163	86.2
Fiber 9	163	87.6
Fiber 10	163	87.5
Fiber 11	163	88.1
Control	163	68.6

(b)

Sample ID	Peak Stress (MPa) Mean	Peak Stress (MPa) STDEV	Failure Strain Mean	Failure Strain STDEV	Stiffness (N/m) Mean	Stiffness (N/m) STDEV
Fiber 1	3.5	1.3	16.0%	11.5%	91.1	63.0
Fiber 2	1.3	0.3	8.4%	4.1%	22.6	7.3
Fiber 3	1.9	0.6	8.8%	4.6%	35.9	19.8
Fiber 4	11.4	6.1	24.1%	13.3%	457.9	434.7
Fiber 5	12.1	2.9	23.4%	14.0%	404.7	69.5
Fiber 6	23.0	8.1	11.1%	10.8%	1844.3	847.6
Fiber 7	28.4	3.7	4.2%	1.5%	2456.4	240.0
Fiber 8	22.7	4.1	4.8%	1.9%	1914.2	275.2
Fiber 9	9.9	1.6	12.3%	4.1%	687.1	200.4
Fiber 10	7.3	0.9	21.9%	9.8%	516.2	75.7
Fiber 11	14.7	4.2	5.2%	3.0%	1165.1	433.5

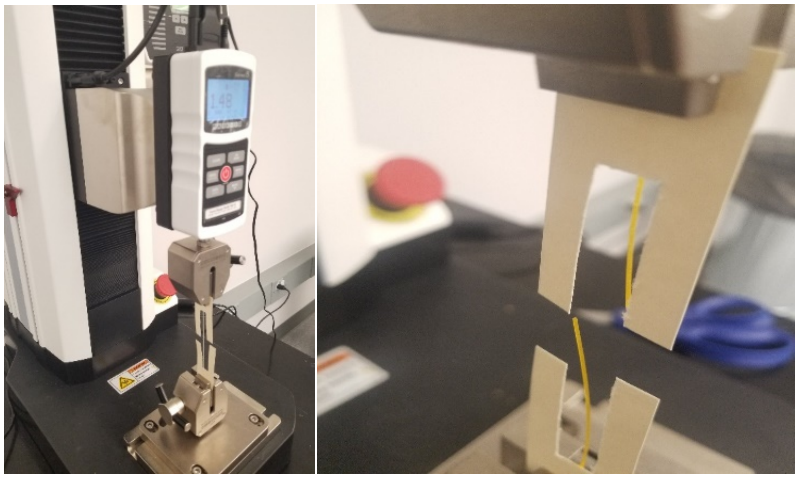

(a) **(b)**

Figure 3. (a) Tensile test setup for sodium-alginate fibers and (b) broken sodium-alginate fiber.

5.1.3. Optimum Preparation Procedure for Sodium-Alginate Fibers with Rejuvn8

Based on the results presented in Table 7 from the TGA and UTS tests, a rejuvenator to shell material ratio of 1:1.5, a 30% emulsifier content, and 40% plasticizer content were selected as the optimum production parameters for the fiber synthesis (i.e., Fibers 7). Figure 4(a) shows a Scanning Electron Microscope (SEM) image of the selected fibers. It is noticed in Figure 4(a) that the developed fibers had a rough morphology, which may help improve the bonding of the fibers with the asphalt binder. In addition, the strain-hardening property of the developed fibers is shown in the load-deformation plot obtained from the UTS test in Figure 4(b). TGA results for Fibers 7 are also shown in Figure 4(c).

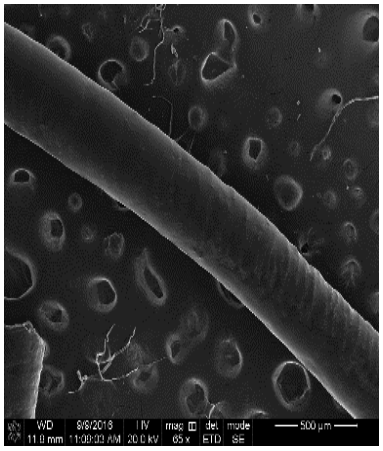

(a)

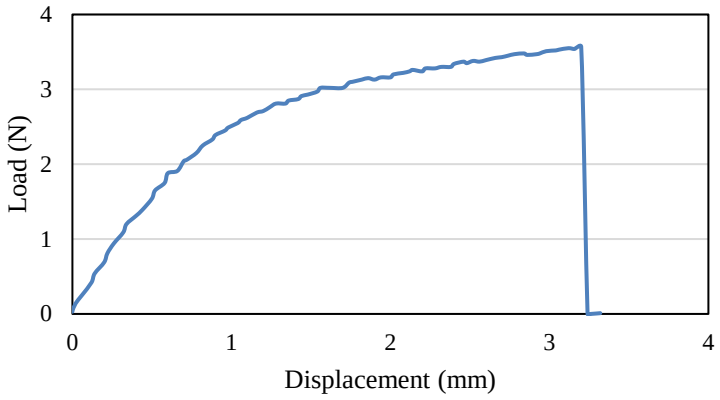

(b)

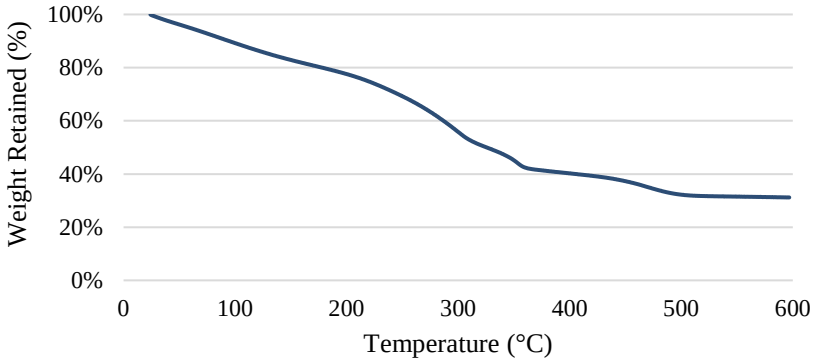

(c)

Figure 4. Fibers with optimum parameters (a) sem picture with 65x magnification, (b) uts test results, and (c) tga test results.

5.2. Self-Healing Efficiency of Sodium-Alginate Fibers in HMA Mixtures

The objective of the second experiment was to evaluate the self-healing ability of the developed sodium-alginate fibers containing a rejuvenator product. Light microscope images were obtained after inducing cracks on rectangular specimens before the healing period. The six

specimens for each selected mixture were divided into two groups: Group I was subjected to room-temperature healing condition and Group II was subjected to a temperature of 50°C utilizing a conventional oven. The initial average crack width was calculated using digital image analysis. After taking the initial crack measurements, beam specimens were subjected to the applicable environmental conditioning. The crack widths of the specimens were measured at 1, 2, 5, and 6 days during the healing period by capturing images utilizing a light microscope and based on digital image analysis.

5.2.1. Healing Quantification for HMA Mixtures with Binder PG 70-22

A self-healing experiment was conducted on the asphalt mixtures prepared with binder PG 70-22 to quantify the self-healing abilities of the developed fibers.

Effect of Sodium-Alginate Fibers in the Healing Ability of Virgin Binder PG 70-22: The healing recovery of the prepared asphalt mixtures was calculated based on Equation (1). For asphalt mixtures prepared with PG 70-22, Figure 5 shows that the healing of the conventional asphalt mixture (70CO) was equivalent to the mixture prepared with the hollow fibers (70PG5F) after 6-day of healing period at room-temperature condition. The varied amount of rejuvenator released in the different samples from mixture 70PG5F resulted in a high-variability in the healing efficiency of the mixture as shown in Figure 5.

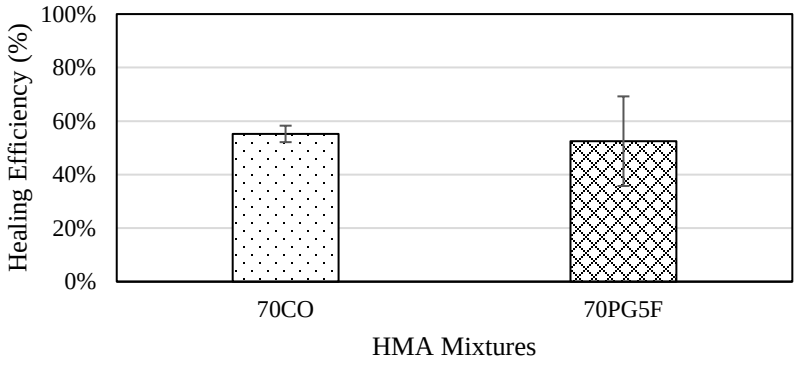

Figure 5. Healing efficiency of virgin HMA mixtures with binder PG 70-22 after 6-day of healing at room temperature.

Effect of Recycled Materials on the Healing Ability of Sodium-Alginate Fibers: The self-healing experiment was conducted on mixtures containing either RAS or RAP as recycled materials. Figure 6 shows the healing efficiency of the evaluated mixtures containing RAS with various fiber contents at room-temperature curing condition. As shown in Figure 6 the fiber content was varied from 1, 3 and 5% by weight of virgin binder to identify the optimum fiber content that enhances the self-healing ability of asphalt binders. Figure 6 shows that the addition of RAS did not have a negative effect on the healing efficiency after the 6-days healing period as it had a similar healing efficiency (i.e. 53%) as the conventional mixture 70CO, 55%. However, the addition of 1% fibers showed a slight enhancement in the healing of the mixture containing RAS by increasing the healing efficiency to 57% after the 6-days healing period. An opposite trend was observed with the addition of 3% fibers as it resulted in a negative effect on the healing efficiency with a decrease in the healing efficiency to 40% after the healing period. The highest healing efficiency was observed in the mixture with 5% fiber content (70PG5P5F) as it had a healing efficiency of 71.3% after the healing period. The variability in

the measurements may be caused by the fact that some fibers did not break during the experiment or that dispersion of the fibers was not consistent in all the mixes. However, it was found that the addition of 5% sodium-alginate fibers enhanced the healing ability of asphalt mixtures containing RAS compared to the conventional asphalt mixture with no fibers; see Figure 6.

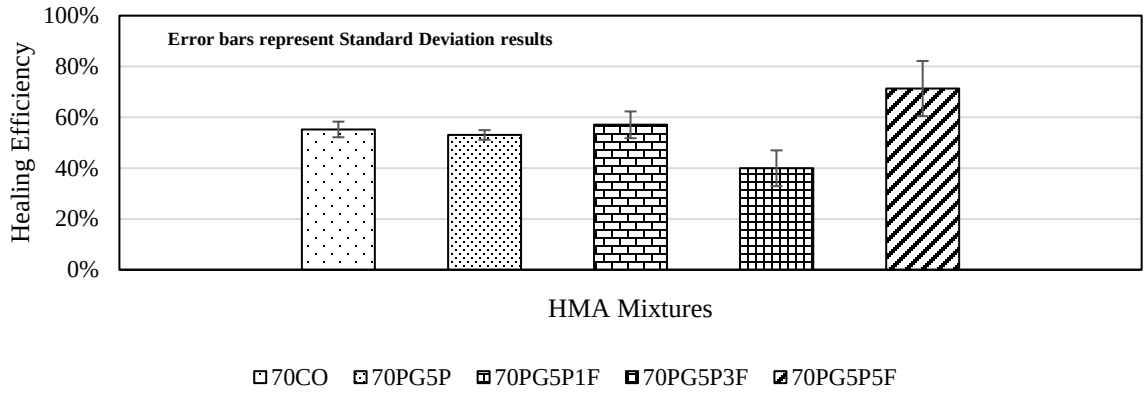

Figure 6. Healing efficiency of HMA mixtures containing RAS with binder PG 70-22.

Test results of the healing experiment at a room-temperature curing condition for asphalt mixtures containing RAP with sodium-alginate fibers are shown in Figure 7. A 5% fiber content was utilized for the mixture containing RAP based on the positive results obtained with mixtures containing RAS. Figure 7 shows that the addition of RAP resulted in an increase in the healing efficiency compared to the conventional mixture. The RAP material used in this study originated from a polymer-modified binder asphalt mixture; this could explain the enhanced healing efficiency of the mixture 70PG20RAP. In addition, Figure 7 shows that the addition of fibers did not have a positive effect on the healing efficiency as the healing efficiency decreased to 51% compared to 68.3% of the mixture containing RAP. It is possible that the fibers did not break during the experiment, which may explain the reduction in healing efficiency. In addition, a chemical reaction between the SBS-polymer in the RAP and the produced fibers could have resulted in a negative effect in the healing recovery of mixture 70PG20RAP5F.

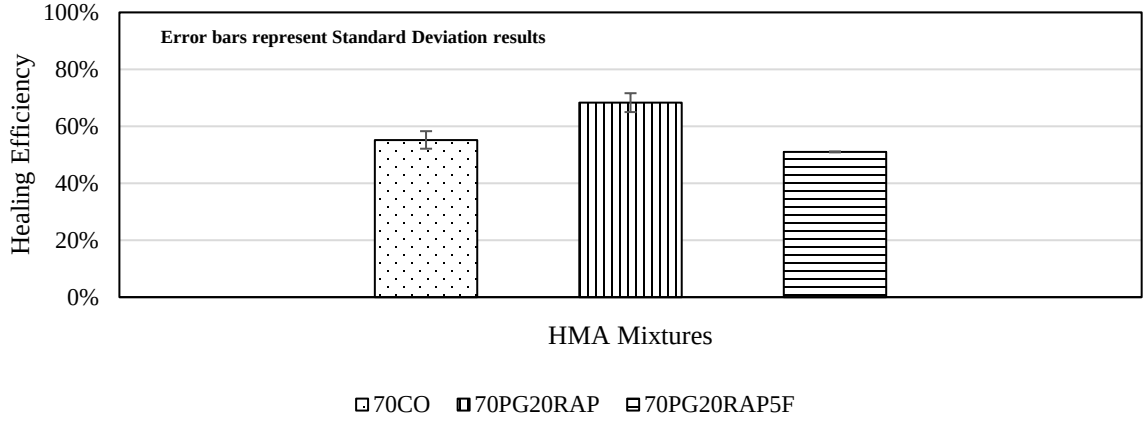

Figure 7. Healing efficiency of HMA mixtures containing RAP with binder PG 70-22.

Effect of Curing Conditions on the Healing Efficiency of Sodium-Alginate Fibers: The effect of changing the environmental curing condition from room temperature (i.e., 25°C) to high-temperature (i.e., 50°C) on the healing efficiency of sodium-alginate fibers was evaluated. The comparison between the healing efficiencies at both environmental curing conditions for mixtures is shown in Figure 8. An increase in the healing efficiency of the mixtures was expected due to the thixotropy property of asphalt binders where the viscosity of a binder decreases with the increase in temperature enhancing the self-healing ability of a binder. However, Figure 8 shows that only mixtures 70PG5F, 70PG5P and 70PG20RAP5F exhibited an improvement in the healing efficiency with high temperature curing condition. The aging taking place during the healing period at high-temperature curing condition could have affected the overall healing efficiency of the developed fibers.

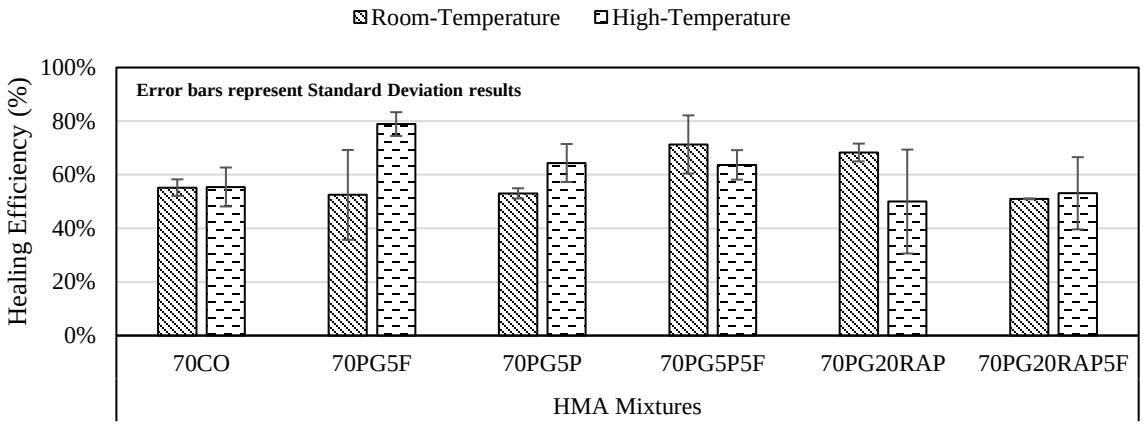

Figure 8. Effect of curing conditions in the healing efficiency of HMA mixtures with binder PG 70-22.

5.2.2. Healing Quantification for HMA Mixtures with Binder PG 64-22

In this phase of the study, a self-healing experiment was conducted on the asphalt mixtures prepared with unmodified binder PG 64-22 to assess the self-healing properties of the synthesized fibers.

Effect of Sodium-Alginate Fibers in the Healing Ability of Virgin Binder PG 64-22: Figure 9 shows that the addition of sodium-alginate fibers decreased the healing recovery for the asphalt mixture prepared with the unmodified binder PG 64-22 after the 6-day healing period as compared to the conventional mixture 64CO after 6-day of healing period at room-temperature.

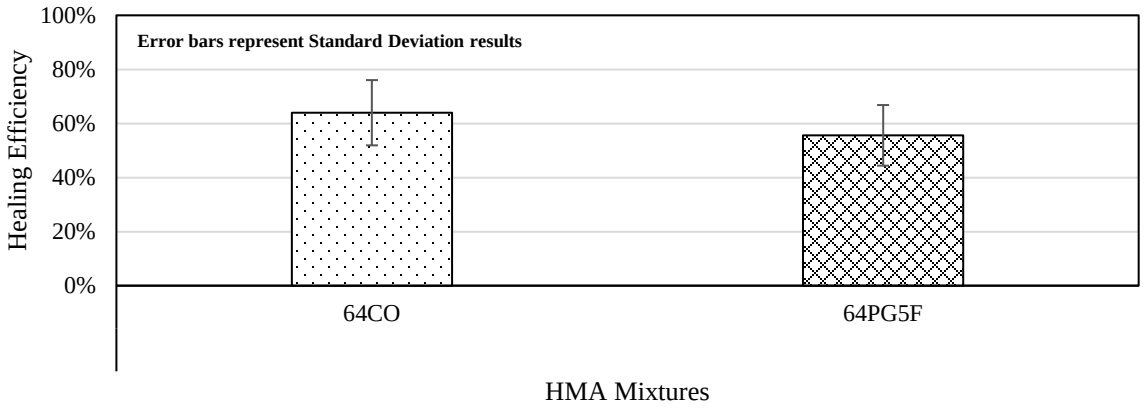

Figure 9. Healing efficiency of virgin HMA mixtures with binder PG 64-22.

Effect of the Type of Recycled Materials on the Healing Ability of Sodium-Alginate Fibers: Figure 10 shows the healing efficiency of the evaluated mixtures containing RAS with binder PG 64-22 at room-temperature curing condition. As shown in Figure 10, the conventional mixture 64CO had the highest healing efficiency after the 6-days healing period. The higher healing efficiency of the conventional mixture 64CO compared to mixture 70CO suggests that the difference in viscosity of the two binders at room temperature affected the healing capacity of the binder. In addition, it was observed that the addition of RAS resulted in a reduction in the healing efficiency of mixture 64PG5P. The aged binder from RAS had a more pronounced negative effect on the softer binder PG 64-22 compared to the mixture containing RAS with binder PG 70-22. Furthermore, Figure 10 shows that the addition of 5% sodium-alginate fibers slightly improved the healing efficiency compared to mixture 64PG5P by increasing the healing efficiency from 44.6% to 48.5%. The increase in healing efficiency with the addition of fibers suggested a partial recovery of the healing ability lost due to the addition of stiffer and brittle materials from RAS.

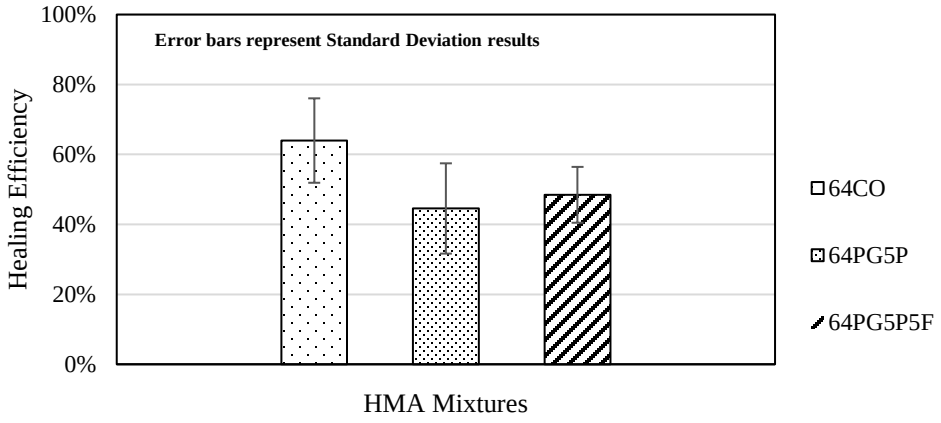

Figure 10. Healing efficiency of HMA mixtures containing RAS with binder PG 64-22 at room temperature.

Test results of the healing experiment at a room-temperature curing condition for HMA mixtures containing RAP with binder PG 64-22 are shown in Figure 11. Contrary to the behavior in the mixture with PG 70-22, the addition of RAP resulted in a decrease in the healing efficiency of the mixture 64PG20RAP. The softer binder PG 64-22 could have been more susceptible to the aged binder from RAP causing the negative effect on the healing efficiency. However, it was also observed that the addition of 5% sodium-alginate fibers resulted in an improvement in the healing efficiency of mixture 64PG20RAP5F with a similar healing ability than the conventional mixture 64CO. The positive effect of the fibers in the healing efficiency of mixture 64PG20RAP5F suggests that some fibers were broken during the 3PB tests releasing the rejuvenator product, and thus improving the flow of the binder around the crack.

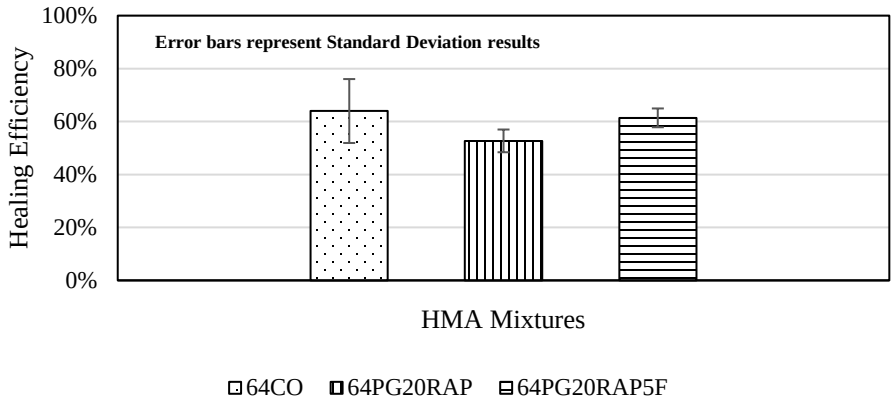

Figure 11. Healing Efficiency of HMA Mixtures containing RAP with Binder PG 64-22 at Room Temperature.

Effect of Curing Conditions on the Healing Ability of Sodium-Alginate Fibers: The asphalt mixtures with binder PG 64-22 were exposed to two different environmental curing conditions to evaluate the effect of temperature on the healing ability of the developed fibers. The two different environmental curing conditions were as follows: room temperature (i.e., 25°C) and high temperature (i.e., 50°C). The comparison between the healing efficiencies at both environmental curing conditions for mixtures with binder PG 64-22 is shown in Figure 11. As previously mentioned, higher healing efficiencies were expected at higher temperatures based on the thixotropic property of asphalt binders. Figure 11 shows that all the evaluated mixtures had a higher healing efficiency at a high-temperature curing condition compared to the room-temperature curing condition. Yet, the improvement was within the test variability. The positive effect of adding sodium-alginate fibers was also observed in mixtures 64PG5F and 64PG5P5F. Yet, the conventional mixture had the highest healing efficiency with 66.9%. Figure 11 shows that the difference in performance between the conventional mixture and mixture containing RAS with fibers was reduced with the increase in temperature during the healing period. Lastly, Figure 11 shows that the exposure to high-temperature reversed the positive effect of adding fibers as the healing efficiency for mixture 64PG20RAP5F decreased from 61.4% to 53.4%.

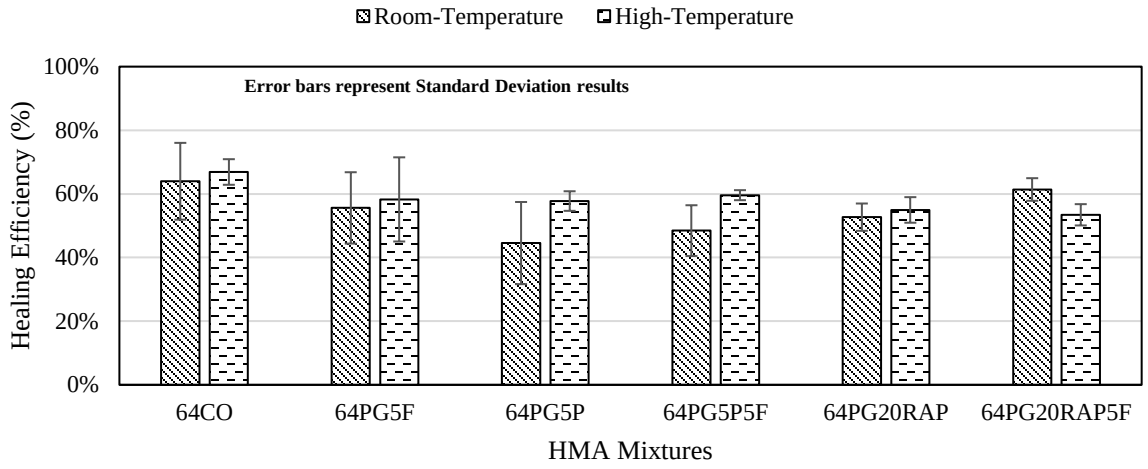

Figure 11. Effect of curing conditions in the healing efficiency of HMA mixtures with binder PG 64-22.

5.2.3. Optimum Parameters to Enhance Healing/Rejuvenation with Sodium-Alginate Fibers

Based on the self-healing experiment performed for mixtures with polymer-modified binders, the addition of sodium-alginate fibers may enhance the healing efficiency of asphalt mixtures when the fibers are added to mixtures containing RAS and the damaged specimens are healed at room temperature. For mixtures with unmodified binders, the developed fibers could enhance the healing efficiency of mixtures containing RAS when the mixes are exposed to a high-temperature during the healing period.

5.3. Strength Recovery Properties of Sodium-Alginate Fibers in HMA Mixtures

In addition to evaluate the healing efficiency of HMA mixtures, a comparison between the strength of beam specimens at different conditions (undamaged, damaged, and healed) was conducted. The strengths at the different conditions were conducted using 3-point bending tests at a deformation rate of 0.5 mm/min. The strength in the undamaged condition was defined as the strength (i.e. peak load) of the first 3-point bending test performed for a beam specimen. The strength in the damaged condition was the peak load of a second 3-point bending test performed right after the first 3-point bending test. In addition, a third 3-point bending test was performed on the beam specimens after the 6-days healing period to determine the strength of the specimens after healing. The strength recovery efficiency in the different conditions was calculated as follows:

$$S_e = (1 - \frac{S_0 - S_t}{S_0}) * 100 \qquad [3]$$

where:
S_e = Strength Recovery efficiency (%);
S_0 = Strength in undamaged condition, kN; and
S_t = Strength in damaged or healed condition, kN.

5.3.1. Strength Recovery for HMA Mixtures with Binder PG 70-22

In this phase of the study, the strength recovery analysis was conducted on the asphalt mixtures prepared with binder PG 70-22 to determine the effect of sodium-alginate fibers on the strength recovery of asphalt mixtures before and after the healing period.

Effect of Sodium-Alginate Fibers in the Strength Recovery Ability of Virgin Binder PG 70-22: The strength recovery of the prepared asphalt mixtures was calculated based on Equation (3). For asphalt mixtures prepared with PG 70-22, Figure 12 shows that the strength recovery of the conventional asphalt mixture (70CO) was equivalent to the mixture prepared with the hollow fibers (70PG5F).

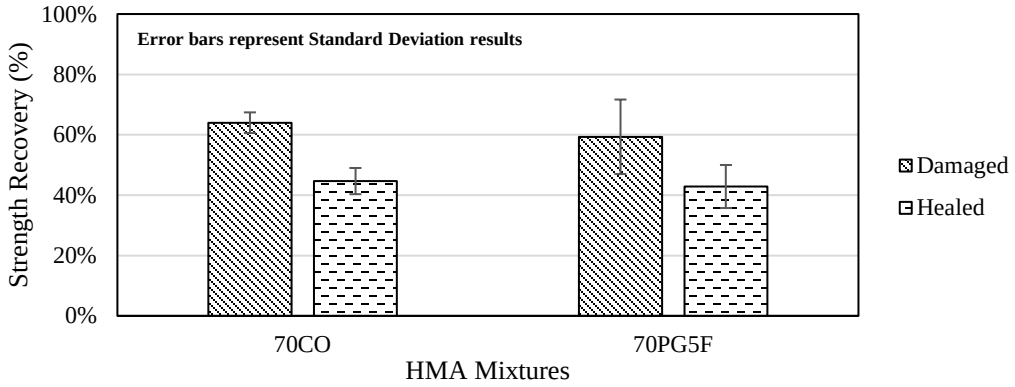

Figure 12. Strength recovery of HMA mixtures containing sodium-alginate fibers with binder PG 70-22.

Effect of Recycled Material on the Strength Recovery Ability of Sodium-Alginate Fibers: The self-healing experiment was conducted in mixtures containing either RAS or RAP as recycled materials. Figure 13 shows the strength recovery of the evaluated mixtures containing RAS at room-temperature curing condition. Figure 13 shows that the addition of RAS did not have a negative impact on the strength recovery of mixture 70PG5P in the damaged state compared to mixture 70CO. However, it is shown in Figure 13 that the strength recovery of mixture 70PG5P was lower than the conventional mixture 70CO after the healing period. The difference in the virgin binder content between mixtures 70CO and 70PG5P could explain the difference in strength recoveries after the healing period. Figure 13 also shows that the mixture containing fibers (70PG5P5F) had a lower strength recovery in both damaged and healed conditions than the mixture containing RAS. The brittle behavior of the binder in the RAS material could explain the difference in strength recoveries after the healing period. In addition, the decrease in the strength recovery of the mixture with fibers in both damaged and healed conditions could be due to the release of the rejuvenator product during the first 3PB test causing softening of the binder. The binder softening caused by the release of the rejuvenator in the early stages of the self-healing experiment could also explain the high healing efficiency of mixture 70PG5P5F observed in Figure 6.

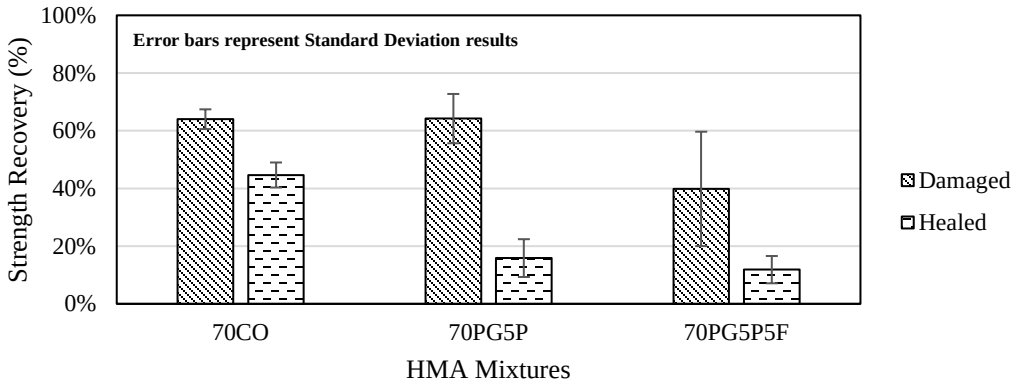

Figure 13. Strength recovery of HMA mixtures containing RAS with binder PG 70-22 at room temperature.

Test results of the strength recovery analysis at room-temperature curing condition for asphalt mixtures containing RAP are shown in Figure 14. The addition of RAP resulted in a more brittle mixture compared to the conventional mixture as mixtures 70PG20RAP and 70PG20RAP5F were more susceptible to fracture as interpreted from the decrease in strength recoveries as compared to mixture 70CO. However, Figure 14 shows that the addition of the fibers (70PG20RAP5F) had a positive effect on the thixotropic property of the binder as a higher strength recovery was observed after the healing period. Based on these results, one may postulate that the 3PB tests performed during the experiment did not break the fibers, as the induced cracks did not pass through them. In this case, the fibers acted as a reinforcement more than as a rejuvenator for mixture 70PG20RAP5F.

Effect of Curing Conditions on the Strength Recovery of Sodium-Alginate Fibers: The effect of changing the environmental curing condition from room temperature (i.e., 25°C) to high-temperature (i.e., 50°C) in the strength recovery ability of sodium-alginate fibers was evaluated. The comparison between the strength recoveries after the 6-days healing period at both environmental curing conditions for mixtures prepared with modified binder PG 70-22 is presented in Figure 15. Figure 15 shows that the increase in temperature enhanced the strength recovery of the evaluated asphalt mixtures. It is shown that the conventional mixture containing sodium-alginate fibers (70PG5F) exhibited a 100% strength recovery at high-temperature curing condition. The higher strength ratios for the beam specimens is due to the high temperature curing condition, which enhanced the flow of the binder and the healing of the cracks.

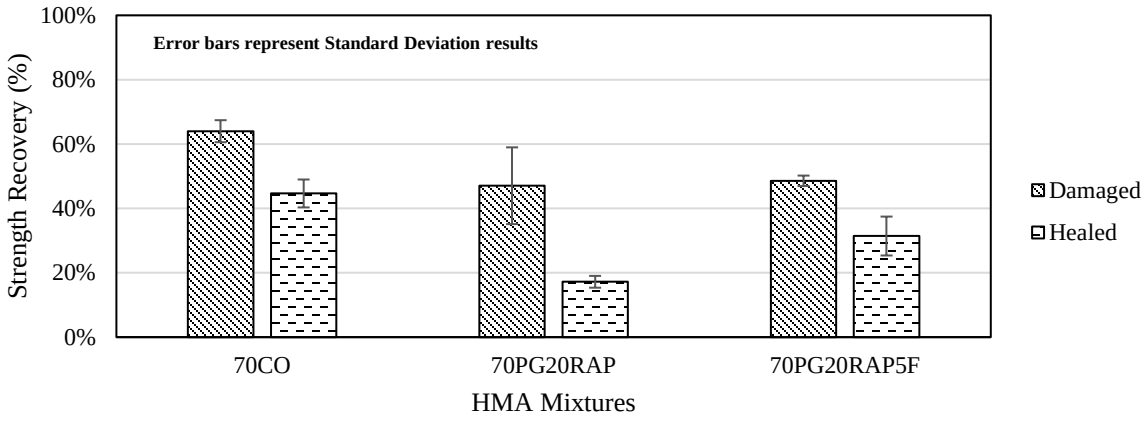

Figure 14. Strength recovery of HMA mixtures containing RAP with binder PG 70-22.

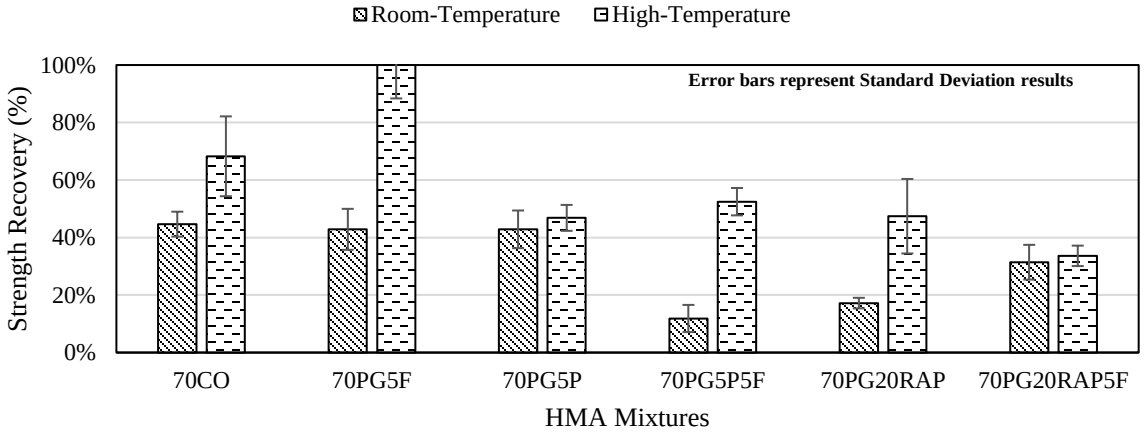

Figure 15. Effect of curing conditions in the strength recovery of HMA mixtures with binder PG 70-22.

5.3.2. Strength Recovery for HMA Mixtures with Binder PG 64-22

In this part of the study, a strength recovery analysis was performed on the asphalt mixtures prepared with binder PG 64-22 from to determine the strength recovery ability of the developed fibers.

Effect of Sodium-Alginate Fibers on the Strength Recovery Ability of Virgin Binder PG 64-22: Figure 16 shows that the addition of sodium-alginate fibers enhanced the strength recovery for the asphalt mixture prepared with the unmodified binder PG 64-22 after the 6-day healing period as compared to the conventional mixture 64CO. The difference between the two binders may be due to a chemical interaction between the polymer in the PG 70-22 binder and the sodium-alginate hollow fibers.

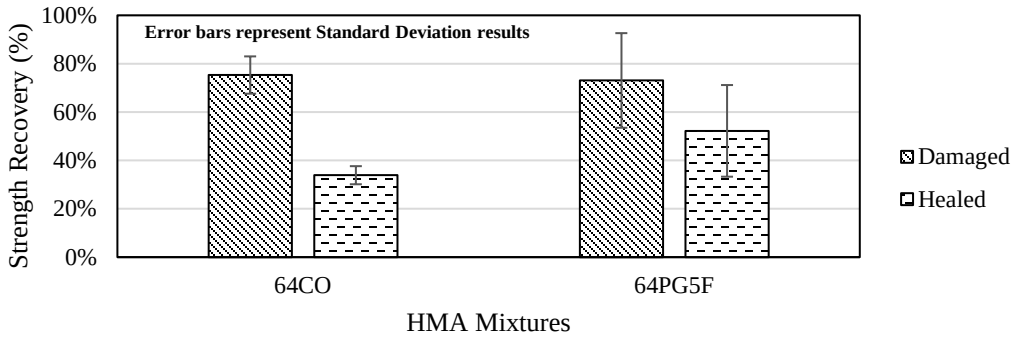

Figure 16. Strength recovery of HMA mixtures containing sodium-alginate fibers with binder PG 64-22.

Effect of the Type of Recycled Material on the Strength Recovery Ability of Sodium-Alginate Fibers: Figure 17 shows the strength recoveries in both the damaged and healed conditions of the evaluated mixtures containing RAS with binder PG 64-22 at room-temperature curing condition. As shown in Figure 17, RAS had a negative effect on the strength recovery in the healed condition as the conventional mixture 64CO had a higher strength recovery after the 6-days healing period. Based on the enhanced healing efficiency of mixture 64PG5P5F, a reduction in the strength recovery was anticipated due to the softening of the rejuvenator. However, Figure 16 also shows that the mixture containing fibers (64PG5P5F) had a similar strength recovery in both the damaged and healed conditions than the mixture containing RAS.

The test results of the strength recovery analysis at room-temperature curing condition for HMA mixtures containing RAP with binder PG 64-22 are shown in Figure 18. The reduction in the strength recoveries for the damaged and healed conditions with the addition of RAP was also observed for the mixtures with binder PG 64-22. A similar trend was observed in Figure 18, which shows that an increase in the healing efficiency of a mixture containing fibers would result in a decrease in the strength recovery due to the softening effect of the rejuvenator product as observed in mixture 64PG20RAP5F. Similar to mix 70PG5P5F, the fibers did not break during the experiment and acted as a reinforcement enhancing the strength recovery of mixture 64PG20RAP5F after the 6-day healing.

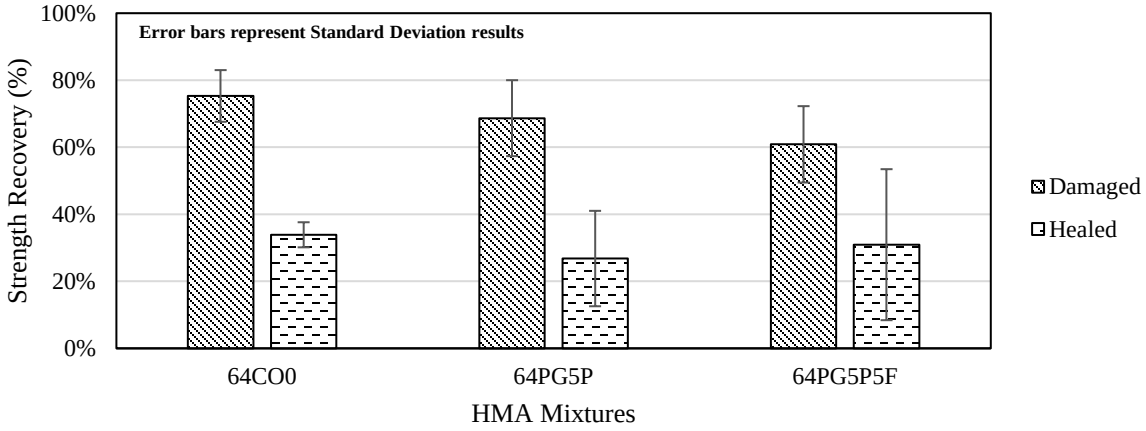

Figure 17. Strength recovery of HMA mixtures containing RAS with binder PG 64-22 at room temperature.

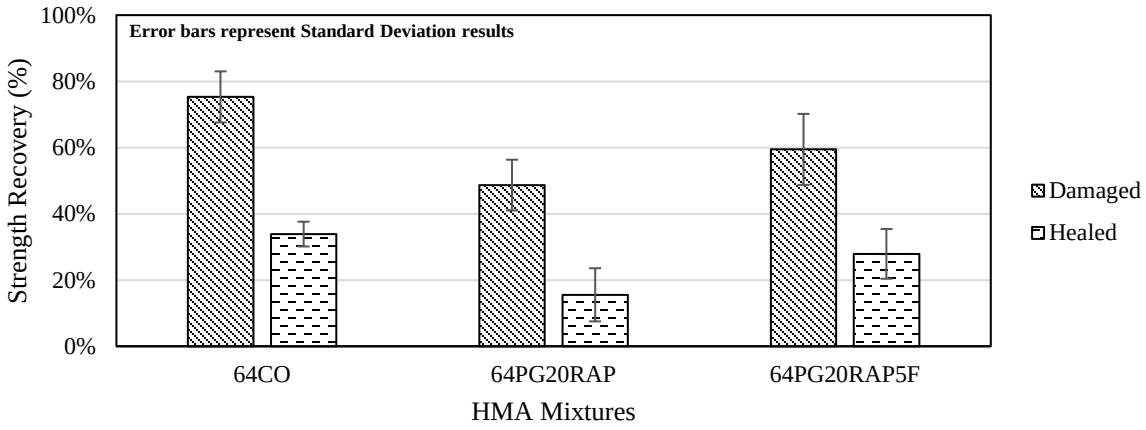

Figure 18. Strength recovery of HMA mixtures containing RAP with binder PG 64-22 at room temperature.

Effect of Curing Conditions on the Strength Recovery Ability of Sodium-Alginate Fibers: The comparison between the strength recoveries after the 6-days healing period at both environmental curing conditions for mixtures with binder PG 64-22 is shown in Figure 19. Similar to the trends observed for the PG 70-22 binder, the conventional mixture with fibers, 64PG5F, had the highest strength recovery at high-temperature curing condition after 6-day of healing period. In addition, it is shown that the mixture containing sodium-alginate fibers had the best strength recovery at the high-temperature curing condition.

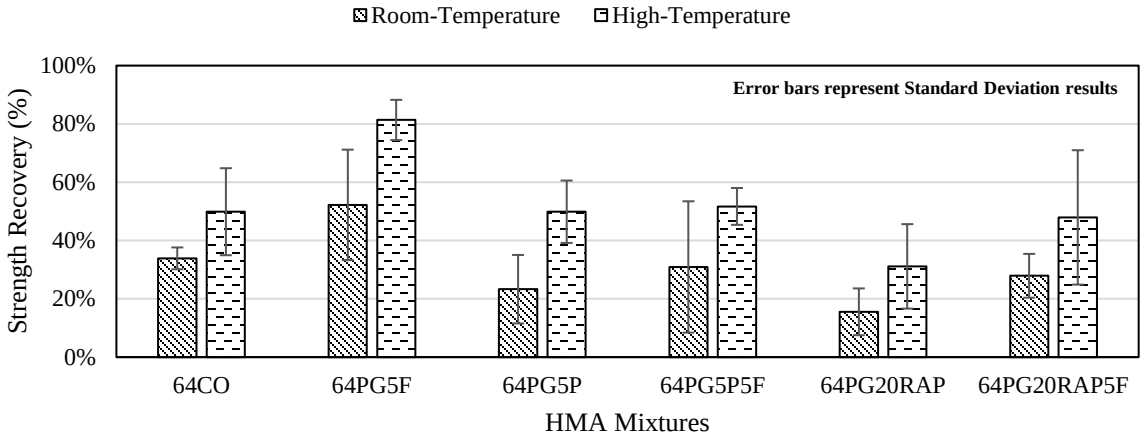

Figure 19. Effect of curing conditions in the strength recovery of HMA mixtures with binder PG 64-22.

5.4. Validation of the Optimum Fiber Content for Binder Blends and Asphalt Mixtures

A binder test and a mixture test were performed to validate the optimum fiber content determined from the self-healing experiment. A MSCR test was performed to evaluate the effect of increasing the content of the developed fibers from 1 to 5% by weight of virgin binder on the performance of the evaluated binder blends against permanent deformation. The MSCR test results for the optimization process are shown in Table 8 suggests that the addition of

extracted binder from RAS improved the rutting susceptibility of the virgin binder by decreasing the non-recoverable creep compliance (J_{nr}). J_{nr} is a measure of the amount of residual strain left in the binder after repeated creep and recovery, relative to the amount of stress applied. Thus, a reduction in the J_{nr} indicates a decrease in the rutting susceptibility of a binder. In addition, MSCR test results showed that the addition of 5% fiber content resulted in similar J_{nr} values compared with blend 70PG5P at both stress levels. Although a decrease in the (J_{nr}) was observed in the blends with RAS and fibers, the percentage recovery of the blends decreased at both stress levels compared to the virgin binder. The reduction in the percentage recovery could be related to the lack of time to fully recover due to the time-dependent behavior of asphalt binders. Overall, MSCR test results suggest that the addition of 5% of sodium-alginate fibers and extracted binder from RAS resulted in an improved performance against permanent deformation compared to a conventional binder PG 70-22.

Table 8. MSCR test results for optimization of fiber content.

Binder Blends	$J_{nr0.1}$ @ 67 °C, kPa^{-1}	$J_{nr3.2}$ @ 67 °C, kPa^{-1}	$\%J_{nr}$ diff	% Recovery Stress, 0.1 kPa	% Recovery Stress, 3.2 kPa
70CO	0.803	1.195	48.82%	49.10%	30.17%
70PG5P	0.636	0.899	41.52%	45.47%	28.36%
70PG5P1F	0.667	0.901	35.08%	40.85%	25.12%
70PG5P3F	0.736	1.035	41.06%	42.28%	24.86%
70PG5P5F	0.662	0.952	43.69%	42.40%	24.10%

The SCB test was also performed on asphalt mixtures from Table 2 to validate the optimum fiber content determined from the self-healing experiment. The SCB test at intermediate temperature was performed to evaluate the effect of the developed fibers on the fracture resistance of the evaluated asphalt mixtures. Figure 20 shows the critical strain energy release rate (J_c) for the evaluated mixtures. The results indicated that the addition of 5% PCWS adversely affected the intermediate fracture properties as compared to the control mixture as the J_c-value decreased from 0.64 kJ/m^2 to 0.45 kJ/m^2. However, the addition of 5% fibers improved the intermediate fracture properties as the J_c-value increased from 0.45 kJ/m^2 to 0.55 kJ/m^2 suggesting an improved resistance against fracture. The combination of MSCR and SCB test results showed not only an improvement in the rutting susceptibility of a virgin binder with the addition of extracted binder from RAS and 5% fiber content, but also a recovery in the fracture properties of the evaluated asphalt mixture compared with the mixture containing RAS without sodium-alginate fibers. Therefore, 5% fiber content was used to evaluate the effect of adding the developed fibers on the rheological properties of binder blends and on the mechanical properties of asphalt mixtures.

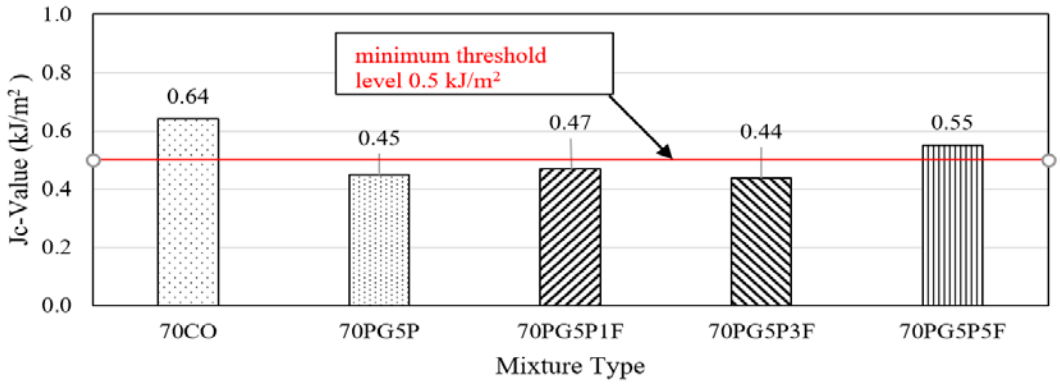

Figure 20. Effect of fiber content in the fracture resistance of asphalt mixtures.

5.5. Chemical Analysis of Binder Blends with Fibers

5.5.1. Molecular Weight Distribution

HP-GPC was used to measure asphalt blends molecular weight distributions, i.e., the percentage of asphaltenes to maltenes that are present in the binder bends. Determining the percentage of asphaltenes and maltenes before and after blending the virgin binders with recycled materials and fibers provided information about the efficiency of the fibers to act as a rejuvenator. The HP-GPC results for binder blends prepared with Binder PG 70-22 are shown in Table 9. The maltenes, Low-Molecular Weight (LMW), were defined as the molecules with a weight less than 3k Daltons; asphaltenes, High-Molecular Weight (HMW), were defined as the molecules between 3k and 19k Daltons; polymer and other components, were defined as the molecules with weight greater than 19k Daltons *(27)*. Table 9 shows that the extracted binders from RAS and RAP had the highest high-molecular weight/ low-molecular weight ratio (HMW/LMW) among the evaluated binder blends. Furthermore, it is shown in Table 9 that the addition of sodium-alginate fibers resulted in an increase in the HMW/LMW ratio. The increase of the HMW fraction suggests that some of the fibers, which are polymers, caused the increase in the HMW/LMW ratios.

Table 9. Chemical composition of evaluated binder blends.

Sample	Others	HMW	LMW	HMW/LMW Ratio
70CO	4.92%	21.73%	73.35%	0.30
70PG5P	6.42%	22.82%	70.76%	0.32
70PG5P5F	6.71%	23.33%	69.59%	0.34
70P20RAP	6.28%	23.73%	70.26%	0.34
70PG20RAP5F	5.38%	26.19%	70.89%	0.37
70PG5P20RAP	6.81%	22.31%	70.89%	0.31
70PG5P20RAP5F	6.7%	21.96%	71.34%	0.31
64CO	0.52%	17.35%	82.13%	0.21
64PG5P	1.82%	23.63%	74.55%	0.32
64PG6P5F	1.9%	24.8%	73.3%	0.34
64PG20RAP	3.44%	25.35%	71.21%	0.36
64PG20RP5F	3.33%	23.46%	70.89%	0.33
64PG5P0RAP	3.83%	23.94%	72.23%	0.33
64PG5P20RAP5F	4.14%	24.61%	71.2%	0.35
RAS	8.1%	26.69%	65.21%	0.41
RAP	13.31%	30.31%	56.38%	0.54

5.5.2. Characterization of Oxidative Asphalt Aging

The carbonyl Index (ICO) was calculated to evaluate the formation of carbonyl molecules in the binder blends, which is related to the oxidation process in the aging process of asphalt binders. Figure 21 shows that the addition of extracted binder from either RAS and/or RAP resulted in an increase in the ICO index. Also, it is shown that the addition of fibers in blends containing recycled materials resulted in an increase in the ICO, which suggests that the rejuvenating product facilitates the extraction of aged binder from the recycled materials and thus, increased the asphaltene content leading to stiffer blends.

Figure 22 shows that the overall ICO indices for blends prepared with binder PG 70-22 were higher than the ICO index for blends prepared with binder PG 64-22. The higher ICO indices suggest that binder PG 70-22 would be more susceptible to aging compared to a softer binder such as PG 64-22. In addition, a similar trend was observed with the addition of fibers as the ICO index increased compared to the blends containing recycled materials, which confirms the increase in the HMW/LMW ratios observed in the HP-GPC test results.

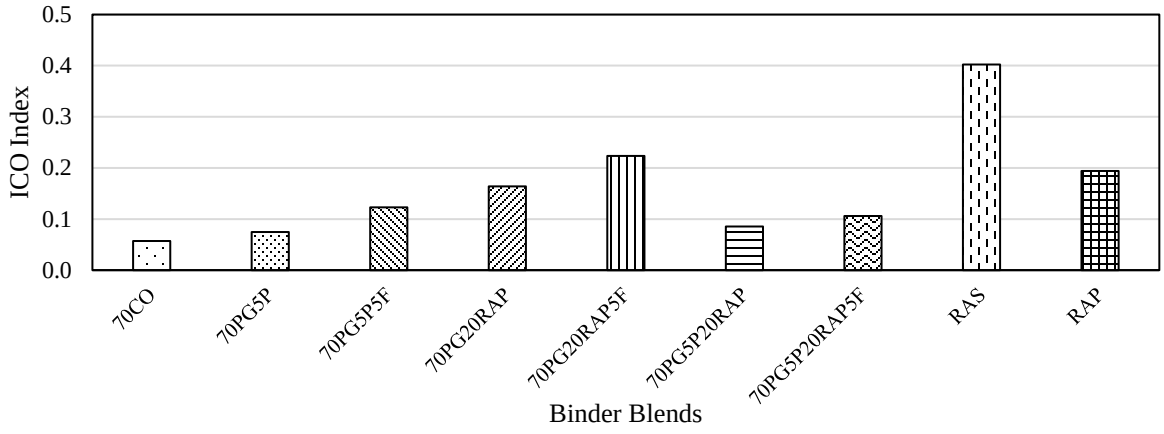

Figure 21. ICO aging index for binder PG 70-22.

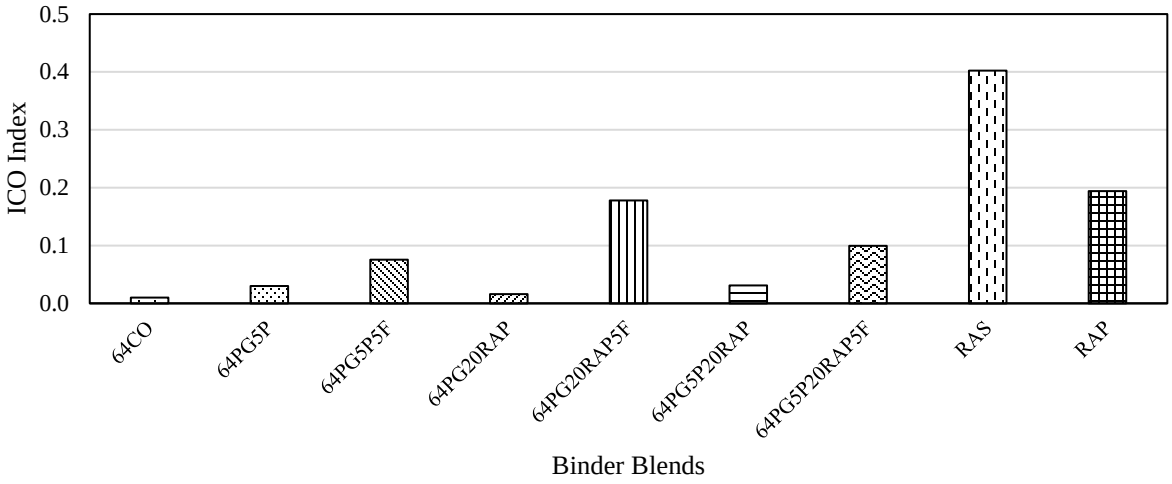

Figure 22. ICO aging index for binder PG 64-22.

5.6. Rejuvenation of Asphalt Binders with Sodium-Alginate Fibers

Twenty asphalt binder blends were prepared and evaluated in this study to assess the effects of adding sodium-alginate fibers containing a rejuvenating product on the rheological properties of the blends. In addition, extracted binder from recycled materials (i.e., PCWS and/or RAP) was added at different percentages of the virgin binder. A Silverson mechanical stirrer was used at 3,600 rpm for 30 minutes and at a mixing temperature of 163°C to achieve good mixing and dispersion of the fibers and extracted binder in the asphalt binder blends. It is noted that the length of the fibers was less than 1 mm, which did not affect the rheological testing procedure of the prepared asphalt binder blends.

5.6.1. PG Grading of Binder Blends

Table 10 presents the measured PG Grading of the asphalt binder blends prepared with binder PG 70-22 based on laboratory testing conducted using a Dynamic Shear Rheometer (DSR) and Bending Beam Rheometer (BBR). Table 10 shows that the addition of the hollow fibers did not change the PG grading of the virgin binder, 70CO; yet, a decrease in the low-temperature performance grade (LTPG) was observed with the addition of 3, 5 and 10% fiber contents compared to the virgin binder. The same decrease in the LTPG was observed in the binder blends 70PG5P5F and 70PG20RAP5F with the addition of hollow fibers.

Table 10 also shows that the addition of the extracted binder from PCWS and/or RAP resulted in an increase in the PG grading compared to the virgin binder from PG 70-22 to PG 76-22 (70PG5P); PG 82-16 (70PG20RAP); and PG 88-16 (70PG5P20RAP). The increase in the high temperature grade of the binder blends containing recycled materials may be due to the increase in asphaltene contents from the recycled materials as observed in the HP-GPC test results. Based on the PG grading results, the addition of the developed fibers did not seem to enhance the final PG of the binder blends except for blend 70PG5P20RAP5F. Yet, the marginal effect of the hollow fibers on the PG grading of the binder blends was expected based on the increase in HMW/LMW ratios and ICO Index on the chemical analysis test results. However, the continuous PG showed a reduction in the HTPG in the binder blends containing the hollow fibers, which may indicate a softening effect of the aged binders from recycled materials except for 70PG5P5F.

Table 10. Summary of PG grading results for binder PG 70-22.

Binder Blend	PG-Grading	Continuous PG-Grading
70CO	70-22	73.8-27.4
70PG3F	70-22	73.3-24.4
70PG5F	70-22	73.7-23.2
70PG10F	70-22	73.3-24.5
70PG5P	76-22	78.2-25.3
70PG5P5F	76-22	79.7-24.1
70PG20RAP	82-16	87.3-21.9
70PG20RAP5F	82-16	85.4-20.4
70PG5P20RAP	88-16	88.8-18.2
70PG5P20RAP	82-16	85.9-20.6

The results of the PG grade for the binder blends prepared with binder PG 64-22 are presented in Table 11. Similar to the results of PG 70-22, the addition of the hollow fibers did not change the PG grade of the binder blends prepared with PG 64-22 except for 64PG5P20RAP5F, which

was the stiffest binder blend. The PG grading of blend 64PG5P20RAP5F could be correlated with the HP-GPC test results as this blend had the second highest HMW/LMW ratio for blends prepared with PG 64-22 as shown on Table 9. However, similar to binder PG 70-22, the continuous PG showed a reduction in the HTPG for the binder blends containing the hollow fibers, which may indicate softening of the aged binders. Also, it was noted in the continuous PG grading that the LTPG improved in the binder blends with sodium-alginate fibers, which may indicate an improvement in the low-temperature performance of the binder blends containing only extracted binder from recycled materials.

Table 11. Summary of PG grading results for binder PG 64-22.

Binder Blend	PG-Grading	Continuous PG-Grading
64CO	64-22	68-23.6
64PG3F	64-22	68-24.4
64PG5F	64-22	69.5-23.8
64PG10F	64-22	67-23.7
64PG5P	70-22	71.8-22.3
64PG5P5F	70-22	70.3-22.6
64PG20RAP	76-16	81.8-16.8
64PG20RAP5F	76-16	80.8-19.4
64PG5P20RAP	76-16	81.8-18.0
64PG5P20RAP5F	82-16	82.4-18.0

5.6.2. MSCR of Binder Blends

The MSCR test results for binder PG 70-22 are shown in Table 12 It is shown in Table 12 that the addition of 3 and 5% fiber content increased the rutting susceptibly as the non-recoverable creep compliance increased and the percentage of recovery decreased compared to the virgin binder 70CO. However, it can be observed that the addition of 10% fiber content enhanced the rutting performance as the non-recoverable creep compliance decreased compared to the virgin binder. In addition, Table 12 shows that the addition of extracted binder from recycled materials improved the rutting resistance of the virgin binder (70CO) as the non-recoverable creep compliance values decreased at both stress levels and an improvement in the percentage of recovery was also observed. The increase in the non-recoverable creep compliance of the binder blends containing recycled materials with the addition of the hollow-fibers suggests a release of the rejuvenator product from the fibers during the blending process, which is supported by the increase in the HMW/LMW ratios and ICO Index observed in the chemical analysis test results shown in Table 9 and Figure 21.

Table 12. MSCR test results for binder PG 70-22.

Asphalt Binder Blends	$J_{nr0.1}$ @ 67 °C, kPa^{-1}	$J_{nr3.2}$ @ 67 °C, kPa^{-1}	$\%J_{nr}$ diff	% Recovery Stress, 0.1 kPa	% Recovery Stress, 3.2 kPa
70CO	0.80	1.20	48.82	49.10	30.17
70PG3F	1.15	1.59	55.15	32.95	14.78
70PG5F	1.02	1.42	38.38	35.20	16.82
70PG10F	0.66	0.88	32.67	38.60	22.40
70PG5P	0.64	0.90	41.52	45.47	28.36
70PG5P5F	0.66	0.95	43.69	42.40	24.10
70PG20RAP	0.20	0.26	31.58	59.54	48.75
70PG20RAP5F	0.24	0.32	31.97	53.55	41.65
70PG5P20RAP	0.13	0.18	31.38	63.57	53.78
70PG5P20RAP	0.26	0.36	34.89	55.13	42.34

The MSCR test results for binder PG 64-22 are shown in Table 13. Similar to binder PG 70-22, the binder blends containing extracted binder from recycled materials showed a decrease in the non-recoverable creep compliance and an increase in the percentage recovery, which indicate an improved rutting resistance compared to the virgin binder PG 64-22. Also, a softening effect from the release of the rejuvenating product from the hollow fibers was observed in Table 13 as noted from the increase in the non-recoverable creep compliance. The reduction in the percentage recovery of the blends containing sodium-alginate fibers could be related to the lack of time to fully recover due to the time-dependent behavior of asphalt binders.

Overall, MSCR test results suggest that the addition of sodium-alginate fibers and extracted binder from recycled materials resulted in an improved performance against permanent deformation compared to the conventional virgin binder.

Table 13. MSCR Test Results for Binder PG 64-22.

Asphalt Binder Blends	$J_{nr0.1}$ @ 67 °C, kPa^{-1}	$J_{nr3.2}$ @ 67 °C, kPa^{-1}	$\%J_{nr}$ diff	% Recovery Stress, 0.1 kPa	% Recovery Stress, 3.2 kPa
64CO	3.47	3.77	8.65	1.62	-0.50
64PG3F	3.76	4.11	9.15	1.26	-0.72
64PG5F	3.63	4.00	10.49	1.85	-0.65
64PG10F	4.36	4.85	11.25	1.44	-1.04
64PG5P	2.32	2.60	12.31	4.86	0.58
64PG5P5F	2.54	2.89	13.90	4.99	0.42
64PG20RAP	0.43	0.49	15.00	21.80	13.59
64PG20RAP5F	0.51	0.59	43.12	20.85	11.86
64PG5P20RAP	0.45	0.51	15.93	22.36	13.17
64PG5P20RAP5F	0.38	0.45	16.18	24.41	14.82

5.6.3. Linear Amplitude Sweep

Figure 23 shows the LAS test results for binder blends prepared with PG 70-22. Based on the equation of the fatigue law, a higher "A" parameter indicates an increase in fatigue life, while a higher "B" parameter indicates a decrease in fatigue life at a constant A. Figure 23(a) shows that the addition of hollow fibers to the virgin binder resulted in a decrease in the "A" parameter, which indicates a reduction in the elastic behavior of the binder. Interestingly, it is shown that the addition of extracted binder from RAS enhanced the resistance to damage in blend 70PG5P compared to the virgin binder. The enhancement in the "A" parameter with the addition of RAS could be due to the presence of polymer in the RAS source as shown in Table 9. The opposite behavior was observed with the addition of RAP as the "A" parameter decreased dramatically compared to the virgin binder. The sampled RAP in this study presented the highest HMW/LMW ratio, which could have affected the elastic property of the virgin binder in blends 70PG20RAP and 70PG20RAP5F. The addition of hollow fibers in blends 70PG5P5F and 70PG5P20RAP5F resulted in binder blends with better elastic properties during the loading cycles compared to the virgin binder as an increase in the "A" parameter was observed. Figure 23(b) shows that the addition of RAP in blends 70PG20RAP

and 70PG5P20RAP increased the sensitivity of the virgin binder to the change in strain level. Results from Figure 23(b) also shows that binder blends containing sodium-alginate fibers would have a similar deterioration rate as the strain level was increased compared to the virgin binder PG 70-22.

The opposite trend was observed with binder blends prepared with PG 64-22. Figure 24(a) shows that the addition of 5% and 10% fiber content in virgin binder enhanced the elastic properties of virgin binder PG 64-22 as the "A" parameter increased. Also, it is shown that the addition of aged binder from either RAS or RAP would result in a binder blend more susceptible to cracking as a decrease in the "A" parameter was observed for blends 64PG5P, 64PG20RAP and 64PG5P20RAP compared to the virgin binder. However, the addition of the hollow fibers partially reversed the negative impact of adding an aged binder and the ability of binder blends 64PG5P5F and 64PG20RAP5F to resist fatigue damage. Yet, Figure 24(b) shows that the addition of fibers did not have a pronounced effect on improving the susceptibility of blends to a change in strain levels as the calculated "B" parameter was equal to or higher than the virgin binder PG 64-22.

Overall, Figure 23(b) and Figure 24(b) shows that addition of SBS polymer in binder PG 70-22 resulted in a decrease in the absolute value of "B" parameter, which indicates that binder PG 70-22 would have a lower deterioration rate than binder PG 64-22. In addition, Figure 23 and Figure 24 shows that the high HMW/LMW ratios and high percentage content of RAP utilized in the study may explain the increase in fracture susceptibility of blends containing RAP as observed in the "A" parameter and absolute "B" parameter values in the LAS test results. Also, the polymer content in RAS (i.e., based on HP-GPC test results) and low percentage content of RAS (i.e., 5%) utilized in the blends could have reduced the negative impact in the fracture susceptibility of blends containing RAS compared to blends containing RAP.

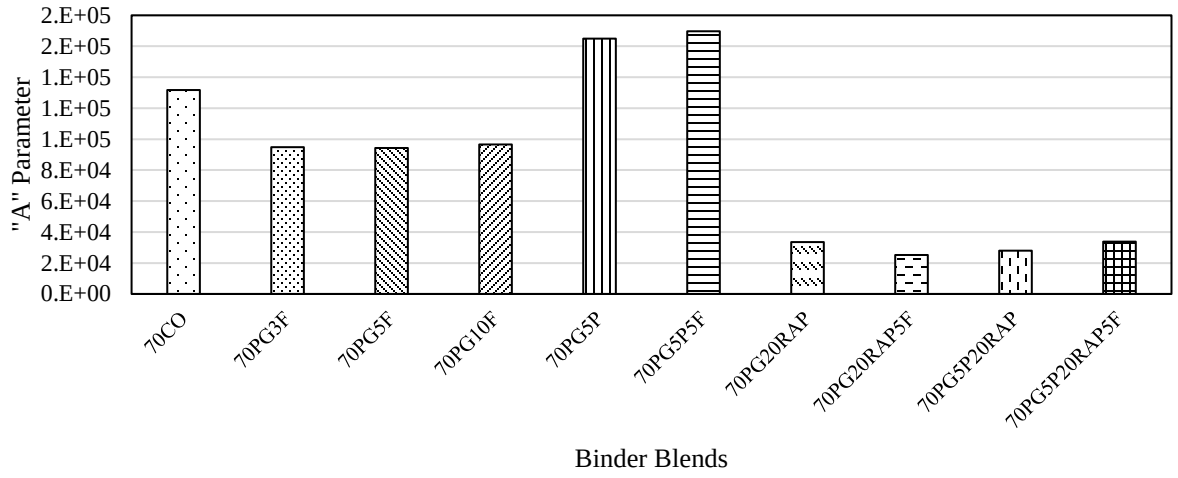

(a)

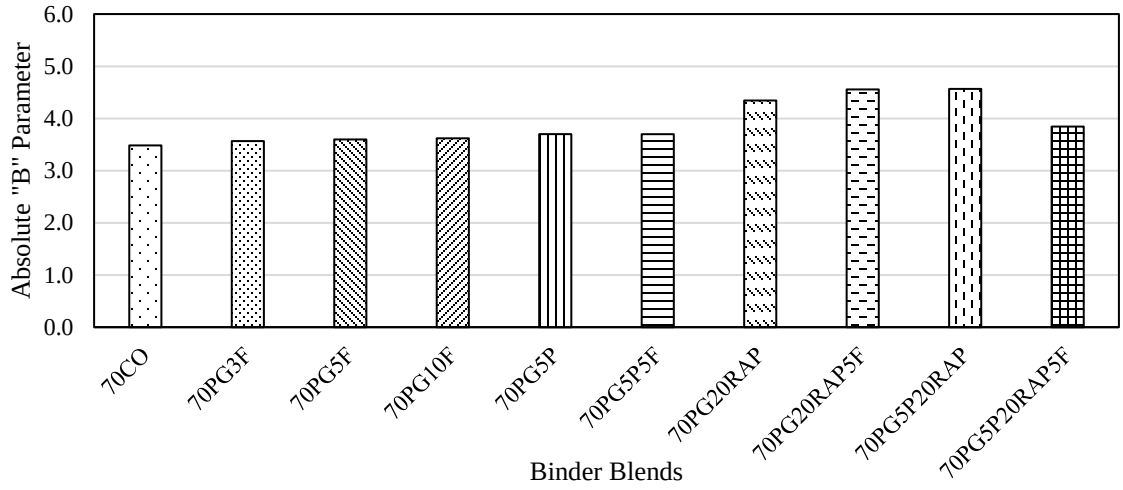

(b)

Figure 23. LAS test results for binder PG 70-22: (a) "A" parameter fatigue law and (b) absolute "B" parameter fatigue law.

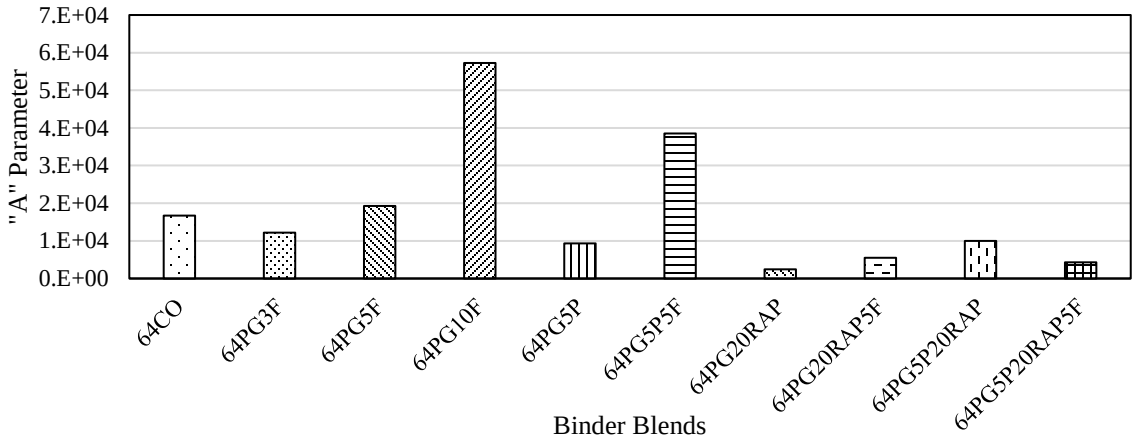

(a)

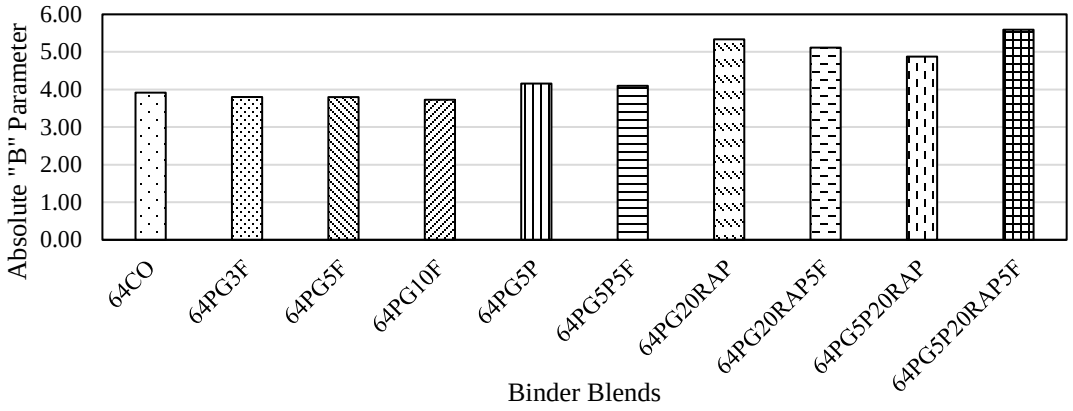

(b)

Figure 24. LAS test results for binder PG 70-22: (a) "A" parameter fatigue law and (b) absolute "B" parameter fatigue law.

5.7. Performance of Asphalt Mixtures with Sodium-Alginate Fibers

Fourteen different Superpave HMA mixtures were prepared to evaluate the effects of adding sodium-alginate fibers on the mix performance against rutting, fatigue cracking, and low-temperature cracking. Prior to mixing, all mix constituents were preheated to 200°C for 3 hrs. Aggregate and recycled materials were mixed first and then, reheated to 163°C for 1 h. The binder was added to the mixture and fibers were added gradually to the mix to avoid a conglomeration of fibers within the mix. After adding the fibers, the mixture was reheated for 10-15 minutes in a 163°C oven to regain workability. Lastly, the mixture was aged in the oven at 163°C for 2 h prior to compacting the specimens for the different mixture tests.

5.7.1. Rutting Performance

The study evaluated the resistance to permanent deformation of the mixtures by using the LWT, where cylindrical specimens were submerged in water at 50°C, and a 703-N steel wheel passed across the surface until attainment of 20,000 cycles at a rate of 56 passes per minute. The failure criteria adopted in this study is a maximum rut depth of 6 mm or completing 20,000 passes at 50°C.

Figure 25 presents the terminal permanent deformation depths for the evaluated mixtures from the LWT test. It is shown in Figure 25 that the maximum allowable rut depth threshold in Louisiana (6 mm) was satisfied for all the mixes. The addition of recycled materials decreased the terminal rut depth as compared to the conventional mixture (70CO). However, results show that the addition of the hollow fibers slightly increased the rut depth as compared to the mixtures containing recycled materials with no fibers. The small increase in the rut depth can be attributed to the breakage of fibers during the LWT test, which released the rejuvenating product and caused a softening effect.

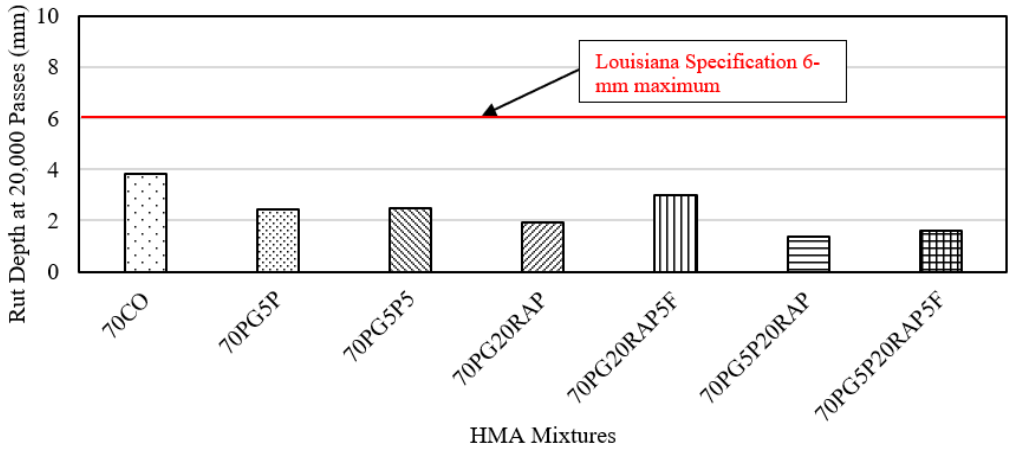

Figure 25. Rutting susceptibility of HMA mixtures with binder PG 70-22.

Figure 26 shows that the conventional asphalt mixture (64CO) had a rut depth greater than the maximum allowable rut depth threshold in Louisiana (6 mm). Furthermore, Figure 26 shows that the addition of recycled materials improved the rutting susceptibility of the mixtures by reducing the rut depth after 20,000 cycles. Similarly, as observed in Figure 25, a small increase in the rut depth was observed in the mixtures containing recycled materials with the addition of hollow fibers.

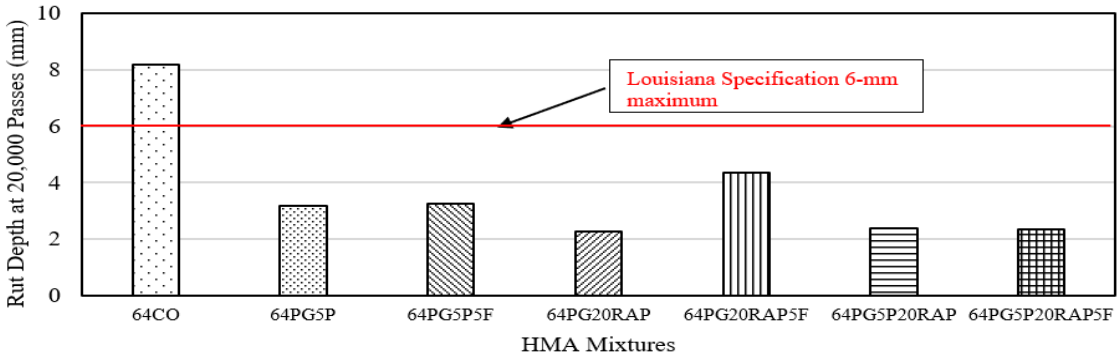

Figure 26. Rutting susceptibility of HMA mixtures with binder PG 64-22.

5.7.2. Fracture Resistance at Intermediate Temperature

Mix susceptibility to cracking at intermediate temperature was characterized using the SCB test. The SCB test was conducted using semi-circular specimens with three different notch

depths (25.4 mm, 31.8 mm, and 38mm) at a testing temperature of 25°C. The SCB test consists of applying a monotonic load under a constant displacement rate of 0.5 mm/min until fracture failure. The test was conducted according to the standard presented in ASTM D 8044.

Figure 27 shows the critical strain energy release rate for the evaluated asphalt mixtures. Figure 27 shows a decrease in the J_c value when RAS and RAS/RAP were added in mixes 70PG5P and 70PG5P20RAP as compared to the conventional mixture (70CO). The addition of RAP resulted in a similar fracture resistance at intermediate temperature as the conventional mixture (70CO). Figure 27 also shows that the addition of fibers in the mix containing RAS (70PG5P5F) had a positive effect as an increase in the J_c value was noted from 0.45 to 0.55 kJ/m^2. The same positive effect due to the addition of fibers was observed in mix 70PG5P20RAP5F as an increase in J_c value was observed as shown in Figure 27. The rejuvenating properties of the hollow fibers may explain the enhancement of the fracture properties of mixes 70PG5P5F and 70PG5P20RAP5F.

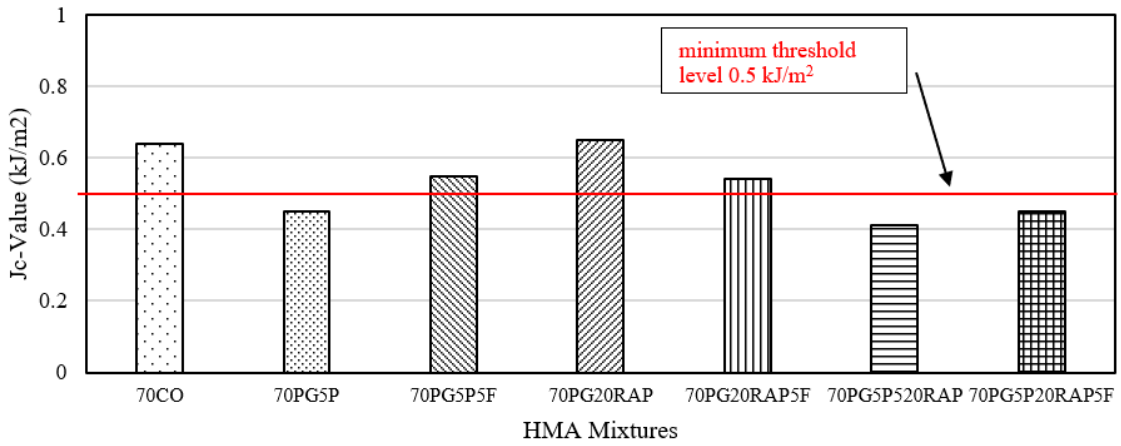

Figure 27. Fracture resistance of HMA mixtures with binder PG 70-22.

Figure 28 shows that all asphalt mixtures prepared with PG 64-22 did not satisfy the minimum threshold level of 0.5 kJ/m^2 which confirms the advantage of using polymer-modified binders. However and similar to the trends observed with PG 70-22, the addition of hollow fibers enhanced the fracture properties of mixtures containing RAS 64PG5P5F) and RAS/RAP (64PG5P20RAP5F). Yet, the addition of hollow fibers decreased the fracture resistance of the mixture prepared with 20% RAP (64PG20RAP compared to 64PG20RAP5F).

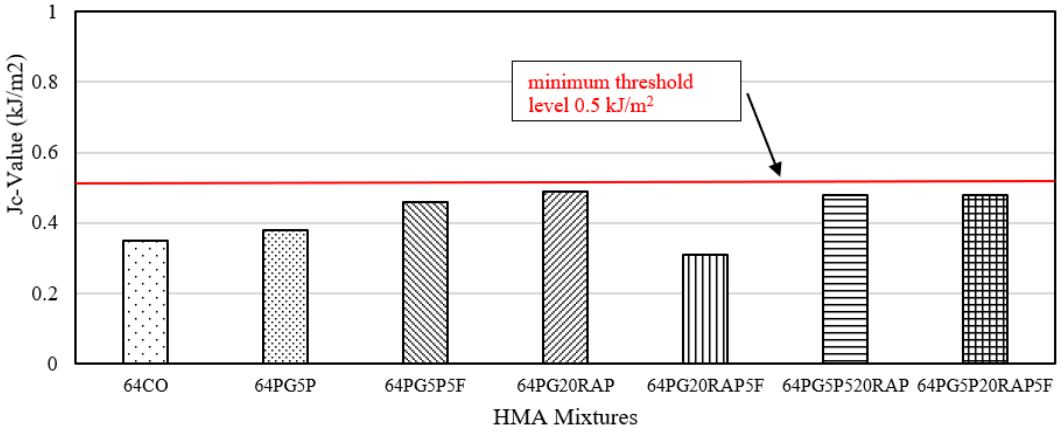

Figure 28. Fracture resistance of HMA mixtures with binder PG 64-22.

5.7.3. Low-Temperature Cracking Resistance

Low-temperature cracking susceptibility of the evaluated mixtures was evaluated by performing the Thermal Stress Restrained Specimen Test (TSRST) in accordance with AASHTO TP10. The test consists of cooling a beam specimen at a rate of 10°C /min while the specimen is restrained from contracting. As the temperature drops, thermal stresses build up until the beam specimen fractures. Samples were long-term aged before conducting the TSRST test. Figure 29 shows the fracture load for the evaluated asphalt mixtures. Mixture aging was performed according to AASHTO R30-02. Figure 29(a) shows that the addition of RAS or RAP resulted in higher fracture load compared to the conventional mixture. Furthermore, it is shown in Figure 29(a) that the addition of the hollow fibers enhanced the fracture load of mixtures containing recycled materials (70PG5P vs. 70PG5P5F; 70PG20RAP vs. 70PG20RAP5F; and 70PG5P20RAP vs. 70PG5P20RAP5F). Therefore, the addition of RAS or RAP with the hollow fibers resulted in asphalt mixtures with higher load capacity at low-temperature.

Figure 29(b) shows a similar improvement in the fracture resistance of mixtures prepared with PG 64-22 with the addition of RAS and/or RAP. The fracture load also improved with the addition of hollow fibers in mixtures containing recycled materials. As a result, the addition of RAS or RAP with the hollow fibers resulted in asphalt mixtures with higher load capacity at low-temperature.

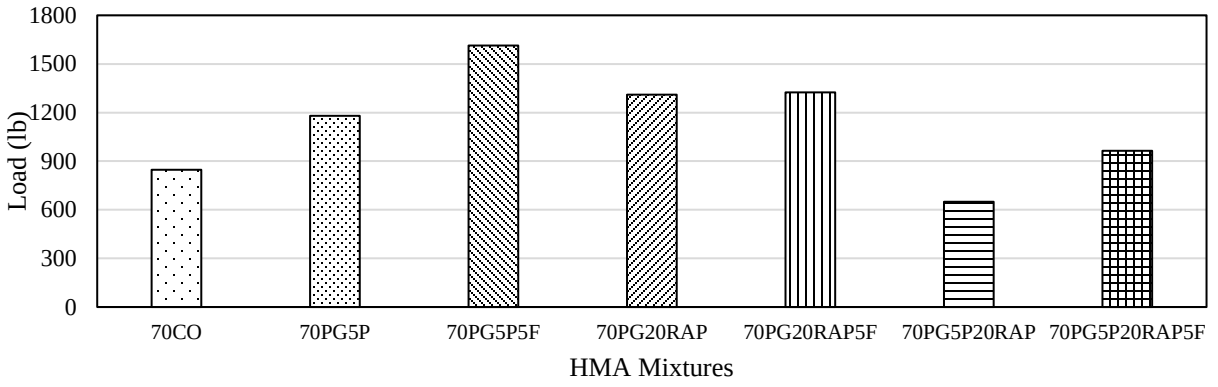

(a)

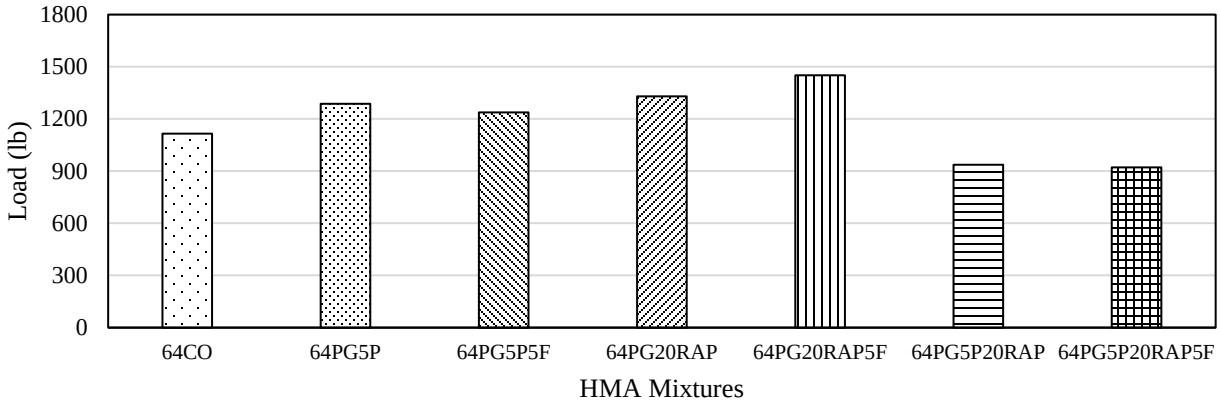

(b)

Figure 29. Failure load: (a) mixtures with PG 70-22 and (b) mixtures with PG 64-22.

The failure temperature of the evaluated mixtures from the TSRST test results are shown in Figure 30. Figure 30(a) shows that the addition of RAS or RAP resulted in a similar failure temperature as the conventional mixture 70CO. Also, it is shown in Figure 30(a) that the addition of the hollow fibers did not enhance the fracture temperature of mixtures containing recycled materials; thus, they had a similar failure temperature than the conventional mixture. A drop in the failure temperature was observed in the mixtures containing RAS and RAP, which in conjunction with results from Figure 29, shows that the evaluated mixtures containing both recycled materials would be more susceptible to fracture at low-temperatures. Similar trends were observed with the mixtures prepared with binder PG 64-22, see Figure 30(b).

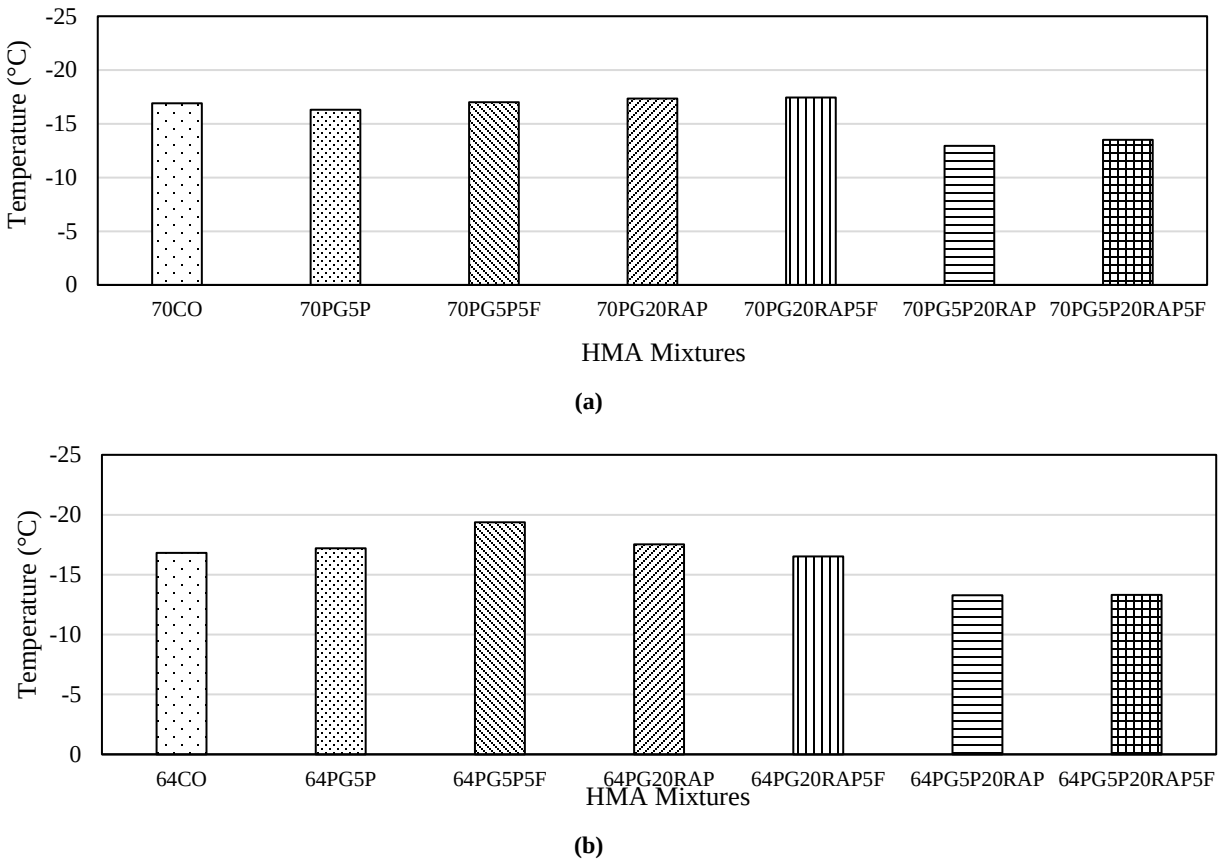

Figure 30. Failure temperature for: (a) mixtures with PG 70-22 and (b) mixtures with PG 64-22.

5.8. Statistical Analysis of Experimental Results

A statistical analysis was performed to determine whether the differences in performance observed in the self-healing experiment and mixture testing results were significant. An Analysis of Variance (ANOVA) at a 5% confidence level was performed for each self-healing and mixture test to identify statistically significant differences in the test results. A Tukey's HSD test was also performed on all possible combinations to identify the mixes that were statistically different based on the previous results from ANOVA. The statistical results for each grouping were ranked by using letters A, B, C, and so forth. The letter A was assigned to the mix with the best performance, followed by the letter B and so forth. Double letters (e.g., A/B, B/C) indicate that the mixture might be categorized in both groups.

5.8.1. Statistical Analysis of Healing Efficiency for Mixtures with Binder PG 70-22

A statistical analysis was conducted to evaluate the effect of the type of recycled materials and environmental curing conditions on the healing efficiency of the evaluated mixtures.

Effect of Sodium-Alginate Fibers on the Healing Ability of Virgin Binder PG 70-22: Table 14 shows that the healing recovery of the conventional asphalt mixture (70CO) was statistically equivalent to the mixture prepared with the hollow fibers (70PG5F). The presence of SBS polymer in binder PG 70-22 could have reduced the benefits of adding sodium-alginate fibers in the healing recovery of mixture 70PG5F.

Table 14. Statistical analysis of healing recovery for virgin HMA mixtures with binder PG 70-22.

Mixture Type	HE (%) Mean	HE (%) COV	HE (%) Rank
70CO	55.2%	5.6%	A
70PG5F	52.5%	31.9%	A

Effect of the Type of Recycled Material on the Healing Efficiency of Sodium-Alginate Fibers: Table 15 shows the statistical analysis of the asphalt mixtures containing RAS with PG 70-22 for the self-healing experiment at room-temperature curing condition. The statistical comparison showed that the addition of sodium-alginate fibers resulted in an asphalt mixture with a similar healing efficiency as a conventional mixture with no recycled materials. In addition, it is shown in Table 15 that the 3% fiber content had a negative impact on the healing efficiency, as it was statistically different from the mixture with the highest healing efficiency, 70PG5P5F.

Table 15. Statistical analysis of self-healing efficiency for HMA mixtures containing RAS with binder PG 70-22.

Mixture Type	HE (%) Mean	HE (%) COV	HE (%) Rank
70CO	55.2%	5.6%	A/B
70PG5P	53.1%	3.6%	A/B
70PG5P1F	57.0%	9.2%	A/B
70PG5P3F	39.9%	17.6%	B
70PG5P5F	71.3%	15.2%	A

The statistical analysis of the mixtures containing RAP with PG 70-22 is shown in Table 16. Table 16 supports that the addition of RAP improved the healing efficiency of the mixture compared to the conventional mixture (70CO). The addition of fibers resulted in a negative effect on the healing efficiency of mixture 70PG20RAP5F, but it had a similar performance as the conventional mixture based on the statistical analysis results.

Table 16. Statistical analysis of self-healing efficiency for HMA mixtures containing RAP with binder PG 70-22.

Mixture Type	HE (%) Mean	HE (%) COV	HE (%) Rank
70CO	55.2%	5.6%	B
70PG20RAP	68.3%	4.9%	A
70PG20RAP5F	51.0%	0.3%	B

Effect of Curing Conditions on the Healing Efficiency of Sodium-Alginate Fibers: A t-test analysis was performed for each type of mixture to evaluate the effect of curing conditions on the healing efficiency. Although Figure 8 shows an increase in the healing efficiency of the mixtures 70PG5F, 70PG5P and 70PG20RAP5F, Table 17 shows that the differences in healing efficiencies observed by the change in temperature during the healing period were not significant.

Table 17. Statistical analysis of the effect of curing conditions in the healing ability of HMA mixtures with binder PG 70-22.

Mixture Type	HE (%) at RT Mean	HE (%) at RT COV	HE (%) at RT Rank	HE (%) at HT Mean	HE (%) at HT COV	HE (%) at HT Rank
70CO	55.2%	5.6%	A	55.4%	13.1%	A
70PG5F	52.5%	31.9%	A	78.9%	5.6%	A
70PG5P	53.1%	3.6%	A	63.4%	11.0%	A
70PG5P1F	57.0%	9.2%	A	68.7%	11.4%	A
70PG5P3F	39.9%	17.6%	A	57.2%	18.6%	A
70PG5P5F	71.3%	15.2%	A	63.7%	8.6%	A
70PG20RAP	68.3%	4.9%	A	50.0%	38.8%	A
70PG20RAP5F	51.0%	0.3%	A	53.1%	25.4%	A

5.8.2. Statistical Comparison of Healing Efficiency for Mixtures with Binder PG 64-22

The differences in the healing efficiencies of the evaluated mixtures prepared with binder PG 64-22 by changing the type of recycled materials and environmental curing conditions were analyzed by performing a statistical analysis.

Effect of Sodium-Alginate Fibers in the Healing Ability of Virgin Binder PG 64-22: Table 18 shows that the healing recovery of the conventional asphalt mixture (64CO) was statistically equivalent to the mixture prepared with the hollow fibers (64PG5F). The lower healing efficiency of the mixture containing the produced fibers might indicate that fibers did not break during the process of inducing damaged in the beam specimens.

Table 18. Statistical analysis of healing recovery for virgin HMA mixtures with binder PG 64-22.

Mixture Type	HE (%) Mean	HE (%) COV	HE (%) Rank
64CO	64.0%	18.9%	A
64PG5F	55.6%	20.2%	A

Effect of the Type of Recycled Materials on the Healing Efficiency of Sodium-Alginate Fibers: Table 19 shows that even though the conventional mixture had the highest healing efficiency at room-temperature curing condition, the performance of the conventional mixture was the same statistically as the mixture containing RAS with and without sodium-alginate fibers. Comparing the results in Table 15 and Table 19, it may be deducted that the healing efficiencies of the sodium-alginate fibers were enhanced when they were combined with a polymer-modified binder.

Table 19. Statistical analysis of self-healing efficiency for HMA mixtures containing RAS with binder PG 64-22.

Mixture Type	HE (%) Mean	HE (%) COV	HE (%) Rank
64CO	64.0%	18.9%	A
64PG5P	44.6%	29.0%	A
64PG5P5F	48.5%	16.5%	A

The statistical analysis of the mixtures containing RAP with PG 64-22 is shown in Table 20. Table 20 indicates that the addition of RAP resulted in a similar performance in the healing efficiency of the mixture compared to the conventional mixture 64CO.

Table 20. Statistical analysis of self-healing efficiency for HMA mixtures containing RAP with binder PG 64-22.

Mixture Type	HE (%) Mean	HE (%) COV	HE (%) Rank
64CO	64.0%	18.9%	A
64PG20RAP	52.7%	8.1%	A
64PG20RAP5F	53.4%	5.8%	A

Effect of Curing Conditions on the Healing Efficiency of Sodium-Alginate Fibers: The improvement in the healing efficiency of the evaluated mixtures prepared with binder PG 64-22 due to the two environmental conditions was evaluated by performing a t-test analysis for each mixture type. As observed for the mixtures prepared with binder PG 70-22, the differences in healing efficiencies between the two environmental curing conditions were insignificant based on the statistical analysis shown in Table 21.

Table 21. Statistical analysis of the effect of curing conditions in the healing efficiency of HMA mixtures with binder PG 64-22.

Mixture Type	HE (%) at RT Mean	HE (%) at RT COV	HE (%) at RT Rank	HE (%) at HT Mean	HE (%) at HT COV	HE (%) at HT Rank
64CO	64.0%	18.9%	A	66.9%	6.0%	A
64PG5F	55.6%	20.2%	A	58.3%	22.7%	A
64PG5P	44.6%	29.0%	A	57.8%	5.3%	A
64PG5P5F	48.5%	16.5%	A	59.6%	2.6%	A
64PG20RAP	52.7%	8.1%	A	55.0%	7.3%	A
64PG20RAP5F	53.4%	5.8%	A	61.4%	6.3%	A

5.8.3. Statistical Comparison of Strength Recovery for Mixtures with Binder PG 70-22

A statistical analysis was performed to evaluate the effect of the type of recycled materials and environmental curing conditions on the strength recovery of the evaluated mixtures.

Effect of Sodium-Alginate Fibers in the Strength Recovery Ability of Virgin Binder PG 70-22: Table 22 shows that the strength recovery of the conventional asphalt mixture (70CO) was statistically equivalent to the mixture prepared with the hollow fibers (70PG5F). The presence of SBS polymer in binder PG 70-22 could have reduced the benefits of adding sodium-alginate fibers in the strength recovery of mixture 70PG5F.

Table 22. Statistical analysis of strength recovery for virgin HMA mixtures with binder PG 70-22.

Mixture Type	HE (%) Mean	HE (%) COV	HE (%) Rank
70CO	44.7%	9.7%	A
70PG5F	42.9%	16.6%	A

Effect of the Type of Recycled Materials on the Strength Recovery of Sodium-Alginate Fibers: Table 23 shows the statistical analysis of the evaluated mixtures containing RAS with PG 70-22 for the strength recovery analysis at room-temperature curing condition. The pairwise comparison showed that the conventional mixture had the best strength recovery after the healing period compared to the mixtures containing RAS. Although the addition of sodium-alginate fibers enhanced the self-healing efficiency of mixture 70PG5P5F, they did not have

an improvement effect on the strength recovery of the mixture. A soft location is possibly induced when the rejuvenator is released and when the fibers are broken during a 3-point bending test in the self-healing experiment, which may explain the lack of improvement in the strength recovery.

Table 23. Statistical analysis of strength recovery for HMA mixtures containing RAS with binder PG 70-22.

Mixture Type	HE (%) Mean	HE (%) COV	HE (%) Rank
70CO	44.7%	9.7%	A
70PG5P	15.9%	41.3%	B
70PG5P5F	11.8%	39.9%	B

The statistical analysis of the mixtures containing RAP with PG 70-22 is shown in Table 24. Tables 23 and 24 indicate that the addition of recycled materials such as RAS and RAP had a negative effect on the strength recovery compared to the conventional mixture. However, Table 24 shows that the fibers improved the strength recovery for mixture 70PG20RAP5F, as the observed differences were statistically significant. This may be due that the fibers acted as a reinforcement because they were not broken during the experiment.

Table 24. Statistical analysis of strength recovery for HMA mixtures containing RAP with binder PG 70-22.

Mixture Type	HE (%) Mean	HE (%) COV	HE (%) Rank
70CO	44.7%	9.7%	A
70PG20RAP	17.2%	10.7%	C
70PG20RAP5F	31.4%	19.2%	B

Effect of Curing Conditions on the Strength Recovery Ability of Sodium-Alginate Fibers: A t-test analysis was performed for each type of mixture to evaluate the effect of curing conditions on the strength recovery ability of the evaluated asphalt mixtures. Table 25 shows that the increase in temperature during the healing period had a significant effect on the strength recovery of the mixtures containing recycled materials with the exception of mixture 70PG20RAP5F. As previously discussed, the aging due to the exposure to high-temperature during the healing period contributed to the increase in strengths of the mixtures. The aging process had a higher effect on mixtures containing recycled materials due to the lower virgin binder content compared to the conventional mixture.

Table 25. Statistical analysis of the effect of curing conditions in the strength recovery ability of HMA mixtures with binder PG 70-22.

Mixture Type	HE (%) at RT Mean	HE (%) at RT COV	HE (%) at RT Rank	HE (%) at HT Mean	HE (%) at HT COV	HE (%) at HT Rank
70CO	44.7%	9.7%	B	68.3%	20.3%	A
70PG5F	42.9%	16.6%	B	100%	-	A
70PG5P	15.9%	41.3%	B	46.8%	11.8%	A
70PG5P5F	11.8%	39.9%	B	52.5%	9.1%	A
70PG20RAP	17.2%	10.7%	B	47.4%	27.3%	A
70PG20RAP5F	31.4%	19.2%	A	33.6%	10.6%	A

5.8.4. Statistical Comparison of Strength Recovery for Mixtures with Binder PG 64-22

The differences in the strength recovery of the evaluated mixtures prepared with binder PG 64-22 by changing the type of recycled materials and environmental curing conditions were analyzed by performing a statistical analysis.

Effect of Sodium-Alginate Fibers in the Strength Recovery Ability of Virgin Binder PG 64-22: Table 26 shows that the addition of sodium-alginate fibers enhanced the strength recovery for the asphalt mixture prepared with the unmodified binder PG 64-22 after the 6-day healing period as compared to the conventional mixture 64CO. In this case, differences were statistically significant. The difference between the two binders may be due to chemical interaction between the polymer in the PG 70-22 binder and the sodium-alginate hollow fibers.

Table 26. Statistical analysis of strength recovery for virgin HMA mixtures with binder PG 64-22.

Mixture Type	HE (%) Mean	HE (%) COV	HE (%) Rank
64CO	33.9%	11.0%	B
64PG5F	52.2%	36.3%	A

Effect of the Type of Recycled Material in the Healing Ability of Sodium-Alginate Fibers: Table 27 shows that the strength recovery after 6-days healing period of the conventional mixture was not significantly different from the mixtures containing RAS contrary to what was observed for mixtures prepared with binder PG 70-22. The addition of sodium-alginate fibers enhanced the strength recovery of mixture 64PG5P5F, but its performance was not significantly different from the other evaluated mixtures.

Table 27. Statistical analysis of strength recovery for HMA mixtures containing RAS with binder PG 64-22.

Mixture Type	HE (%) Mean	HE (%) COV	HE (%) Rank
64CO	33.9%	11.0%	A
64PG5P	23.3%	50.4%	A
64PG5P5F	30.9%	72.8%	A

Table 28 also shows that the addition of a recycled materials had an adverse impact on the strength recovery in mixture 64PG20RAP compared to the conventional mixture 64CO as the differences in strength recovery were statistically significant. However, it is shown in Table 28 that the enhancement in the strength recovery of mixture 64PF20RAP5F with the addition of fibers resulted in an asphalt mixture with a similar strength recovery to a conventional mixture. Therefore, as explained before, the addition of fibers acted as a reinforcement in this case resulting in an increase in the stiffness of the asphalt mixture.

Table 28. Statistical analysis of strength recovery for HMA mixtures containing RAP with binder PG 64-22.

Mixture Type	HE (%) Mean	HE (%) COV	HE (%) Rank
64CO	33.9%	11.0%	A
64PG20RAP	15.5%	51.6%	B
64PG20RAP5F	27.9%	26.9%	A/B

Effect of Curing Conditions in the Healing Ability of Sodium-Alginate Fibers: The improvement in the strength recovery of the evaluated mixtures prepared with binder PG 64-22 by changing the environmental curing conditions was evaluated by performing a t-test analysis for each type of mixture. Table 29 shows that the enhancement in the strength recovery of the mixtures by increasing the temperature from 25°C to 50°C during the healing period was not significantly different. The variability observed in the strength recovery analysis test results could have contributed to neglect the effect of increasing the temperature from 25°C to 50°C during the healing period in the strength recovery of the mixtures as observed in the mixtures prepared with binder PG 70-22.

Table 29. Statistical analysis of the effect of curing conditions in the strength recovery ability of HMA mixtures with binder PG 64-22.

Mixture Type	HE (%) at RT Mean	HE (%) at RT COV	HE (%) at RT Rank	HE (%) at HT Mean	HE (%) at HT COV	HE (%) at HT Rank
64CO	33.9%	11.0%	A	49.9%	29.9%	A
64PG5F	52.2%	36.3%	A	81.4%	-	A
64PG5P	26.8%	50.4%	A	49.9%	21.5%	A
64PG5P5F	30.9%	72.8%	A	51.7%	12.2%	A
64PG20RAP	15.5%	51.6%	A	31.1%	46.5%	A
64PG20RAP5F	27.9%	26.9%	A	47.9%	48.1%	A

5.8.5. Statistical Comparison of Asphalt Mixture Performance Testing

Table 30 shows the statistical analysis of the performance tests conducted for the PG 70-22 mixtures. Based on the statistical analysis, Table 30 indicates that the performance of mixture 70PG5P20RAP against permanent deformation was significantly different from the conventional mixture. In addition, mixtures 70PG5P, 70PG5P5F, 70PG20RAP5F and 70PG5P20RAP5F showed a similar performance compared to the mixture containing RAP and RAS based on the pairwise comparison shown in Table 30.

For the cracking resistance at intermediate temperature, Table 30 shows that the poor performance of mixture containing RAP and RAS was significantly different from the conventional mixture. However, it is also shown in Table 30 that the recovery in the J_c-value for the mixtures 70PG5P5F, 70PG0RAP5F and 70PG520RAP5F with the addition of sodium-alginate fibers resulted in a mixture with a similar performance as the conventional mixture. Furthermore, the addition of recycled materials and sodium alginates fibers had an improved and significant difference in performance at low-temperature conditions compared to the conventional mixture 70CO.

Table 30. Statistical analysis for mixture testing for HMA mixtures with PG 70-22.

Mixture Type	LWT Mean	LWT COV	LWT Rank	SCB Mean	SCB COV	SCB Rank	TSRST Mean	TSRST COV	TSRST Rank
70CO	3.8 mm	22.1%	B	0.64 kJ/m2	1.1%	A	846.9 lb	22.0%	B
70PG5P	2.5 mm	4.3%	A/B	0.45 kJ/m2	12.6%	A/B	1179.9 lb	17.3%	A/B
70PG5P5F	2.5 mm	30.4%	A/B	0.54 kJ/m2	14.5%	A/B	1613.6 lb	5.0%	A
70PG20RAP	1.9 mm	12.4%	A/B	0.65 kJ/m2	9.7%	A	1310.5 lb	14.5%	A/B
70PG20RAP5F	3.2 mm	22.2%	A/B	0.55 kJ/m2	16.6%	A/B	1324.5 lb	-	A/B
70PG5P20RAP	1.4 mm	52.3%	A	0.40 kJ/m2	8.0%	B	649.6 lb	41.4%	B
70P5P20RAP5F	1.6 mm	11.2%	A/B	0.45 kJ/m2	22.0%	A/B	963.8 lb	24.2%	A/B

Table 31 shows the statistical analysis for the different performance tests conducted for the PG 64-22 mixtures. Table 31 shows that the performance against permanent deformation was enhanced with the addition of recycled materials and sodium-alginate fibers, as the conventional mixture 64CO was significantly different and inferior from the other mixtures. It can also be observed that the conventional mixture 64CO would not satisfy the 6-mm rut depth of the Louisiana's specifications.

For the cracking resistance at intermediate temperature, Table 31 shows that mixtures containing recycled materials and sodium-alginate fibers, except for mixture 64PG20RAP5F, were not statistically different in performance against cracking compared to the conventional mixture 64CO. Therefore, Table 31 suggests that asphalt mixtures containing recycled materials and sodium-alginate fibers would have similar mechanical fracture properties at intermediate temperature than a conventional mixture. Furthermore, the addition of recycled materials and sodium-alginate fibers did not have a significant effect on low-temperature cracking, as the statistical analysis did not show significant differences in the failure load between all evaluated mixtures.

Table 31. Statistical analysis for mixture testing for HMA mixtures with PG 64-22.

Mixture Type	LWT Mean	LWT COV	LWT Rank	SCB Mean	SCB COV	SCB Rank	TSRST Mean	TSRST COV	TSRST Rank
64CO	8.2 mm	3.8%	C	0.35 kJ/m2	8.4%	A/B	1115.4 lb	7.5%	A
64PG5P	3.2 mm	18.9%	B/C	0.38 kJ/m2	31.1%	A/B	1287.0 lb	4.4%	A
64PG5P5F	3.3 mm	6.3%	B/C	0.46 kJ/m2	35.0%	A	1237.6 lb	-	A
64PG20RAP	2.3 mm	1.3%	A	0.49 kJ/m2	36.4%	A	1329.8 lb	0.6%	A
64PG20RAP5F	4.4 mm	11.1%	B	0.31 kJ/m2	50.2%	B	1451.0 lb	17.6%	A
64PG5P20RAP	2.4 mm	24.5%	A	0.48 kJ/m2	4.9%	A	936.6 lb	21.2%	A
64PG5P20RAP5F	2.4 mm	30.9%	A	0.48 kJ/m2	17.8%	A	956.3 lb	-	A

6. CONCLUSIONS

Based upon the results obtained from the different tests performed in this study, it can be concluded that self-healing mechanisms in asphalt pavements are a promising concept that could improve mechanical properties of asphalt mixtures and enhance the service life of a pavement. Sodium-alginate fibers containing a commercial rejuvenator product as core material were successfully synthesized with optimum thermal and tensile properties to resist the asphalt mixing processes. In addition, the following findings and conclusions are drawn based on the outcome of this study:

With respect to the optimum fiber content:

- The addition of 5% fiber content in mixture 70PG5P5F resulted in a greater enhancement of the healing efficiency of the damaged specimens compared to 1% and 3% fiber content.
- A validation of the 5% fiber content as an optimum fiber content was performed by conducting the MSCR and SCB tests. The proposed optimum fiber content resulted in an enhancement in the fracture susceptibility at intermediate temperature of long-term aged asphalt mixtures containing RAS.

With respect to healing efficiency and strength recovery:

- Results of the self-healing experiment showed that the enhancement in the healing recovery depends on the breakage of the fibers. When the fibers break, the rejuvenator is released resulting in softening of the mix. In contrast, when the fibers do not break, they act as reinforcement to the mix.
- The self-healing experiment test results showed that the addition of sodium-alginate fibers improved the strength recovery of mixtures prepared with unmodified binder. For mixtures prepared with polymer-modified binder, the strength recovery of the conventional asphalt mixture was statistically equivalent to the mixture prepared with the hollow fibers.
- The increase in temperature from 25°C to 50°C during the healing period resulted in higher strength recovery percentages in all the evaluated mixtures. Furthermore, the conventional mixture containing sodium-alginate fibers exhibited a 100% strength recovery at high-temperature curing condition.

With respect to the effects of the fibers on the chemical composition of asphalt binder:

- HP-GPC test results showed that the addition of fibers in blends containing recycled materials resulted in an increase in the HMW/LMW ratio. The increase of the asphaltene fraction suggests that some fibers were broken during the blending process, which released the core material and facilitate the blending between aged and virgin binder in the blends.

- FTIR results showed that the addition of extracted binder from either RAS and/or RAP resulted in an increase in the ICO index. The addition of fibers in blends containing recycled materials also resulted in an increase in the ICO, which suggests that the rejuvenating product facilitates the extraction of aged binder from the recycled materials and thus, increased the asphaltene content resulting in stiffer blends.

With respect to the effects of the fibers on the rheological properties of asphalt binder:

- Rheological properties of the binder blends containing recycled materials and sodium-alginate fibers suggested that the fibers did not have a noticeable effect on the final PG grade.

- MSCR test results showed that a binder blend with extracted binder from recycled materials and sodium-alginate fibers would have less rutting susceptibility than a conventional virgin binder would.

- LAS test results showed that the hollow fibers recovered some of the elastic behavior lost due to the addition of aged binder from RAS and/or RAP. However, the addition of fibers in virgin binders resulted in a decrease in the "A" parameter of the fatigue law except with 10% fiber content in binder PG 64-22.

With respect to the effects of the fibers on the laboratory performance of asphalt mixtures:

- LWT test results showed that the addition of sodium-alginate fibers in the mixtures containing recycled materials resulted in an increase in the rut depth; yet, the mixtures performed better than the conventional mixture and satisfied the Louisiana specifications.
- SCB test results suggested that the conventional mixture would have the best performance against fracture as it had the highest Jc-value. However, SCB test results showed that the addition of fibers slightly enhanced the mechanical properties against fracture at intermediate temperature of mixtures containing RAS and RAS/RAP.
- TSRST test results showed that the addition of fibers improved marginally the loading capacity of mixtures containing recycled materials compared to the conventional mixtures. Yet, the failure temperature of mixtures containing recycled materials with fibers did not show significance differences from the conventional mixtures.

7. RECOMMENDATIONS

Based on the outcome of this study, the authors recommend conducting further research prior to implementing the developed fibers in practice. It is recommended to test the developed fibers with other softer (i.e. non-modified) binders, other RAP and RAS sources to evaluate their effects on the rheological properties of the binders and their enhancement of the mechanical properties of the mixtures. In addition, the authors recommend performing a life cycle cost assessment to determine the cost savings associated with the use of recycled materials and sodium-alginate fibers. Other commercial rejuvenator products should also be evaluated as core materials to enhance the reversing of the aging process of the binder from recycled materials. Field-testing is recommended to evaluate the performance of asphalt mixtures with the developed fibers in full-scale environmental and traffic conditions. Finally, it is recommended to determine the optimum fiber content based on a performance-based characterization against common distresses such as rutting, fatigue cracking and low-temperature cracking.

REFERENCES

1. W. S. Mongawer, A. Booshehrian, S. Vahidi and A. J. Austerman, "Evaluating the effect of rejuvenators on the degree of bleeding and performance of high RAP, RAS,and RAP/RAS mixtures," Road Materials and Pavement Design, vol. 14, no. 82, pp. 193-213.

2. C. Chiu and M. Lee, "Effectiveness of seal rejuvenators for bituminous pavement surfaces," J. Test. Eval., vol. 34, pp. 390-394, 2006.

3. A. Shah, R. S. McDaniel, G. A. Huber and V. Gallivan, "Investigation of properties of plant-produced reclaimed asphalt pavement mixtures," Journal of the Transportation Research Board, 2007.

4. X. Li, M. O. Marasteanu, R. C. Williams and T. R. Clyne, "Effect of reclaimed asphalt pavement (proportion and type) and binder grade on asphalt mixtures," Journal of the Transportation Research Board, 2008.

5. J. R. Willis and P. Turner, "Characterization of apshalt binder extractedfrom reclaimed asphalt shingles," NCAT Report 16-01, 2016.

6. G. W. Maupin Jr, "Investigation of the Use of Tear-Off Shingles in Asphalt concrete," Charottesville, 2010.

7. D. E. Watson, A. Johnson and H. R. Sharma, "Georgia's Experience with Recycled Roofing Shingles in Asphaltic concrete," In Transportation Research Record 1638, pp. 15-20, 1998.

8. J. Brownride, "The role of an asphalt rejuvenator in pavement preservation: use and need for asphalt rejuvenation," Tricor Refining, LLC, 2010.

9. R. Karlsson and U. Isacsson, "Material-related aspectsof asphalt recycling-state of the art," Journal of Materials in Civil Engineer, vol. 18, 2006.

10. E. R. Brown, "Preventative Maintenance Of Asphalt Concrete Pavements," 1988.

11. D. I. Anderson, D. E. Peterson, M. L. Wiley and W. B. Betenson, "Evaluation of selected softening agents used in flexible plavement recycling," FHWA-TS-79-204, 1978.

12. G. Peterson, R. Davison, C. Glover and J. Bullin, "Effect of Composition on Asphalt Recycling Agent Performance," Transportation Research Record, 1994.

13. J. Shen, S. Amirkhanian and J. Aune Miller, "Effects of rejuvenating agents on Superpave mixtures containing reclaimed asphalt pavement," Journal of Materials in Civil Engineering, vol. 19, no. 5, pp. 376-384, 2007.

14. S. Cooper, L. N. Mohammad and M. A. Elseifi, "Laboratory Performance of Asphalt Mixtures Containing Recycled Asphalt Shingles," Journal of the Transportation Research Board, vol. 2445, pp. 94-102, 2014.

15. M. A. Aguirre, M. M. Hassan, S. Shirzad, W. H. Daly and L. Mohammad, "Micro-encapsulation of asphalt rejuvenators using Melamine-Formaldehyde," Construction and Building Materials, vol. 114, pp. 29-39, 2016.

16. S. Shirzad, M. M. Hassan, M. A. Aguirre, L. N. Mohammad and W. H. Daly, "Evaluation of sunflower Oil as a Rejuvenator and Its Microencapsulation as a Healing Agent," J. Mater. Civil. Eng., 2016.

17. M. A. Aguirre, M. M. Hassan, S. Shirzad, L. N. Mohammad, S. Cooper and I. I. Negulescu, "Laboratory Testing of Self-Healing Microcapsules in Asphalt Mixtures Prepared with Recycled Asphalt Shingles," Journal of Materials in Civil Engineering, 2017.

18. T. Al-Mansoori, J. Norambuena-Contreras and A. Garcia, "Effect of capsule addition and healing temperature on the self-healing potential of asphalt mixtures," Materials and Structure, pp. 51-53, 2018.

19. J. Norambuena-Contreras, E. Yalcin, A. Garcia, T. Al-Mansoori, M. Yilmaz and R. Hudson-Griffiths, "Effect of mixing and ageing on the mechanical and self-healing properties of asphalt mixtures containing polymeric capsules," Construction and Building Materials, vol. 175, pp. 254-266, 2018.

20. A. Garcia, J. Jelfs and C. J. Austin, "Internal asphalt mixture rejuvenation using capsules," Construction Building Materials, vol. 101, no. 8, 2015.

21. F. A. Anderson, "Final report on the safety assessment of melamine/formaldehyde resin," J. Am. Coll. Toxicology, vol. 14, pp. 373-385, 1995.

22. D. Palin, V. Wiktor and H. M. Jonkers, "Bacteria-based agent for self-healing marine concrete," 5th Int. Conf. on Self-healing materials, 2015.

23. S. van der Zwaag, "Review of current strategies to induce self-healing behaviour in fibre reinforced polymer based composites," Mater. Sci. Technol., vol. 30, no. 9, 2014.

24. A. Tabakovic, D. Braak, M. Van Gerwen, O. Copuroglu, W. Post, S. J. Garcia and E. Schlangen, "The compartmented alginate fibres optimisation for bitumen rejuvenator encapsulation," Journal of Traffic and Transportation Engineering, pp. 1-13, 2017.

25. A. Tabakovic, L. Schuyffel, A. Karac and E. Schlangen, "An Evaluation of the Efficiency of Compartmented Alginate Fibers Encapsulating a Rejuvenator as an Asphalt Pavement Healing System," Applied Sciences, 2017.

26. S. D. Mookhoek, H. R. Fischer and S. Van der Zwaag, "Alginate fibers ontaining discrete liquid filled vacuoles for controlled delivery," Composites Part A: Applied Science and Manufacturing, vol. 43, no. 12, pp. 2176-2182, 2012.

27. R. H. McDowell, Properties of alginates, London (UK): Alginate Industries, 1977.

28. A. M. Hartman, M. D. Gilchrist and G. Walsh, "Effect of mixture compaction on indirect tensile stiffness and fatigue," J. Transp. Eng., vol. 127, no. 5, 2001.

29. J. Bonnot, "Selection and use of the procedure for laboratory compaction of bitumen mixtures," Performance Related Test Procedures for Bitumen Mixtures, 1997.

30. AASHTO, "Standard method of test for quantitative extraction of asphalt binder from hot mix asphalt HMA," AASHTO T164, Washington, DC, 2014.

31. AASHTO, "Standard practice for recovery of asphalt binder from solution by Abson method," AASHTO R59, Washington, DC, 2011.

32. ASTM D8044-16, "Standard Test Method for Evaluation of Asphalt Mixture Cracking Resistance using the Semi-Circular Bend Test (SCB) at Intermediate Temperatures," ASTM International, West Conshohocken, PA, 2016.

33. AASHTO, "Standard specification for performance-graded for asphalt binder," AASHTO M320, Washington, DC, 2015.

34. AASHTO, "Standard Method of Test for Estimating Fatigue Resistance of Asphalt Binders Using the Linear Amplitude Sweep," 2016.

35. G. Liu, E. Nielsen, J. Komacka, G. Leegwater and M. Ven, "Influence of the soft bitumen on the chemical and rheological properties of reclaimed polymer-modified binders from the "old" surface-layer asphalt," Construction Building Material, vol. 79, pp. 129-135, 2015.

APPENDIX A: PG GRADING RESULTS

Table A-1. PG grading for binder PG 64-22.

Test	Specification	Temperature ºC	Blend1	Blend2	Blend3	Blend4	Blend5	Blend6	Blend7
DSR ($G^*/\sin\delta$), 10 rad/s, AASHTO T315	>1.0 kPa	64 ºC	1.92 kPa	2.73 kPa	2.19 kPa	8.53 kPa	-	8.67 kPa	8.07 kPa
DSR (G*/sinδ), 10 rad/s, AASHTO T315	>1.0 kPa	70 ºC	0.88 kPa	1.24 kPa	1.02 kPa	3.86 kPa	3.03 kPa	3.90 kPa	3.80 kPa
DSR ($G^*/\sin\delta$), 10 rad/s, AASHTO T315	>1.0 kPa	76 ºC	-	0.61 kPa	0.509 kPa	1.82 kPa	1.40 kPa	1.84 kPa	1.82 kPa
DSR ($G^*/\sin\delta$), 10 rad/s, AASHTO T315	>1.0 kPa	82 ºC	-	-	-	0.896 kPa	0.697 kPa	0.906 kPa	0.92 kPa
DSR ($G^*/\sin\delta$), 10 rad/s, AASHTO T315	>2.2 kPa	64 ºC	3.75 kPa	-	-	21.5	-	-	
DSR (G*/sinδ), 10 rad/s, AASHTO T315	>2.2 kPa	70 ºC	1.68 kPa	2.55 kPa	2.35 kPa	9.69	-	9.47 kPa	10.2 kPa
DSR ($G^*/\sin\delta$), 10 rad/s, AASHTO T315	>2.2 kPa	76 ºC	-	1.21 kPa	1.12 kPa	4.5	3.93 kPa	4.44 kPa	4.80 kPa
DSR ($G^*/\sin\delta$), 10 rad/s, AASHTO T315	>2.2 kPa	82 ºC	-	-	-	2.15	1.9 kPa	2.14 kPa	2.31 kPa
DSR ($G^*/\sin\delta$), 10 rad/s, AASHTO T315	>2.2 kPa	88 ºC	-	-	-	-	-	-	1.17 kPa
DSR ($G^*.\sin\delta$), 10 rad/s, AASHTO T315	<5000 kPa	34 ºC	-	-	-	-	-	-	4350 kPa
DSR ($G^*.\sin\delta$), 10 rad/s, AASHTO T315	<5000 kPa	31 ºC	-	-	-	-	3730 kPa	3690 kPa	5550 kPa
DSR ($G^*.\sin\delta$), 10 rad/s, AASHTO T315	<5000 kPa	28 ºC	-	-	-	6835 kPa	5106 kPa	5020 kPa	69620 kPa
DSR ($G^*.\sin\delta$), 10 rad/s, AASHTO T315	<5000 kPa	25 ºC	3920 kPa	4885 kPa	2405 kPa	5195 kPa	6760 kPa	6680 kPa	8180 kPa
DSR ($G^*.\sin\delta$), 10 rad/s, AASHTO T315	<5000 kPa	22 ºC	5795 kPa	6925 kPa	3515 kPa	-	-		-
DSR ($G^*.\sin\delta$), 10 rad/s, AASHTO T315	<5000 kPa	19 ºC	-	-	5015 kPa	-	-		-
BBR-S- AASHTO T313	<300 MPa	-6 ºC	92.05	97.95 MPa	75.9 MPa	139	109.5	161.5	141.5
BBR-S- AASHTO T313	<300 MPa	-12 ºC	197 MPa	189.5 MPa	151 MPa	323	219	299	284.5
BBR-S- AASHTO T313	<300 MPa	-18 ºC	351 MPa	360 MPa	281 MPa	646	440	510	471.5
BBR-m- AASHTO T313	>0.3	-6 ºC	0.374	0.357	0.364	0.326	0.324	0.316	0.315
BBR-m- AASHTO T313	>0.3	-12 ºC	0.312	0.302	0.306	0.259	0.282	0.269	0.27
BBR-m- AASHTO T313	>0.3	-18 ºC	0.268	0.264	0.28	0.179	0.223	0.231	0.212
PG- Grading	--------		**64-22**	**70-22**	**70-22**	**76-16**	**76-16**	**76-16**	**82-16**
Continuous PG- Grading	--------		**68-23.6**	**71.8-22.3**	**70.3-22.6**	**81.8-16.8**	**80.8-19.4**	**81.8-18.0**	**82.4-18.0**

Table A-2. PG grading for binder PG 70-22.

Test	Specification	Temperature ºC	Blend8	Blend9	Blend10	Blend11	Blend12	Blend13	Blend14
DSR (G*/sinδ), 10 rad/s, AASHTO T315	>1.0 kPa	64 ºC	3.35 kPa	4.99 kPa	4.92 kPa	5.6 kPa	-	-	-
DSR (G*/sinδ), 10 rad/s, AASHTO T315	>1.0 kPa	70 ºC	1.77 kPa	2.65 kPa	2.58 kPa	3.02 kPa	4.54 kPa	6.78 kPa	-
DSR (G*/sinδ), 10 rad/s, AASHTO T315	>1.0 kPa	76 ºC	0.97 kPa	1.44 kPa	1.42 kPa	1.66 kPa	2.49 kPa	3.60 kPa	-
DSR (G*/sinδ), 10 rad/s, AASHTO T315	>1.0 kPa	82 ºC	-	-	-	0.939 kPa	1.37 kPa	1.91 kPa	1.44 kPa
DSR (G*/sinδ), 10 rad/s, AASHTO T315	>1.0 kPa	88 ºC	-	-	-	-	0.78 kPa	1.08 kPa	0.82 kPa
DSR (G*/sinδ), 10 rad/s, AASHTO T315	>1.0 kPa	94 ºC	-	-	-	-	-	0.62 kPa	-
DSR (G*/sinδ), 10 rad/s, AASHTO T315	>2.2 kPa	64 ºC	6.04 kPa	8.51 kPa	-	-	-	-	-
DSR (G*/sinδ), 10 rad/s, AASHTO T315	>2.2 kPa	70 ºC	3.23 kPa	4.39 kPa	4.48 kPa	9.69 kPa	-	-	-
DSR (G*/sinδ), 10 rad/s, AASHTO T315	>2.2 kPa	76 ºC	1.73 kPa	2.36 kPa	2.38 kPa	5.12 kPa	4.73 kPa	-	-
DSR (G*/sinδ), 10 rad/s, AASHTO T315	>2.2 kPa	82 ºC	-	-	-	2.77 kPa	2.57 kPa	3.25 kPa	2.31 kPa
DSR (G*/sinδ), 10 rad/s, AASHTO T315	>2.2 kPa	88 ºC	-	-	-	-	1.42 kPa	1.80 kPa	1.29 kPa
DSR (G*.sinδ), 10 rad/s, AASHTO T315	<5000 kPa	28 ºC	-	-	-	4380 kPa	4060 kPa	4830 kPa	3670 kPa
DSR (G*.sinδ), 10 rad/s, AASHTO T315	<5000 kPa	25 ºC	3180 kPa	3030 kPa	2690 kPa	5945 kPa	5470 kPa	6470 kPa	5080 kPa
DSR (G*.sinδ), 10 rad/s, AASHTO T315	<5000 kPa	22 ºC	4660 kPa	4525 kPa	3900 kPa	-	-	-	-
DSR (G*.sinδ), 10 rad/s, AASHTO T315	<5000 kPa	19 ºC	6620 kPa	6505 kPa	5550 kPa	-	-	-	-
BBR-S- AASHTO T313	<300 MPa	-6 ºC	83 MPa	81.2 MPa	77.9 MPa	149.5 MPa	125 MPa	121 MPa	103.5 MPa
BBR-S- AASHTO T313	<300 MPa	-12 ºC	178 MPa	161 MPa	145 MPa	272 MPa	217 MPa	233 MPa	194 MPa
BBR-S- AASHTO T313	<300 MPa	-18 ºC	317 MPa	323 MPa	281 MPa	476 MPa	475 MPa	443 MPa	379 MPa
BBR-m- AASHTO T313	>0.3	-6 ºC	0.396	0.380	0.375	0.340	0.335	0.326	0.338
BBR-m- AASHTO T313	>0.3	-12 ºC	0.336	0.330	0.314	0.299	0.287	0.254	0.288
BBR-m- AASHTO T313	>0.3	-18 ºC	0.290	0.275	0.273	0.240	0.238	0.230	0.234
PG- Grading	--------		**70-22**	**76-22**	**76-22**	**82-16**	**82-16**	**88-16**	**82-16**
Continuous PG- Grading	--------		**73.8-27.4**	**78.2-25.3**	**79.7-24.1**	**87.3-21.9**	**85.4-20.4**	**88.8-18.2**	**85.9-20.6**

APPENDIX B: STATISTICAL ANALYSIS FOR THE HEALING QUANTIFICATION (PG 70-22)

B.1 Effect of Sodium-Alginate Fibers in the Healing Ability of Virgin Binder PG 70-22

Table B-1. Means comparison.

t	Alpha
2.77645	0.05

Table B-2. LSD threshold matrix.

Binder	70CO	70PG5F
70CO	-27.295	-24.575
70PG5F	-24.575	-27.295

Table B-3. Connecting letters report.

Level		Mean
70CO	A	55.213333
70PG5F	A	52.493333

B.2 Effect of Type of Recycled Material in the Healing Ability of Sodium-Alginate Fibers

B.2.1. Recycled Material: RAS

Table B-4. One-way Anova.

Rsquare	0.783445
Adj Rsquare	0.687199
Root Mean Square Error	6.776551
Mean of Response	55.46786
Observations (or Sum Wgts)	14

Table B-5. Analysis of variance.

Source	DF	Sum of Squares	Mean Square	F Ratio	Prob > F
HMA Mixture Type	4	1495.2044	373.801	8.1400	0.0046*
Error	9	413.2948	45.922		
C. Total	13	1908.4992			

Table B-6. Means for One-way Anova.

Level	Number	Mean	Std Error	Lower 95%	Upper 95%
70CO	3	55.2133	3.9124	46.363	64.064
70PG5P	2	53.0500	4.7917	42.210	63.890
70PG5P1F	3	57.0367	3.9124	48.186	65.887
70PG5P3F	3	39.9333	3.9124	31.083	48.784
70PG5P5F	3	71.3000	3.9124	62.449	80.151

Table B-7. HSD threshold matrix.

Level	70PG5P5F	70PG5P1F	70CO	70PG5P	70PG5P3F
70PG5P5F	-18.605	-4.342	-2.519	-2.551	12.761
70PG5P1F	-4.342	-18.605	-16.782	-16.815	-1.502
70CO	-2.519	-16.782	-18.605	-18.638	-3.325
70PG5P	-2.551	-16.815	-18.638	-22.787	-7.685
70PG5P3F	12.761	-1.502	-3.325	-7.685	-18.605

Table B-8. Connecting letters report.

Level			Mean
70PG5P5F	A		71.300000
70PG5P1F	A	B	57.036667
70CO	A	B	55.213333
70PG5P	A	B	53.050000
70PG5P3F		B	39.933333

B.2.2. Recycled Material: RAP

Table B-9. One-way Anova.

Rsquare	0.913305
Adj Rsquare	0.878627
Root Mean Square Error	2.860068
Mean of Response	59.075
Observations (or Sum Wgts)	8

Table B-10. Analysis of variance.

Source	DF	Sum of Squares	Mean Square	F Ratio	Prob > F
HMA Mixture Type	2	430.86627	215.433	26.3366	0.0022*
Error	5	40.89993	8.180		
C. Total	7	471.76620			

Table B-11. Means for One-way Anova.

Level	Number	Mean	Std Error	Lower 95%	Upper 95%
70CO	3	55.2133	1.6513	50.969	59.458
70PG20RAP	3	68.3133	1.6513	64.069	72.558
70PG20RAP5F	2	51.0100	2.0224	45.811	56.209

Table B-12. HSD threshold matrix.

Level	70PG20RAP	70CO	70PG20RAP5F
70PG20RAP	-7.5985	5.5015	8.8079
70CO	5.5015	-7.5985	-4.2921
70PG20RAP5F	8.8079	-4.2921	-9.3063

Table B-13. Connecting letters report.

Level			Mean
70PG20RAP	A		68.313333
70CO		B	55.213333
70PG20RAP5F		B	51.010000

B.3. Effect of Curing Conditions in the Healing Ability of Sodium-Alginate Fibers

B.3.1. One-way Analysis of 70CO By Environmental Curing Condition

Table B-14. Means comparisons.

t	Alpha
2.77645	0.05

Table B-15. LSD threshold matrix.

Level	High-Temperature	Room-Temperature
High-Temperature	-12.648	-12.424
Room-Temperature	-12.424	-12.648

Table B-16. Connecting letters report.

Level		Mean
High-Temperature	A	55.436667
Room-Temperature	A	55.213333

B.3.2. One-way Analysis of 70PG5F By Environmental Curing Condition

Table B-17. Means Comparisons.

t	Alpha
3.18245	0.05

Table B-18. LSD threshold matrix.

Level	High-Temperature	Room-Temperature
High-Temperature	-44.274	-14.005
Room-Temperature	-14.005	-36.149

Table B-19. Connecting letters report.

Level		Mean
High-Temperature	A	78.905000
Room-Temperature	A	52.493333

B.3.3. One-way Analysis of 70PG5P By Environmental Curing Condition

Table B-20. Means comparisons.

t	Alpha
3.18245	0.05

Table B- 21. LSD threshold matrix.

Level	High-Temperature	Room-Temperature
High-Temperature	-0.15306	-0.05777
Room-Temperature	-0.05777	-0.18747

Table B-22. Connecting letters report.

Level		Mean
High-Temperature	A	0.64386667
Room-Temperature	A	0.53050000

B.3.4. One-way Analysis of 70PG5P1F By Environmental Curing Condition

Table B-23. Means comparisons.

t	Alpha
2.77645	0.05

Table B-24. LSD threshold matrix.

Level	High-Temperature	Room-Temperature
High-Temperature	-0.15155	-0.03445
Room-Temperature	-0.03445	-0.15155

Table B-25. Connecting Letters Report.

Level		Mean
High-Temperature	A	0.68746667
Room-Temperature	A	0.57036667

B.3.5. One-way Analysis of 70PG5P3F By Environmental Curing Condition

Table B- 26. Means Comparisons.

t	Alpha
2.77645	0.05

Table B- 27. LSD threshold matrix.

Level	High-Temperature	Room-Temperature
High-Temperature	-0.20472	-0.03235
Room-Temperature	-0.03235	-0.20472

Table B-28. Connecting letters report.

Level		Mean
High-Temperature	A	0.57170000
Room-Temperature	A	0.39933333

B.3.6. One-way Analysis of 70PG5P5F By Environmental Curing Condition

Table B-29. Means comparisons.

t	Alpha
2.77645	0.05

Table B-30. LSD threshold matrix.

Level	Room-Temperature	High-Temperature
Room-Temperature	-0.19514	-0.11888
High-Temperature	-0.11888	-0.19514

Table B-31. Connecting letters report.

Level		Mean
Room-Temperature	A	0.71300000
High-Temperature	A	0.63673333

B.3.7. One-way Analysis of 70PG20RAP By Environmental Curing Condition

Table B-32. Means comparisons.

t	Alpha
2.77645	0.05

Table B-33. LSD threshold matrix.

Level	Room-Temperature	High-Temperature
Room-Temperature	-0.31511	-0.13198
High-Temperature	-0.13198	-0.31511

Table B-34. Connecting letters report.

Level		Mean
Room-Temperature	A	0.68313333
High-Temperature	A	0.50000000

B.3.8. One-way Analysis of 70PG20RAP5F By Environmental Curing Condition

Table B-35. Means comparisons.

t	Alpha
4.30265	0.05

Table B-36. LSD threshold matrix.

Level	High-Temperature	Room-Temperature
High-Temperature	-0.41007	-0.38927
Room-Temperature	-0.38927	-0.41007

Table B-37. Connecting letters report.

Level		Mean
High-Temperature	A	0.53090000
Room-Temperature	A	0.51010000

APPENDIX C: STATISTICAL ANALYSIS FOR HEALING QUANTIFICATION (PG 64-22)

C.1. Effect of Sodium-Alginate Fibers in the Healing Ability of Virgin Binder PG 64-22

Table C-1. Means Comparisons.

t	Alpha
3.18245	0.05

Table C-2. LSD threshold matrix.

Binder	64CO	64PG5F
64CO	-30.638	-25.884
64PG5F	-25.884	-37.523

Table C-3. Connecting letters report.

Level		Mean
64CO	A	63.970000
64PG5F	A	55.600000

C.2. Effect of Type of Recycled Material in the Healing Ability of Sodium-Alginate Fibers

C.2.1. Recycled Material: RAS

Table C-4. One-way Anova.

Rsquare	0.45702
Adj Rsquare	0.276027
Root Mean Square Error	11.19485
Mean of Response	52.32667
Observations (or Sum Wgts)	9

Table C-5. Analysis of Variance.

Source	DF	Sum of Squares	Mean Square	F Ratio	Prob > F
HMA Mixture Type	2	632.9065	316.453	2.5251	0.1601
Error	6	751.9479	125.325		
C. Total	8	1384.8544			

Table C-6. Means for One-way Anova.

Level	Number	Mean	Std Error	Lower 95%	Upper 95%
64CO	3	63.9700	6.4633	48.155	79.785
64PG5P	3	44.5533	6.4633	28.738	60.369
64PG5P5F	3	48.4567	6.4633	32.641	64.272

Table C-7. HSD threshold matrix.

Binder	64CO	64PG5P5F	64PG5P
64CO	-28.045	-12.531	-8.628
64PG5P5F	-12.531	-28.045	-24.141
64PG5P	-8.628	-24.141	-28.045

Table C-8. Connecting letters report.

Level		Mean
64CO	A	63.970000
64PG5P5F	A	48.456667
64PG5P	A	44.553333

C.2.2. Recycled Material: RAP

Table C-9. One-way Anova.

Rsquare	0.405139
Adj Rsquare	0.206852
RootMean Square Error	7642331
Mean of Response	56.7
Observations (or Sum Wgts)	9

Table C-10. Analysis of variance.

Source	DF	Sum of Squares	Mean Square	F Ratio	Prob > F
HMA Mixture Type	2	238.66687	119.333	2.0432	0.2105
Error	6	350.43133	58.405		
C. Total	8	589.09820			

Table C-11. Means for one-way Anova.

Level	Number	Mean	Std Error	Lower 95%	Upper 95%
64CO	3	63.9700	4.4123	53.173	74.767
64PG20RAP	3	52.6933	4.4123	41.897	63.490
64PG20RAP5F	3	53.4367	4.4123	42.640	64.233

Table C-12. HSD threshold matrix.

Level	64CO	64PG20RAP5F	64PG20RAP
64CO	-19.145	-8.612	-7.868
64PG20RAP5F	-8.612	-19.145	-18.402
64PG20RAP	-7.868	-18.402	-19.145

Table C-13. Connecting letters report.

Level		Mean
64CO	A	63.970000
64PG20RAP5F	A	53.436667
64PG20RAP	A	52.693333

C.3. Effect of Curing Conditions in the Healing Ability of Sodium-Alginate Fibers

C.3.1. One-way Analysis of 64CO By Environmental Curing Condition

Table C-14. Means comparisons.

t	Alpha
3.18245	0.05

Table C-15. LSD threshold matrix.

Level	High-Temperature	Room-Temperature
High-Temperature	-32.216	-26.489
Room-Temperature	-26.489	-26.304

Table C-16. Connecting letters report.

Level		Mean
High-Temperature	A	66.890000
Room-Temperature	A	63.970000

C.3.2. One-way Analysis of 64PG5F By Environmental Curing Condition

Table C-17. Means comparisons.

t	Alpha
3.18245	0.05

Table C-18. LSD threshold matrix.

Level	High-Temperature	Room-Temperature
High-Temperature	-32.706	-33.893
Room-Temperature	-33.893	-40.056

Table C-19. Connecting letters report.

Level		Mean
High-Temperature	A	58.273333
Room-Temperature	A	55.6000

C3.3. One-way Analysis of 64PG5P By Environmental Curing Condition

Table C-20. Means comparisons.

t	Alpha
2.77645	0.05

Table C-21. LSD threshold matrix.

Level	High-Temperature	Room-Temperature
High-Temperature	-21.266	-8.062
Room-Temperature	-8.062	-21.266

Table C-22. Connecting letters report.

Level		Mean
High-Temperature	A	57.756667
Room-Temperature	A	44.553333

C.3.4. One-way Analysis of 64PG5P5F By Environmental Curing Condition

Table C-23. Means comparisons.

t	Alpha
3.18245	0.05

Table C-24. LSD threshold matrix.

Level	High-Temperature	Room-Temperature
High-Temperature	-20.956	-7.981
Room-Temperature	-7.981	-17.110

Table C-25. Connecting letters report.

Level		Mean
High-Temperature	A	59.605000
Room-Temperature	A	48.456667

C.3.5. One-way Analysis of 64PG20RAP By Environmental Curing Condition

Table C-26. Means comparisons.

t	Alpha
2.77645	0.05

Table C-27. LSD threshold matrix.

Level	High-Temperature	Room-Temperature
High-Temperature	-9.4225	-7.1525
Room-Temperature	-7.1525	-9.4225

Table C-28. Connecting letters report.

Level		Mean
High-Temperature	A	54.963333
Room-Temperature	A	52.693333

C.3.6. One-way Analysis of 64PG20RAP5F By Environmental Curing Condition

Table C-29. Means comparisons.

t	Alpha
2.77645	0.05

Table C-30. LSD threshold matrix.

Level	Room-Temperature	High-Temperature
Room-Temperature	-7.8137	0.1430
High-Temperature	0.1430	-7.8137

T

Table C-31. Connecting letters report.

Level			Mean
Room-Temperature	A		61.393333
High-Temperature		B	53.436667

APPENDIX D: STATISTICAL ANALYSIS FOR THE STRENGTH RECOVERY (BINDER PG 70-22)

D.1. Effect of Sodium-Alginate Fibers in the strength Recovery Ability of Virgin Binder PG 70-22

Table D-1.One-way Anova.

Rsquare	0.033482
Adj Rsquare	-0.20815
Root Mean Square Error	0.059003
Mean of Response	0.437533
Observations (or Sum Wgts)	6

Table D-2. Analysis of variance.

Source	DF	Sum of Squares	Mean Square	F Ratio	Prob > F
HMA Mixture	1	0.00048241	0.000482	0.1386	0.7286
Error	4	0.01392547	0.003481		
C. Total	5	0.01440787			

Table D-3. Means for one-way Anova.

Level	Number	Mean	Std Error	Lower 95%	Upper 95%
70CO	3	0.446500	0.03407	0.35192	0.54108
70PG5F	3	0.428567	0.03407	0.33399	0.52315

Table D-4. LSD threshold matrix.

Binder	70CO	70PG5F
70CO	-0.13376	-0.11582
70PG5F	-0.11582	-0.13376

Table D-5. Connecting letters report.

Level		Mean
70CO	A	0.44650000
70PG5F	A	0.42856667

D.2. Effect of Type of Recycled Material in the Strength Recovery Ability of Sodium-Alginate Fibers

D.2.1. Recycled Material: RAS

Table D-6. One-way Anova.

Rsquare	0.936355
Adj Rsquare	0.910898
Root Mean Square Error	0.050078
Mean of Response	0.251488
Observations (or Sum Wgts)	8

Table D-7. Analysis of variance.

Source	DF	Sum of Squares	Mean Square	F Ratio	Prob > F
HMA Mixture Type	2	0.18447462	0.092237	36.7807	0.0010*
Error	5	0.01253883	0.002508		
C. Total	7	0.19701345			

Table D-8. Means for one-way Anova.

Level	Number	Mean	Std Error	Lower 95%	Upper 95%
70CO	3	0.446500	0.02891	0.37218	0.52082
70PG5P	2	0.158550	0.03541	0.06753	0.24957
70PG5P5F	3	0.118433	0.02891	0.04411	0.19275

Table D-9. HSD threshold matrix.

Level	70CO	70PG5P	70PG5P5F
70CO	-0.13304	0.13920	0.19502
70PG5P	0.13920	-0.16295	-0.10863
70PG5P5F	0.19502	-0.10863	-0.13304

Table D-10. Connecting letters report.

Level			Mean
70CO	A		0.44650000
70PG5P		B	0.15855000
70PG5P5F		B	0.11843333

D.2.2 Recycled Material: RAP

Table D-11. One-way Anova.

Rsquare	0.933096
Adj Rsquare	0.906334
Root Mean Square Error	0.040256
Mean of Response	0.310525
Observations (or Sum Wgts)	8

Table D-12. Analysis of variance.

Source	DF	Sum of Squares	Mean Square	F Ratio	Prob > F
HMA Mixture Type	2	0.11300748	0.056504	34.8669	0.0012*
Error	5	0.00810277	0.001621		
C. Total	7	0.12111026			

Table D-13. Means for one-way Anova.

Level	Number	Mean	Std Error	Lower 95%	Upper 95%
70CO	3	0.446500	0.02324	0.38675	0.50625
70PG20RAP	3	0.172067	0.02324	0.11232	0.23181
70PG20RAP5F	2	0.314250	0.02847	0.24108	0.38742

Table D-14. HSD threshold matrix.

Level	70CO	70PG20RAP5F	70PG20RAP
70CO	-0.10695	0.01267	0.16748
70PG20RAP5F	0.01267	-0.13099	0.02261
70PG20RAP	0.16748	0.02261	-0.10695

Table D-15. Connecting letters report.

Level				Mean
70CO	A			0.44650000
70PG20RAP5F		B		0.31425000
70PG20RAP			C	0.17206667

D.3. Effect of Curing Conditions in the Healing Ability of Sodium-Alginate Fibers

D.3.1 One-way Analysis of 70CO By Environmental Curing Condition

Table D-16. Means comparisons.

t	Alpha
2.77645	0.05

Table D-17. LSD threshold matrix.

Level	High-Temperature	Room-Temperature
High-Temperature	-0.23325	0.00278
Room-Temperature	0.00278	-0.23325

Table D-18. Connecting letters report.

Level			Mean
High-Temperature	A		0.68253333
Room-Temperature		B	0.44650000

D.3.2. One-way Analysis of 70PG5F By Environmental Curing Condition

Table D-19. Means comparisons.

t	Alpha
3.18245	0.05

Table D-20. LSD threshold matrix.

Level	High-Temperature	Room-Temperature
High-Temperature	-0.28248	0.38847
Room-Temperature	0.38847	-0.23064

Table D-21. Connecting letters report.

Level			Mean
High-Temperature	A		1.0
Room-Temperature		B	0.4285667

D.3.3 One-way Analysis of 70PG5P By Environmental Curing Condition

Table D-22. Means comparisons.

t	Alpha
3.18245	0.05

Table D-23. LSD threshold matrix.

Level	High-Temperature	Room-Temperature
High-Temperature	-0.15285	0.13895
Room-Temperature	0.13895	-0.18721

Table D-24. Connecting letters report.

Level			Mean
High-Temperature	A		0.46840000
Room-Temperature		B	0.15855000

D.3.4. One-way Analysis of 70PG5P5F By Environmental Curing Condition

Table D-25. Connecting letters report.

t	Alpha
2.77645	0.05

Table D-26. LSD threshold matrix.

Level	High-Temperature	Room-Temperature
High-Temperature	-0.10757	0.29869
Room-Temperature	0.29869	-0.10757

Table D-27. Connecting letters report.

Level			Mean
High-Temperature	A		0.52470000
Room-Temperature		B	0.11843333

D.3.5. One-way Analysis of 70PG20RAP By Environmental Curing Condition

Table D-28. Means comparisons.

t	Alpha
2.77645	0.05

Table D-29. LSD threshold matrix.

Level	High-Temperature	Room-Temperature
High-Temperature	-0.20972	0.09248
Room-Temperature	0.09248	-0.20972

Table D-30. Connecting letters report.

Level			Mean
High-Temperature	A		0.47426667
Room-Temperature		B	0.17206667

D.3.6. One-way Analysis of 70PG20RAP5F By Environmental Curing Condition

Table D-31. Means comparisons.

t	Alpha
4.30265	0.05

Table D-32. LSD threshold matrix.

Level	High-Temperature	Room-Temperature
High-Temperature	-0.21341	-0.19131
Room-Temperature	-0.19131	-0.21341

Table D-33. Connecting letters report.

Level		Mean
High-Temperature	A	0.33635000
Room-Temperature	A	0.31425000

APPENDIX E: STATISTICAL ANALYSIS FOR STRENGTH RECOVERY (BINDER PG 64-22)

E.1. Effect of Sodium-Alginate Fibers in the Strength Recovery Ability of Virgin Binder PG 64-22

Table E-1. One-way Anova.

Rsquare	0.403397
Adj Rsquare	0.254247
Root Mean Square Error	0.136581
Mean of Response	0.430567
Observations (or Sum Wgts)	6

Table E-2. Analysis of variance.

Source	DF	Sum of Squares	Mean Square	F Ratio	Prob > F
HMA Mixture	1	0.05045334	0.050453	2.7046	0.1754
Error	4	0.07461775	0.018654		
C. Total	5	0.12507109			

Table E-3. Means for one-way Anova.

Level	Number	Mean	Std Error	Lower 95%	Upper 95%
64CO	3	0.338867	0.07886	0.11993	0.55780
64PG5F	3	0.522267	0.07886	0.30333	0.74120

Table E-4. LSD threshold matrix.

Binder	64PG5F	64CO
64PG5F	-0.30962	-0.12622
64CO	-0.12622	-0.30962

Table E-5. Connecting Letters Report.

Level		Mean
64PG5F	A	0.52226667
64CO	B	0.33886667

E.2. Effect of Type of Recycled Material in the Strength Recovery Ability of Sodium-Alginate Fibers

E.2.1. Recycled Material: RAS

Table E-6. One-way Anova.

Rsquare	0.11958
Adj Rsquare	-0.17389
Root Mean Square Error	0.14826
Mean of Response	0.293756
Observations (or Sum Wgts)	9

Table E-7. Analysis of variance.

Source	DF	Sum of Squares	Mean Square	F Ratio	Prob > F
HMA Mixture Type	2	0.01791300	0.008956	0.4075	0.6824
Error	6	0.13188597	0.021981		
C. Total	8	0.14979896			

Table E-8. Means for one-way Anova.

Level	Number	Mean	Std Error	Lower 95%	Upper 95%
64CO	3	0.338867	0.08560	0.12942	0.54832
64PG5P	3	0.233000	0.08560	0.02355	0.44245
64PG5P5F	3	0.309400	0.08560	0.09995	0.51885

Table E-9. HSD threshold matrix.

Level	64CO	64PG5P5F	64PG5P
64CO	-0.37141	-0.34194	-0.26554
64PG5P5F	-0.34194	-0.37141	-0.29501
64PG5P	-0.26554	-0.29501	-0.37141

Table E-10. Connecting letters report.

Level		Mean
64CO	A	0.33886667
64PG5P5F	A	0.30940000
64PG5P	A	0.23300000

E.2.2. Recycled Material: RAP

Table E-11. One-way Anova.

Rsquare	0.660674
Adj Rsquare	0.547566
Root Mean Square Error	0.067041
Mean of Response	0.257778
Observations (or Sum Wgts)	9

Table E-12. Analysis of variance.

Source	DF	Sum of Squares	Mean Square	F Ratio	Prob > F
HMA Mixture Type	2	0.05250478	0.026252	5.8411	0.0391*
Error	6	0.02696674	0.004494		
C. Total	8	0.07947152			

Table E-13. Means for one-way Anova.

Level	Number	Mean	Std Error	Lower 95%	Upper 95%
64CO	3	0.338867	0.03871	0.24416	0.43358
64PG20RAP	3	0.155433	0.03871	0.06072	0.25014
64PG20RAP5F	3	0.279033	0.03871	0.18432	0.37374

Table E-14. HSD threshold matrix.

Level	64CO	64PG20RAP5F	64PG20RAP
64CO	-0.16795	-0.10811	0.01549
64PG20RAP5F	-0.10811	-0.16795	-0.04435
64PG20RAP	0.01549	-0.04435	-0.16795

Table E-15. Connecting letters report.

Level			Mean
64CO	A		0.33886667
64PG20RAP5F	A	B	0.27903333
64PG20RAP		B	0.15543333

E.3. Effect of Curing Conditions in the Healing Ability of Sodium-Alginate Fibers

E.3.1. One-way Analysis of 64CO By Environmental Curing Condition

Table E-16. Means comparisons.

t	Alpha
2.77645	0.05

Table E-17. LSD threshold matrix.

Level	High-Temperature	Room-Temperature
High-Temperature	-0.24657	-0.08657
Room-Temperature	-0.08657	-0.24657

Table E-18. Connecting letters report.

Level		Mean
High-Temperature	A	0.49886667
Room-Temperature	A	0.33886667

E.3.2. One-way Analysis of 64PG5F By Environmental Curing Condition

Table E-19. Means comparisons.

t	Alpha
2.77645	0.05

Table E-20. LSD Threshold Matrix.

Level	High-Temperature	Room-Temperature
High-Temperature	-0.32329	-0.03206
Room-Temperature	-0.03206	-0.32329

Table E-21. Connecting Letters Report.

Level		Mean
High-Temperature	A	0.8135
Room-Temperature	A	0.5222

E.3.3. One-way Analysis of 64PG5P By Environmental Curing Condition

Table E-22. Means comparisons.

t	Alpha
3.18245	0.05

Table E-23. LSD threshold matrix.

Level	High-Temperature	Room-Temperature
High-Temperature	-0.31163	-0.11765
Room-Temperature	-0.11765	-0.38167

Table E-24. Connecting letters report.

Level		Mean
High-Temperature	A	0.49876667
Room-Temperature	A	0.26800000

E.3.4. One-way Analysis of 64PG5P5F By Environmental Curing Condition

Table E-25. Means comparisons.

t	Alpha
3.18245	0.05

Table E-26. LSD threshold matrix.

Level	High-Temperature	Room-Temperature
High-Temperature	-0.59675	-0.33721
Room-Temperature	-0.33721	-0.48724

Table E-27. Connecting letters report.

Level		Mean
High-Temperature	A	0.51695000
Room-Temperature	A	0.30940000

E.3.5. One-way Analysis of 64PG20RAP By Environmental Curing Condition

Table E-28. Means comparisons.

t	Alpha
2.77645	**0.05**

Table E-29. LSD threshold matrix.

Level	High-Temperature	Room-Temperature
High-Temperature	-0.26552	-0.10962
Room-Temperature	-0.10962	-0.26552

Table E-30. Connecting letters report.

Level		Mean
High-Temperature	A	0.31133333
Room-Temperature	A	0.15543333

E.3.6 One-way Analysis of 64PG20RAP5F By Environmental Curing Condition

Table E-31. Means comparisons.

t	Alpha
2.77645	0.05

Table E-32. LSD threshold matrix.

Level	High-Temperature	Room-Temperature
High-Temperature	-0.38867	-0.18843
Room-Temperature	-0.18843	-0.38867

Table E-33. Connecting letters report.

Level		Mean
High-Temperature	A	0.47926667
Room-Temperature	A	0.27903333

APPENDIX F: STATISTICAL ANALYSIS FOR HMA MIXTURE TESTS

F.1. One-way Analysis of HMA Mixtures PG64-22 for LWT Test

Table F-1. One-way Anova.

Rsquare	0.970768
Adj Rsquare	0.945713
Root Mean Square Error	0.477905
Mean of Response	3.705
Observations (or Sum Wgts)	14

Table F-2. Analysis of variance.

Source	DF	Sum of Squares	Mean Square	F Ratio	Prob > F
HMA Mixture Type	6	53.093800	8.84897	38.7445	<.0001*
Error	7	1.598750	0.22839		
C. Total	13	54.692550			

Table F-3. Means for one-way Anova.

Level	Number	Mean	Std Error	Lower 95%	Upper 95%
64CO	2	8.17000	0.33793	7.3709	8.9691
64PG20RAP	2	2.25000	0.33793	1.4509	3.0491
64PG20RAP5F	2	4.35000	0.33793	3.5509	5.1491
64PG5P	2	3.18500	0.33793	2.3859	3.9841
64PG5P20RAP	2	2.37000	0.33793	1.5709	3.1691
64PG5P20RAP5F	2	2.35500	0.33793	1.5559	3.1541
64PG5P5F	2	3.25500	0.33793	2.4559	4.0541

Table F-4. HSD threshold matrix.

Level	64CO	64PG20RAP 5F	64PG5P5 F	64PG5 P	64PG5P20RAP	64PG5P20RAP5 F	64PG20R AP
64CO	-1.8944	1.9256	3.0206	3.0906	3.9056	3.9206	4.0256
64PG20RAP5F	1.9256	-1.8944	-0.7994	-0.7294	0.0856	0.1006	0.2056
64PG5P5F	3.0206	-0.7994	-1.8944	-1.8244	-1.0094	-0.9944	-0.8894
64PG5P	3.0906	-0.7294	-1.8244	-1.8944	-1.0794	-1.0644	-0.9594
64PG5P20RAP	3.9056	0.0856	-1.0094	-1.0794	-1.8944	-1.8794	-1.7744
64PG5P20RAP 5F	3.9206	0.1006	-0.9944	-1.0644	-1.8794	-1.8944	-1.7894
64PG20RAP	4.0256	0.2056	-0.8894	-0.9594	-1.7744	-1.7894	-1.8944

Table F-5. Connecting letters report.

Level				Mean
64CO	A			8.1700000
64PG20RAP5F		B		4.3500000
64PG5P5F		B	C	3.2550000
64PG5P		B	C	3.1850000
64PG5P20RAP			C	2.3700000
64PG5P20RAP5F			C	2.3550000
64PG20RAP			C	2.2500000

F.2. One-way Analysis of HMA Mixtures PG64-22 for SCB Test

Table F-6. One-way Anova.

Rsquare	0.578137
Adj Rsquare	0.26174
Root Mean Square Error	0.131347
Mean of Response	0.496
Observations (or Sum Wgts)	15

Table F-7. Analysis of variance.

Source	DF	Sum of Squares	Mean Square	F Ratio	Prob > F
HMA Mixture Type	6	0.18914333	0.031524	1.8273	0.2108
Error	8	0.13801667	0.017252		
C. Total	14	0.32716000			

Table F-8. Means for one-way Anova.

Level	Number	Mean	Std Error	Lower 95%	Upper 95%
64CO	2	0.670000	0.09288	0.45583	0.88417
64PG20RAP	2	0.525000	0.09288	0.31083	0.73917
64PG20RAP5F	2	0.310000	0.09288	0.09583	0.52417
64PG5P	3	0.383333	0.07583	0.20846	0.55821
64PG5P20RAP	2	0.580000	0.09288	0.36583	0.79417
64PG5P20RAP5F	2	0.515000	0.09288	0.30083	0.72917
64PG5P5F	2	0.545000	0.09288	0.33083	0.75917

Table F-9. HSD threshold matrix.

Level	64CO	64PG5P20RAP	64PG5P5F	64PG20RAP	64PG5P20RAP5F	64PG5P	64PG20RAP5F
64CO	-0.50145	-0.41145	-0.37645	-0.35645	-0.34645	-0.17109	-0.14145
64PG5P20RAP	-0.41145	-0.50145	-0.46645	-0.44645	-0.43645	-0.26109	-0.23145
64PG5P5F	-0.37645	-0.46645	-0.50145	-0.48145	-0.47145	-0.29609	-0.26645
64PG20RAP	-0.35645	-0.44645	-0.48145	-0.50145	-0.49145	-0.31609	-0.28645
64PG5P20RAP5F	-0.34645	-0.43645	-0.47145	-0.49145	-0.50145	-0.32609	-0.29645
64PG5P	-0.17109	-0.26109	-0.29609	-0.31609	-0.32609	-0.40943	-0.38443
64PG20RAP5F	-0.14145	-0.23145	-0.26645	-0.28645	-0.29645	-0.38443	-0.50145

Table F-10. Connecting letters report.

Level		Mean
64CO	A/B	0.67000000
64PG5P20RAP	A	0.58000000
64PG5P5F	A	0.54500000
64PG20RAP	A	0.52500000
64PG5P20RAP5F	A	0.51500000
64PG5P	A/B	0.38333333
64PG20RAP5F	B	0.31000000

F.3. One-way Analysis of HMA Mixtures PG64-22 for TSRST Test

Table F-11. One-way Anova.

Rsquare	0.7715
Adj Rsquare	0.4973
Root Mean Square Error	151.7394
Mean of Response	1202.783
Observations (or Sum Wgts)	12

Table F-12. Analysis of variance.

Source	DF	Sum of Squares	Mean Square	F Ratio	Prob > F
HMA Mixture Type	6	388701.73	64783.6	2.8136	0.1381
Error	5	115124.16	23024.8		
C. Total	11	503825.90			

Table F-13. Means for one-way Anova.

Level	Number	Mean	Std Error	Lower 95%	Upper 95%
64CO	2	1115.39	107.30	839.6	1391.2
64PG20RAP	2	1329.81	107.30	1054.0	1605.6
64PG20RAP5F	2	1451.01	107.30	1175.2	1726.8
64PG5P	2	1287.03	107.30	1011.2	1562.8
64PG5P20RAP	2	936.55	107.30	660.7	1212.4
64PG5P20RAP5F	1	956.28	151.74	566.2	1346.3
64PG5P5F	1	1237.56	151.74	847.5	1627.6

Table F-14. HSD threshold matrix.

Level	64PG20RAP5F	64PG20RAP	64PG5P	64PG5P5F	64CO	64PG5P20RAP5F	64PG5P20RAP
64PG20RAP5F	-679.17	-557.98	-515.19	-618.37	-343.56	-337.09	-164.72
64PG20RAP	-557.98	-679.17	-636.39	-739.56	-464.75	-458.28	-285.91
64PG5P	-515.19	-636.39	-679.17	-782.35	-507.54	-501.07	-328.70
64PG5P5F	-618.37	-739.56	-782.35	-960.49	-709.64	-679.21	-530.80
64CO	-343.56	-464.75	-507.54	-709.64	-679.17	-672.70	-500.33
64PG5P20RAP5F	-337.09	-458.28	-501.07	-679.21	-672.70	-960.49	-812.08
64PG5P20RAP	-164.72	-285.91	-328.70	-530.80	-500.33	-812.08	-679.17

Table F-15. Connecting letters report.

Level		Mean
64PG20RAP5F	A	1451.0050
64PG20RAP	A	1329.8100
64PG5P	A	1287.0250
64PG5P5F	A	1237.5600
64CO	A	1115.3900
64PG5P20RAP5F	A	956.2800
64PG5P20RAP	A	936.5500

F.4. One-way Analysis of HMA Mixtures PG 70-22 for LWT Test

Table F-16. One-way Anova.

Rsquare	0.792474
Adj Rsquare	0.614594
Root Mean Square Error	0.583205
Mean of Response	2.398571
Observations (or Sum Wgts)	14

Table F-17. Analysis of variance.

Source	DF	Sum of Squares	Mean Square	F Ratio	Prob > F
HMA Mixture Type	6	9.091871	1.51531	4.4551	0.0355*
Error	7	2.380900	0.34013		
C. Total	13	11.472771			

Table F-18. Means for one-way Anova.

Level	Number	Mean	Std Error	Lower 95%	Upper 95%
70CO	2	3.81500	0.41239	2.8399	4.7901
70PG20RAP	2	1.94000	0.41239	0.9649	2.9151
70PG20RAP5F	2	3.15500	0.41239	2.1799	4.1301
70PG5P	2	2.45500	0.41239	1.4799	3.4301
70PG5P20RAP	2	1.36500	0.41239	0.3899	2.3401
70PG5P20RAP5F	2	1.57500	0.41239	0.5999	2.5501
70PG5P5F	2	2.48500	0.41239	1.5099	3.4601

Table F- 19. HSD threshold matrix.

Level	70CO	70PG20RAP5F	70PG5P5F	70PG5P	70PG20RAP	70PG5P20RAP5F	70PG5P20RAP
70CO	-2.3118	-1.6518	-0.9818	-0.9518	-0.4368	-0.0718	0.1382
70PG20RAP5F	-1.6518	-2.3118	-1.6418	-1.6118	-1.0968	-0.7318	-0.5218
70PG5P5F	-0.9818	-1.6418	-2.3118	-2.2818	-1.7668	-1.4018	-1.1918
70PG5P	-0.9518	-1.6118	-2.2818	-2.3118	-1.7968	-1.4318	-1.2218
70PG20RAP	-0.4368	-1.0968	-1.7668	-1.7968	-2.3118	-1.9468	-1.7368
70PG5P20RAP5F	-0.0718	-0.7318	-1.4018	-1.4318	-1.9468	-2.3118	-2.1018
70PG5P20RAP	0.1382	-0.5218	-1.1918	-1.2218	-1.7368	-2.1018	-2.3118

Table F-20. Connecting letters report.

Level			Mean
70CO	A		3.8150000
70PG20RAP5F	A	B	3.1550000
70PG5P5F	A	B	2.4850000
70PG5P	A	B	2.4550000
70PG20RAP	A	B	1.9400000
70PG5P20RAP5F	A	B	1.5750000
70PG5P20RAP		B	1.3650000

F.5. One-way Analysis of HMA Mixtures PG 70-22 for SCB Test

Table F-21. One-way Anova.

Rsquare	0.751256
Adj Rsquare	0.585426
Root Mean Square Error	0.068055
Mean of Response	0.51875
Observations (or Sum Wgts)	16

Table F-22. Analysis of variance.

Source	DF	Sum of Squares	Mean Square	F Ratio	Prob > F
HMA Mixture Type	6	0.12589167	0.020982	4.5303	0.0217*
Error	9	0.04168333	0.004631		
C. Total	15	0.16757500			

Table F-23. Means for one-way Anova.

Level	Number	Mean	Std Error	Lower 95%	Upper 95%
70CO	2	0.635000	0.04812	0.52614	0.74386
70PG20RAP	2	0.655000	0.04812	0.54614	0.76386
70PG20RAP5F	3	0.546667	0.03929	0.45778	0.63555
70PG5P	2	0.450000	0.04812	0.34114	0.55886
70PG5P20RAP	3	0.403333	0.03929	0.31445	0.49222
70PG5P20RAP5F	2	0.450000	0.04812	0.34114	0.55886
70PG5P5F	2	0.535000	0.04812	0.42614	0.64386

Table F-24. HSD threshold matrix.

Level	70PG20RAP	70CO	70PG20RAP5F	70PG5P5F	70PG5P20RAP5F	70PG5P	70PG5P20RAP
70PG20RAP	-0.25237	-0.23237	-0.12205	-0.13237	-0.04737	-0.04737	0.02128
70CO	-0.23237	-0.25237	-0.14205	-0.15237	-0.06737	-0.06737	0.00128
70PG20RAP5F	-0.12205	-0.14205	-0.20606	-0.21872	-0.13372	-0.13372	-0.06273
70PG5P5F	-0.13237	-0.15237	-0.21872	-0.25237	-0.16737	-0.16737	-0.09872
70PG5P20RAP5F	-0.04737	-0.06737	-0.13372	-0.16737	-0.25237	-0.25237	-0.18372
70PG5P	-0.04737	-0.06737	-0.13372	-0.16737	-0.25237	-0.25237	-0.18372
70PG5P20RAP	0.02128	0.00128	-0.06273	-0.09872	-0.18372	-0.18372	-0.20606

Table F-25. Connecting letters report.

Level			Mean
70PG20RAP	A		0.65500000
70CO	A		0.63500000
70PG20RAP5F	A	B	0.54666667
70PG5P5F	A	B	0.53500000
70PG5P20RAP5F	A	B	0.45000000
70PG5P	A	B	0.45000000
70PG5P20RAP		B	0.40333333

F.6. One-way Analysis of HMA Mixtures PG 70-22 for TSRST Test

Table F-26. One-way Anova.

Rsquare	0.803562
Adj Rsquare	0.656234
Root Mean Square Error	200.8958
Mean of Response	1098.662
Observations (or Sum Wgts)	15

Table F-27. Analysis of variance.

Source	DF	Sum of Squares	Mean Square	F Ratio	Prob > F
HMA Mixture Type	6	1320767.4	220128	5.4542	0.0159*
Error	8	322873.1	40359		
C. Total	14	1643640.5			

Table F-28. Means for one-way Anova.

Level	Number	Mean	Std Error	Lower 95%	Upper 95%
70CO	3	846.96	115.99	579.5	1114.4
70PG20RAP	2	1310.48	142.05	982.9	1638.1
70PG20RAP5F	1	1324.52	200.90	861.3	1787.8
70PG5P	3	1179.86	115.99	912.4	1447.3
70PG5P20RAP	2	649.55	142.05	322.0	977.1
70PG5P20RAP5F	2	963.82	142.05	636.2	1291.4
70PG5P5F	2	1613.64	142.05	1286.1	1941.2

Table F-29. HSD threshold matrix.

Level	70PG5P5F	70PG20RAP5F	70PG20RAP	70PG5P	70PG5P20RAP5F	70CO	70PG5P20RAP
70PG5P5F	-767.0	-650.2	-463.8	-266.4	-117.1	66.5	197.1
70PG20RAP5F	-650.2	-1084.7	-925.3	-741.0	-578.6	-408.1	-264.4
70PG20RAP	-463.8	-925.3	-767.0	-569.5	-420.3	-236.6	-106.0
70PG5P	-266.4	-741.0	-569.5	-626.2	-484.1	-293.3	-169.8
70PG5P20RAP5F	-117.1	-578.6	-420.3	-484.1	-767.0	-583.3	-452.7
70CO	66.5	-408.1	-236.6	-293.3	-583.3	-626.2	-502.7
70PG5P20RAP	197.1	-264.4	-106.0	-169.8	-452.7	-502.7	-767.0

Table F-30. Connecting letters report.

Level			Mean
70PG5P5F	A		1613.6427
70PG20RAP5F	A	B	1324.5200
70PG20RAP	A	B	1310.4750
70PG5P	A	B	1179.8590
70PG5P20RAP5F	A	B	963.8150
70CO		B	846.9569
70PG5P20RAP		B	649.5500